

---

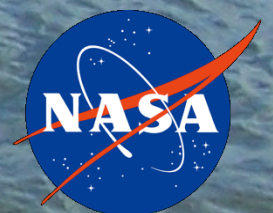
QUALITY ASSESSMENT  
OF THE

VISIBLE INFRARED IMAGING  
RADIOMETER SUITE (VIIRS)

OCEAN COLOR  
ENVIRONMENT DATA RECORDS (EDR)

---

25 March 2013



---

Prepared by the  
Suomi National Polar-orbiting Partnership (S-NPP)  
NASA Science Team Ocean Discipline

**Kevin R. Turpie<sup>1</sup>, Barney Balch<sup>2</sup>, Bruce Bowler<sup>2</sup>, Bryan A. Franz<sup>3</sup>,  
Robert Frouin<sup>4</sup>, Watson Gregg<sup>3</sup>, Charles R. McClain<sup>3</sup>, Cecile  
Rousseaux<sup>5</sup>, David Siegel<sup>6</sup>, Menghua Wang<sup>7</sup>,  
Gene Eplee<sup>8</sup>, Wayne Robinson<sup>8</sup>**

**Affiliations:**

<sup>1</sup>University of Maryland, Baltimore County/JCET,

<sup>2</sup>Bigelow Laboratory for Ocean Sciences,

<sup>3</sup>NASA Goddard Space Flight Center,

<sup>4</sup>Scripps Institution of Oceanography,

<sup>5</sup>Universities Space Research Association,

<sup>6</sup>University of California, Santa Barbara,

<sup>7</sup>NOAA/NESDIS/STAR,

<sup>8</sup>Science Applications International Corporation

Submitted to the NASA Science Mission Directorate's Earth Science Division (SMD/ESD) and the Joint Polar Satellite System (JPSS)/NPP Project Science Office (PSO).

Funded under NASA grant NNH10ZDA001N: Research Opportunities in Space and Earth Science (ROSES-2010), Appendix A.22 – NPP Science Team for Climate Data Records.

The views, opinions, and findings contained in this report are those of the authors and should not be construed as an official NASA, NOAA or U.S. Government position, policy, or decision.

**THIS DOCUMENT DOES NOT CONTAIN ITAR/EAR/EXPORT-CONTROLLED, PROPRIETARY/ SENSITIVE INFORMATION, NOR DOES IT DISCLOSE AN INVENTION.**

---

## ABSTRACT

---

VIIRS is being used by NOAA to routinely generate measurements of the Earth's surface and atmosphere, which are referred to as Environment Data Records (EDR). The ocean color EDR includes normalized water-leaving radiance (a measure of surface reflectance at 410, 443, 486, 551, and 671 nm), inherent optical properties (absorption and phytoplankton backscatter coefficients,  $a$  and  $b_b$ , at the same five wavelengths) and chlorophyll  $a$  concentration. The NASA science team evaluated whether the EDR products would meet NASA science objectives, including continuity of the existing climate data record (CDR) established with earlier NASA ocean color missions, including the Sea-viewing Wide Field of view Sensor (SeaWiFS) and the MODerate resolution Imaging Spectroradiometer (MODIS) aboard the EOS satellite Aqua. Team members at the NASA/Goddard Space Flight Center (GSFC) evaluated the EDR products against NASA evaluation products, the latter of which were based on standard NASA ocean color algorithms; an independent calibration; and were generated with existing computational infrastructure with a full, mission-level reprocessing capability. The independent evaluation processing at GSFC demonstrated that a consistent, high quality data record could be generated from S-NPP VIIRS. Indeed, the NASA evaluation chlorophyll  $a$  concentration from VIIRS agrees remarkably well with MODIS Aqua. Meanwhile, another team member (Wang) also compared the EDR products against those generated with NOAA research algorithms, based on the same standard NASA algorithms, but using the operational calibration. That investigation also looked at estimation of the diffuse attenuation coefficient at 490 nm (i.e.,  $K_d(490)$ ), which is a parameter in the NASA data record, but not part of the EDR suite. Wang also investigated the potential use of the VIIRS Shortwave Infrared (SWIR) bands to improve atmospheric correction over coastal waters. Likewise, other team members demonstrated that VIIRS can support other EOS standard products that are not part of the EDR suite, including Particulate Inorganic Carbon (PIC) and Photosynthetically Available Radiation (PAR). Furthermore, improved consistency between VIIRS and MODIS was demonstrated for the synoptic chlorophyll  $a$  concentration time series using data assimilation techniques. Validation analysis showed that operational and research evaluation products for surface reflectance showed good correlation with *in situ* data. However, closer investigation indicated the existence of biases in surface reflectance that were smaller than the uncertainty of the regression analysis, but were still sufficiently large enough to negatively affect the quality of the EDR chlorophyll  $a$  concentration and potentially other derived products. We concluded that the first year of operational and evaluation data demonstrate that reprocessing and continued refinement of calibration is critical to producing the consistency and accuracy required for continuity of the NASA data record and climate research objectives. Given past experience, it is expected that at least one more year of refinement is needed to bring VIIRS ocean color product quality to the level currently found in the established NASA data record. The EDR data product quality is converging at a slower rate to the NASA evaluation products and there is no reprocessing capability in the operational processing stream used to generate the EDR data products.

---

## ACKNOWLEDGEMENT

---

The Ocean Discipline members of the S-NPP NASA Science Team would like to express their gratitude to the staff of the Ocean Biology Processing Group for their role as Ocean Product Evaluation and Analysis Tools Element (PEATE). Without their stalwart support of our evaluation of the VIIRS ocean color data products, this assessment report would not be possible. Furthermore, we would like to express our thanks to science team member Thomas Stone (USGS) and the VIIRS Characterization Support Team (VCST) for their collaborative support in understanding and calibrating the VIIRS instrument. We are also grateful to the NOAA MOBY project (PI: Ken Voss, University of Miami) for maintaining and distributing *in situ* optical datasets.

---

# TABLE OF CONTENTS

---

<b>ABSTRACT</b> .....	<b>III</b>
<b>ACKNOWLEDGEMENT</b> .....	<b>IV</b>
<b>TABLE OF CONTENTS</b> .....	<b>V</b>
<b>EXECUTIVE SUMMARY</b> .....	<b>1</b>
<b>1. INTRODUCTION</b> .....	<b>6</b>
1.1 BACKGROUND .....	7
1.2 ASSESSMENT OF INSTRUMENT PERFORMANCE .....	8
1.2.1 <i>Prelaunch Assessment</i> .....	8
1.2.2 <i>Postlaunch Assessment</i> .....	10
1.3 CALIBRATION AND VALIDATION (CAL/VAL) ASSESSMENT.....	11
1.3.1 <i>Prelaunch Assessment</i> .....	11
1.3.2 <i>Postlaunch Development</i> .....	11
1.3.3 <i>Striping and Scan Angle Effects</i> .....	13
<b>2. SCIENCE TEAM ASSESSMENT EFFORTS</b> .....	<b>16</b>
2.1 OVERVIEW OF TEAM ACTIVITIES .....	16
2.2 OCEAN PEATE SUPPORT .....	16
2.3 DATA COLLECTION .....	20
2.3.1 <i>Bigelow Laboratory for Ocean Sciences: Balch Laboratory</i> .....	21
2.3.2 <i>Plumes and Blooms – Siegel (UC Santa Barbara)</i> .....	26
2.3.3 <i>SIMBADA measurements – Frouin (Scripps Institute of Oceanography)</i> .....	29
2.4 ALGORITHM DEVELOPMENT .....	31
2.4.1 <i>Diffuse Attenuation Coefficient at 490 nm (<math>K_d(490)</math>)</i> .....	31
2.4.2 <i>Particulate Inorganic Carbon (PIC)</i> .....	32
2.4.3 <i>Estimate Photosynthetically Available Radiation (PAR)</i> .....	35
2.4.4 <i>Chlorophyll concentrations and Inherent Optical Properties</i> .....	43

---

2.4.5 Early Results from the SWIR Method of Atmospheric Correction .....	44
2.4.6 Assimilating Global Ocean Chlorophyll from Suomi NPP-VIIRS: Prospects for Extending the Ocean Color Time Series .....	46
2.5 PRODUCT EVALUATION .....	51
2.5.1 NOAA Effort .....	51
2.5.2 NASA Effort .....	67
<b>3. CONCLUSIONS.....</b>	<b>82</b>
<b>4. RECOMMENDATIONS.....</b>	<b>86</b>
<b>RESULTING PAPERS – 2011-PRESENT.....</b>	<b>87</b>
<b>REFERENCES.....</b>	<b>88</b>
<b>ACRONYMS.....</b>	<b>92</b>

---

## EXECUTIVE SUMMARY

---

**Overview** – This document reports the NASA science team assessment of the VIIRS instrument and the quality of ocean color data that it can produce. As with any past ocean color mission, the quality of the ocean color data depends on a detailed understanding of the sensor, on the on-going refinement of calibration, and algorithm employed to extract ocean surface reflectance values from radiometric measurements made at the top of the atmosphere. **It can be concluded, based on the first year of data, that VIIRS is currently capable of producing high-quality data products that are comparable to heritage NASA ocean color missions, and exceed the quality of those missions at their first year mark. Conversely, the data being produced operationally by the Integrated Data Processing Segment (IDPS) did not realize this potential.**

**Objectives** – The science team had two primary goals: 1) to evaluate the NOAA ocean color Environmental Data Record (EDR) to determine whether it would support continuity of the establish NASA ocean color data record and 2) to determine whether VIIRS could support the development of new algorithms, including those that could generate data products that were originally part of the NASA data record, but were not supported by the S-NPP operational processing stream. Furthermore, the science team also considered whether calibrated radiometry from the VIIRS sensor could support NASA's data continuity objectives to generate a continuous NASA data record.

**Sensor Performance** – The story of the prelaunch assessment is described in detail in Section 1.1, including continued challenges with trending the instrument response. However, the overall performance of VIIRS instrument on orbit is good, and so the sensor appears potentially useful for the generation of number of heritage ocean color data products. **However, the quality of the VIIRS evaluation data products at their one-year anniversary appears better than the quality for corresponding products from the SeaWiFS and MODIS missions at their first anniversary.** This can be attributed to the solid performance of the instrument; the well-seasoned experience of the science team and Ocean PEATE; and the unprecedentedly extensive knowledge gained about the instrument characteristics prior to launch. In addition, the combined engineering resources available across NASA and NOAA to resolve VIIRS instrument anomalies are also much greater than heritage.

**Calibration Assessment** – As with heritage ocean color missions at this stage, some additional work will be needed to bring VIIRS calibration quality to heritage levels. Calibration will continue to be refined as more lunar and calibration buoy data is collected. The calibration system artifacts will need to be investigated and the effects of changing OOB response will need to be quantified and corrected. Corrections for residual striping and scan effects should be applied to bring VIIRS quality in line with MODIS Aqua, as described in Section 1.3.2. Also, the decreasing signal-to-noise ratio for the NIR bands will need to be monitored to be sure that they do not require further mitigation to boost the signal (e.g., pixel aggregation). However, techniques to address all of these tasks already exist and are straightforward because of the experience afforded by previous missions. Thus, a consistent calibration of VIIRS can be achieved, provided regular lunar calibrations are maintained. Likewise, heritage missions (e.g.,

---

SeaWiFS and MODIS) took two to three years for the calibration teams to fully understand and de-trend solar calibrator data; to collect sufficient data for vicarious calibration; and to accumulate sufficient lunar measurements to fully trend long-term trends in the instrument response.

**Prelaunch Processing Assessment** – The prelaunch evaluation identified major issues with the operational system that confuted the premise that the Ocean Color EDR would support NASA science objectives. First, the NOAA operational algorithms for VIIRS are inconsistent with those used to generate the current NASA data record. For instance, they lack a NIR correction in the EDR algorithm, which causes significant differences in chlorophyll *a* concentration in productive or turbid waters. Second, the lack of a mission-level reprocessing capability precludes the generation of a consistent data record. For instance, changes or updates to the calibration, implementation of a vicarious calibration, or making needed updates to algorithms, masks, and flags will only improve the record for the future; the standing record will always hold artifacts, some of which are significant. **Therefore, the operational NOAA ocean color EDR cannot meet NASA continuity objectives.**

**Postlaunch Data Assessment** – Postlaunch data analysis further supports the prelaunch conclusion regarding the EDR data quality. This is plainly illustrated in Fig. 1 for chlorophyll *a* concentration, which is the only derived product in the EDR suite that corresponds to a standard product in the NASA data record. Fig. 2 puts this comparison in context with the NASA ocean color data record, based on observations using the Sea-viewing Wide Field of view Sensor (SeaWiFS) and the MODerate resolution Imaging Spectroradiometer (MODIS) aboard the EOS satellite Aqua. Deep-water averages of monthly composites shown Fig. 2 are not based on common bins, but any the difference between these monthly curves and the 8-day common bin averages were found to be much smaller than the deviation of the EDR. This is expected given that the monthly composites have fuller global sampling, and so coverage gaps have less influence the signal. Therefore, the synoptic averages of the EDR chlorophyll *a* product deviate significantly from the NASA data record spanning 15 years.

**Sea Truth Validation (Radiometry)** – The VIIRS surface radiometry for both the EDR and NASA evaluation products showed good agreement with *in situ* data from fixed stations of the AERosol ROBotic NETwork – Ocean Color (AERONET-OC) (Zibordi et al., 2009). Similar results were observed at sea by Balch, but the biases were larger for most of the bands. However, that analysis involved a sample size at least one order of magnitude smaller and the corresponding regression analysis could be more subject to noise associated with ship measurements (related to viewing geometry, pitch and role of the ship, etc.). The good agreement between satellite and *in situ* surface radiometry seems counterintuitive when considering the poor performance of the EDR chlorophyll *a* deep-water time series. However, the slope confidence intervals for the regressions statistics indicate that there is sufficient uncertainty in the comparison between satellite and surface data to allow for large enough biases to adversely affect one or both products (in this case, only the EDR appears to be affected). Closer investigation of the EDR surface reflectance (i.e.,  $nL_w$ ) indicates that the EDR blue bands are low and the EDR green band is high, relative to the NASA evaluation product. Improvement in EDR chlorophyll should come with vicarious calibration of the operational product.

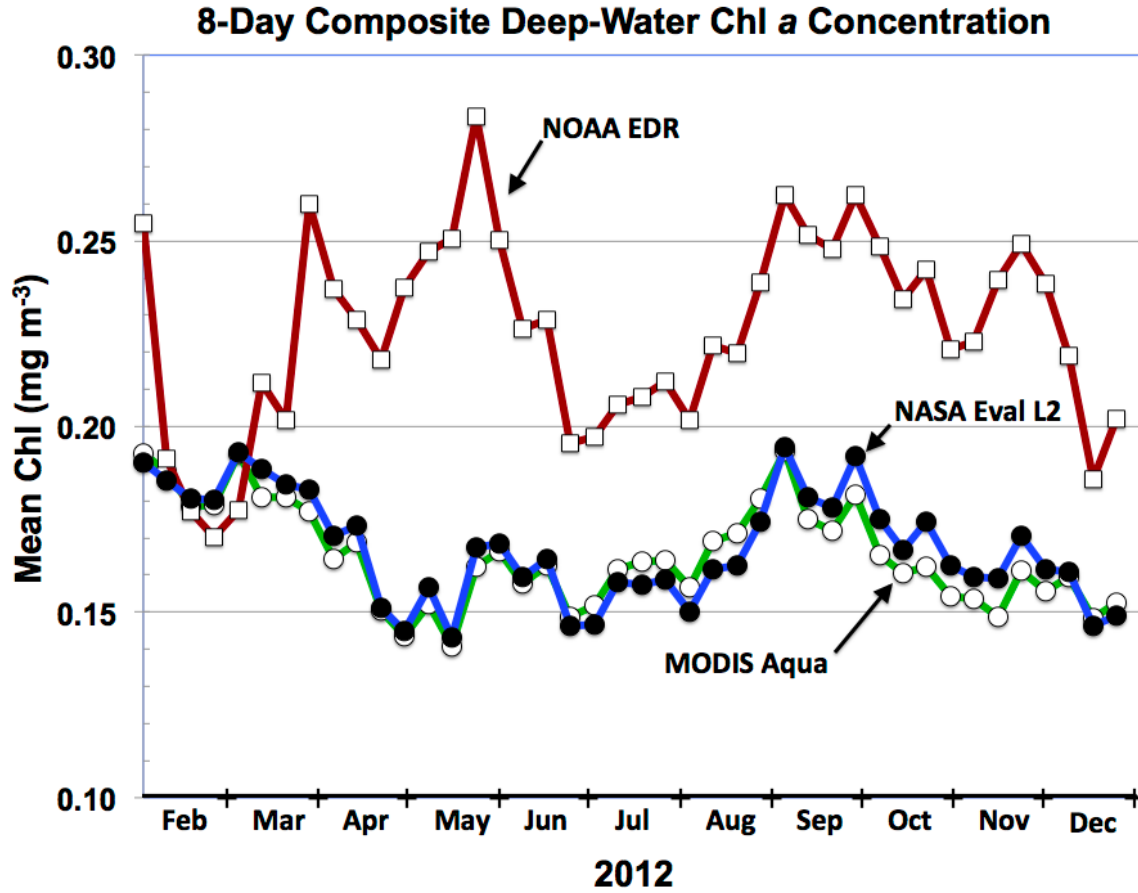


Fig. 1: Chlorophyll Mean Time Series since start of EDR production. 8-day composites of chlorophyll *a* concentration composites were averaged over waters with depth > 1000 m. The red curve is from the NOAA EDR using VIIRS data. The blue curve is from the NASA VIIRS evaluation product, while the green curve is from MODIS Aqua data.

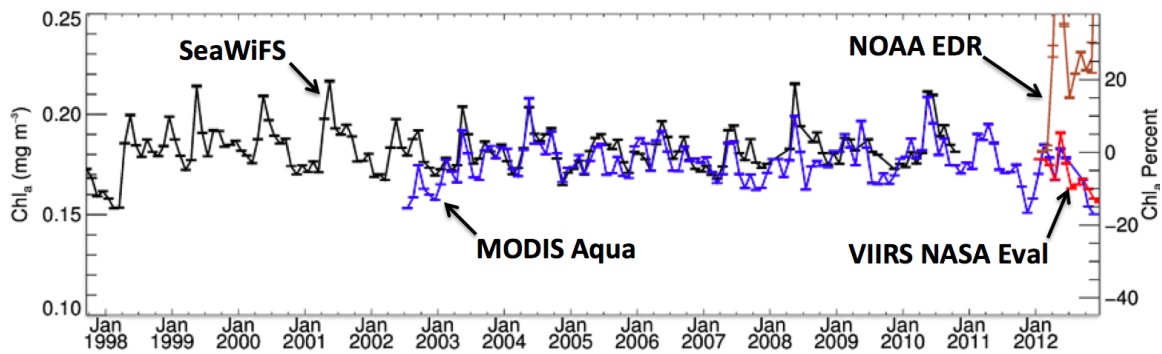


Fig. 2: Comparison with Deep-Water Chlorophyll *a* long-term time series. The black curve covers the 13 years of the SeaWiFS mission and the blue does likewise for MODIS Aqua. Both SeaWiFS and MODIS Aqua Deep-Water Chlorophyll averages are comparable. Likewise, the red curve shows the NASA evaluation Chlorophyll *a* average, which agrees well with MODIS Aqua. Conversely, the brown curve representing the NOAA EDR clearly deviates from the current NASA data records. Averages are not based on common bins, but the difference between these monthly curves and the 8-day common bin averages were found to be much smaller than the deviation of the EDR (Plot courtesy of B. Franz).

---

**Sea Truth Validation (Chlorophyll *a*)** – Comparison between chlorophyll *a* concentration estimates from the satellite with estimate from *in situ* data were limited. Protocols of the SeaWiFS Bio-optical Archive and Storage System (SeaBASS) (Werdell and Bailey, 2005) eliminated all but ten data pairs (all from the Great Belt II cruise), so no meaningful statistical analysis could be done. Field comparisons by Balch showed reasonable matches between fluorometric chlorophyll *a* concentration and the NASA evaluation product (within the known algorithm uncertainty of a factor of two). Siegel also made comparisons between fluorometric chlorophyll *a* concentration taken as part of Plumes and Blooms, but these showed modest, but significant correlation. Similar results arose when the same analysis was applied to MODIS and SeaWiFS. These smaller correlations likely stem from the fact that the region where Plumes and Blooms measurements were taken is particularly challenging for spaceborne remote sensing instruments with limited spatial and spectral resolution.

**Data Collection Strategies** – The amount of *in situ* data available after one year for this analysis was limited. Additional data are expected to be archived into SeaBASS over the next year (PI's have up to one year to deliver data to this archive per NASA policy). Also, per NASA policy, all High-Performance Liquid Chromatography (HPLC) chlorophyll *a* measurements must be performed at a common NASA laboratory to maintain consistency. This necessary approach slows the process for making data available for validation analysis. Furthermore, once all the SeaBASS protocols are applied for matching satellite and *in situ* data, only a small fraction of the collected data remain. However, despite the lack of available chlorophyll *a* data, AERONET-OC stations provided continuous radiometric measurements through most of the year, producing a far greater sample of that parameter than can affordably be collected shipboard during that period. This is not to say that we should not have cruises, because only cruises can target specific regions, e.g., away from terrestrial sources of pollution and continental dust. However, implementation of new strategies, e.g., advanced buoys or gliders that can take a suite of measurements, could cover much more ground at a lower cost. Also, increasing data sharing with domestic and international sources could expand the available data. For instance, further analysis of the VIIRS EDR and NASA evaluation products could include data from the European data collection activity called the Bouée pour l'acquisition de Séries Optiques à Long Terme (BOUSSOLE), including chlorophyll data. New strategies need to be considered to expand the data available for validation and while minimizing cost.

**Validation Challenges** – Another aspect about *in situ* validation was raised by the fact that despite the hundreds of radiometric measurements now available through AERONET-OC, the regression uncertainty was too large to capture significant biases that would have directly explained the poor performance of the chlorophyll *a* algorithm. This is indicative that there are other challenges regarding data collection and analysis that should be addressed. Naturally, there are many sources of uncertainty that can arise when taking measurements at sea and methods to address these are being, and should be, developed. In addition, there is the so-called “scale issue,” in which spurious variation is introduced by matching point measurements with a kilometer-scale satellite pixels. Further work is needed to reduce these sources of uncertainty in the comparison with the *in situ* data.

**New Algorithm Development** – Evaluation of new algorithms further supported the potential of VIIRS to meet data continuity objectives and possibly the development of novel

---

applications. The heritage algorithms, PIC and PAR, were successfully implemented in the NASA evaluation processing stream and appeared to perform well, relative to MODIS and sea truth. The comparisons between VIIRS-derived PIC and chlorophyll estimates are remarkably close to those achieved with MODIS Aqua. The PAR product showed comparable, but slightly higher values with compared to MODIS Aqua and to *in situ* data. This may improve with further refinement of the VIIRS calibration. The experimental algorithm for estimating chlorophyll *a* using the GSM semi-analytic ocean color model demonstrated similar performance for the Plumes and Blooms data for VIIRS, MODIS, and SeaWiFS. Use of the VIIRS SWIR bands to improve atmospheric correction over coastal waters shows promise. A potential challenge facing this algorithm is the proper calibration the SWIR bands. Like the NIR bands, the responsivity of the SWIR bands is also degrading because of prelaunch mirror contamination. Unlike the IR bands, the SWIR bands were not turned on until mid-January, several weeks after the nadir doors of the spacecraft were opened and the degradation began. Therefore, it is difficult to determine much these bands degraded from their prelaunch calibration responses to the point when they were activated. Fortunately, the SWIR algorithm investigated by Wang and his team consider the ratio of two SWIR bands and the same-sign calibration biases in those bands will tend to cancel. Finally, application of data assimilation techniques with a bias correction produces a VIIRS L3 time series of chlorophyll *a* concentration that is more consistent with MODIS Aqua. The technique also provides a method to remove the spurious signal introduced into the climate record by data gaps on regional and global scales.

#### **Recommendations for Ocean Color Data Continuity using VIIRS**

**REPROCESSING** – A mission-level ocean color reprocessing capability should be available for application throughout the mission, as with heritage missions. Moreover, reprocessing should be able to span the multiple sensors of NASA data record to facilitate algorithm updates.

**VIIRS CALIBRATION SUPPORT** – An ocean color-focused calibration should continue for at least the first two to three years, which barring late mission anomalies, is likely a minimum period necessary to bring VIIRS data to NASA data record quality.

**ALGORITHM CONTINUITY AND CONSISTENCY** – Heritage atmosphere correction algorithms should be used to maintain continuity with the NASA ocean color data record. Furthermore, EOS products without an EDR equivalent should be generated (e.g., PIC, PAR, and  $K_d(490)$ ).

**NEW ALGORITHM DEVELOPMENT** – VIIRS is of sufficient quality to be used as an opportunity for the development of new algorithms and remote sensing techniques.

**VALIDATION DATA** – New data collection and validation strategies should be developed for more effective validation and data analyses. These include the following example areas:

- Top-level planning for collection of data over a wide diversity of environments;
- Technology or techniques to increase sample size or reduce noise for *in situ* data;
- Strategies to address differences in scale between satellite and *in situ* data;
- Expanded domestic and international collaboration in data collection.

---

## 1. INTRODUCTION

---

Ocean color remote sensing is the only method by which we can monitor and observe the global ocean and aquatic biosphere with a passive sensor. Using information gleaned from a few wavelengths provide information on biological parameters such as the concentration of phytoplankton pigment or inorganic carbon. These parameters that were derived from ocean radiometry, provide vital information regarding primary production of carbon and input to higher trophic levels, which have research applications such as large-scale modeling biogeochemical cycles and their response to climate change; the influence of phytoplankton growth (including harmful algal blooms) on water quality, ecosystem health, and fisheries and their subsequent affect to societal needs; the prediction of water clarity for naval applications; and the influence of biological activity in the upper layers of the ocean on cloud formation, sea surface temperature, and possibly even severe storm tracks.

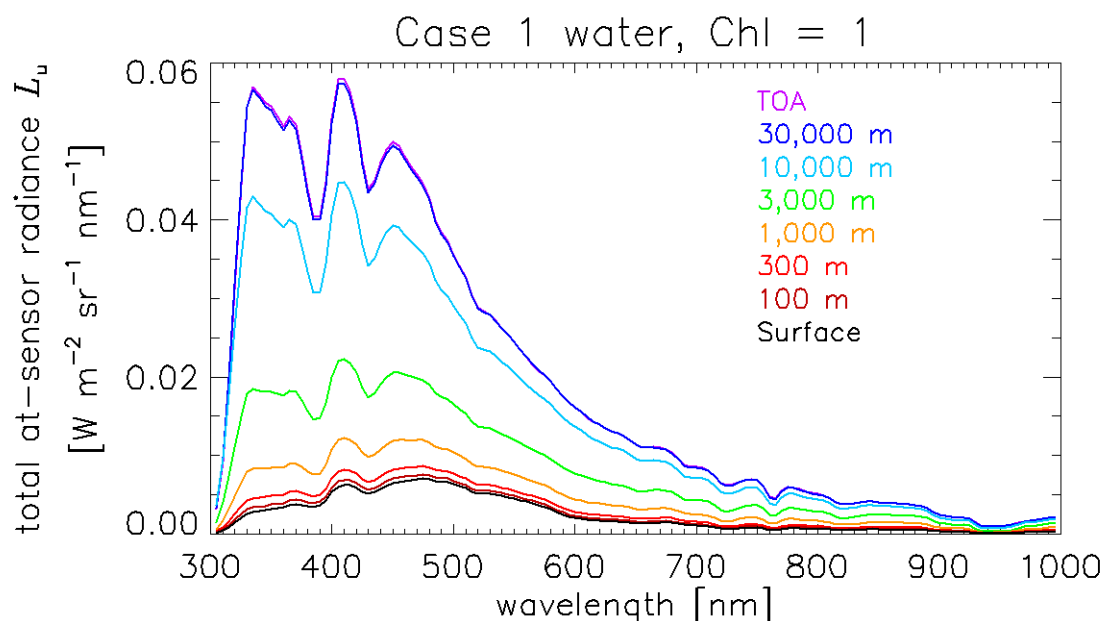


Fig. 3: Comparison of ocean spectrum at the surface and with atmosphere contributions. The black curve is the spectrum for a relatively clear, open ocean. The same ocean at increasing altitudes up to the top of the atmosphere (TOA) is shown, with the top-of-atmosphere in purple. The TOA is what is measured by VIIRS and the surface is what needs to be recovered. Figure from Mobley (2013).

However, retrieval of surface reflectance is a challenging measurement, which requires careful consideration of instrument effects and calibration. Typically, more than 85% of the visible light reaching a spaceborne sensor comes from the atmosphere, as shown in Fig. 3. It is therefore necessary, but not sufficient, to remove this additional signal using modeling of atmospheric and instrumental effects. For this isolation of the ocean signal to work, however, the radiometric measurement must be highly accurate, otherwise, any residual measurements would overwhelm the tiny ocean signal. An error in calibration of the top-of-atmosphere radiance can lead to an error in surface reflectance that is an order of magnitude larger. Over

---

the past two decades of research, NASA-funded investigators developed and fine-tuned techniques to predict the atmospheric contribution, to refine the instrument calibration to a fraction of a percent, and to identify and remove instrument artifacts.

This document reports the NASA science team assessment of the VIIRS instrument and the quality of ocean color data that it can produce. As with any past ocean color mission, the quality of the ocean color data depends on a detailed understanding of the sensor, an ongoing refinement of calibration, and algorithm employed to extract ocean surface reflectance values from radiometric measurements made at the top of the atmosphere. **It can be concluded, based on the first year of data, that VIIRS is currently capable of producing high-quality data products that are comparable to heritage NASA ocean color missions, and exceed the quality of those missions at their first year mark. Conversely, the data being produced operationally by the Integrated Data Processing Segment (IDPS) did not meet this potential.**

## 1.1 BACKGROUND

---

On 28 October 2011, NASA launched the Visible Infrared Imaging Radiometer Suite (VIIRS) aboard the Suomi National Polar-orbiting Partnership (NPP) spacecraft. VIIRS is being used by NOAA to routinely generate measurements of the Earth's surface and atmosphere, which are referred to as Environment Data Records (EDR). The ocean color EDR includes normalized water-leaving radiance ( $nL_w$ ), inherent optical properties (absorption and particle backscatter,  $a$  and  $b_{bp}$  respectively, at five wavelengths) based on an algorithm developed by Carder et al. (1999), and chlorophyll  $a$  concentration using the three-channel version of the empirical algorithm developed by O'Reilly et al. (1998). In the months that followed the launch, the NASA Science Team began evaluating ocean color data products. Their task was to determine whether the NOAA ocean color EDR products would meet NASA science objectives, including continuing the existing climate data record (CDR) established with earlier NASA missions. Their efforts focused primarily on the surface radiance quantities (e.g.,  $nL_w$ ) and chlorophyll  $a$  concentration, as only these were considered part of the standard NASA CDR. Absorption and backscatter are still considered largely experimental, and determining their quality for any mission is still a subject of research.

Before the NPP launch, the science team argued that the NOAA EDR products could not support continuity of the existing NASA ocean color CDR because they were based on outdated algorithms and, perhaps more importantly, because of the lack of support for reprocessing. Both situations would lead to inconsistencies in the continued CDR. To quantify this inconsistency, the science team faced the challenge of developing an independent evaluation data production capability that both used NASA selected algorithms and supported reprocessing. Generation of an independent NASA VIIRS evaluation product for ocean color also had the additional benefit of answering the question as to whether the raw flight data from VIIRS would meet NASA science objectives (i.e., was the instrument performing sufficiently to support NASA ocean color continuity). That effort included development of an independent calibration strategy and leveraged existing processing capabilities at NASA's Goddard Space Flight Center (GSFC) that already supported heritage ocean color data production. Using those resources, NOAA operational ocean color products were compared to products generated by this independent research processing system and data from other sensors. This constructive analysis, led by

---

Turpie and McClain at GSFC, also included comparisons to surface measurements and the MODerate resolution Imaging Spectroradiometer (MODIS) aboard the Aqua satellite. Meanwhile, a parallel evaluation conducted by Wang and his team at NOAA focus directly on the operational data product quality relative to surface measurements and ocean color data from, but also included comparisons to research NOAA algorithms similar to those employed by NASA. It is worth noting that these slightly different approaches were largely independent, only occasionally exchanging information at NASA and NOAA science team meetings, yet they drew largely the same conclusions regarding the EDR quality and the potential of VIIRS to support ocean color continuity.

Other members of the science team were also tasked with collecting data for product validation. These surface measurements were taken under a broad range of conditions, but in many cases focused on targets specific to algorithm development. Nonetheless, these investigators report direct comparisons between *in situ* measurements with VIIR data. Some of that data has not yet been processed and archived into the SeaWiFS Bio-optical Archive and Storage System (SeaBASS) (Werdell and Bailey, 2005). Furthermore, conditions under which many of these measurements were taken do not meet the rather stringent protocols established in the SeaBASS system for matching surface with satellite data. Thus, only a limited set of surface data collected by the science team was available at this time to perform a rigorous comparison between *in situ* data and VIIRS data products. However, both Turpie and Wang did make extensive comparisons to radiometric data that were available in SeaBASS from the AEROSOL ROBOTIC NETWORK – OCEAN COLOR (AERONET-OC) (Zibordi et al., 2009).

Some science team members undertook the development of additional algorithms that could potentially be used with VIIRS. Consideration of data products that were originally supported by NASA heritage missions, but not by NPP, included an estimate of Particulate Inorganic Carbon (PIC) by Balch, Diffuse Attenuation Coefficient at 490 nm (Kd(490)) by Wang, and an estimate of Photosynthetically Available Radiation (PAR), by Frouin. Experimental algorithms were also explored. Gregg investigated a novel application that looked to improve the consistency of the chlorophyll *a* record using data assimilation, while Wang looked at the potential of improving atmospheric correction over coastal regions using VIIRS shortwave infrared (SWIR) bands. Siegel compared performance of the Garver, Siegel, Maritorea (GSM) semi-analytic model for VIIRS and MODIS in optically complex waters.

## **1.2 ASSESSMENT OF INSTRUMENT PERFORMANCE**

---

### **1.2.1 PRELAUNCH ASSESSMENT**

---

Although the launch of Suomi NPP was picture perfect, the prelaunch preparation of the VIIRS sensor met many challenges and delays. Thanks to the dedicated work of many engineers and analysts, most of the challenges with the sensor were met. By the end of 2009, extensive prelaunch sensor testing indicated that no known significant problems remained that would prevent VIIRS from potentially carrying on the ocean color legacy established with the SeaWiFS and the MODIS (Turpie et al., 2011).

---

Extensive characterization testing of the VIIRS instrument was carried out in the last half of 2009 and extensive observatory-level testing that was carried out by NIST early in 2010. An assessment of potential risks to ocean color quality was done based on this prelaunch knowledge of the instrument and an examination of ground system capabilities. A significant instrument issue at the time was the presence of optical communication between bands via the spectral filter array, a phenomenon also known as *optical crosstalk*. What was learned from the characterization data, and later reported, was that the effects of optical crosstalk were markedly smaller than expected from earlier experiments with the engineering design unit and subsequent bench tests with the flight unit integrated filter array (2005-2008). The remaining issues were whether the residual effects were small enough to no longer be of concern and whether the uncertainty in their characterization was also small enough to form a confident assessment of their influence.

Review of the Raytheon Performance Verification Reports (PVR) for the spectral characterization of the VIIRS instrument indicated the uncertainty determination was sufficiently thorough and robust (Raytheon, 2009a, b), and that the predicted uncertainty was sufficiently small to perform credible assessments of the affects to ocean color EDR quality. To assess those potential ramifications, characterization data were incorporated in to the VIIRS Data Simulator (Robinson et al., 2009), which was designed to simulate various instrument effects. Over most of the ocean, the results showed that small effects would be present in water-leaving radiances and that the expected effect would be minimal to chlorophyll *a* concentration, with coastal waters being a possible exception if the effects were left uncorrected (Robinson et al., 2009). Furthermore, sending bands were generally adjacent on the focal plane to bands receiving crosstalk, and thus the spatial effects of optical crosstalk was found to be usually only one to three samples distant. This was confirmed after launch through examination of lunar images taken with VIIRS, which showed no noticeable image ghosting that would result from crosstalk spatial effects. Therefore, this helped confirm that the suggested mitigation to optical crosstalk effects should be applied in the evaluation products generated using NASA algorithms, which was to simply fold the crosstalk spectral effects into the existing correction for other out-of-band response effects into the atmospheric correction algorithm.

As a tradeoff with optical crosstalk, large out-of-band light leaks were observed in the instrument spectral response during testing. Most notable was a 1% bias in the radiometric response for the 410 nm band stemming from NIR wavelengths when observing a solar spectrum and about a 4% bias for the 551 nm band stemming from the blue side of the corresponding band pass. The magnitude of these effects did not exceed that of light leaks associated with the SeaWiFS and MODIS sensors. Although these effects were manifested differently in VIIRS, the belief was that the same correction methodology used for those instruments would be as effective.

The strategy to address both optical crosstalk and out-of-band light leaks was to incorporate the total-band response for each band into the atmospheric correction tables. That response characteristic was represented by the relative spectral response (RSR) curves derived from instrument characterization testing. In 2011, the NPP/JPSS project made RSR curves available that were derived from both the thermal/vacuum test data and NIST observatory-level

---

test data using the Spectral Irradiance and radiance Responsivity Calibrations using Uniform Sources (SIRCUS) system (Brown et al., 2006). Because this test involved flooding the entire focal plane with monochromatic light, the results included the spectral effects of crosstalk. These hybrid RSR curves were used to generate new ocean color atmospheric correction tables late in 2011, and are now being used in the NASA evaluation data processing software, as they are similarly applied in the operational processing of the EDR products.

---

### 1.2.2 POSTLAUNCH ASSESSMENT

---

After launch, it was clear from calibration system measurements that the instrument's response to light was decreasing more rapidly than expected in the 671 nm, 748 nm, and 865 nm channels. NASA assembled a special engineering team, which carefully evaluated the instrument behavior and traced the problem to tungsten oxide contamination of four of the telescope mirrors during their manufacture. It was further determined that this contamination also affected the 1240nm, 1380nm, and 1610nm channels, which had not yet been activated. Tungsten oxide is a photoactive substance that when exposed to UV radiation causes VIIRS to become increasingly less sensitive in the six aforementioned VisNIR and SWIR channels.

It was further found that the Solar Diffuser Stability Monitor (SDSM) detectors were also degrading at similar wavelengths, but project engineers noted that this was an independent phenomenon. In addition, close examination of the Solar Diffuser reflectance using data from the SDSM revealed that the reference panel was yellowing at a unprecedented rate; probably because the calibrator aperture was designed without a cover and open in the ram direction of the spacecraft. To further understand these effects, considerable data are being analyzed and their overall affect on ocean color data products will be monitored.

Fortunately, it appears that the instrument response degradation can be accurately monitored and it is expected to eventually level off so that useful measurements can continue to be made. If the response were to continue to decrease in the NIR channels, alternative methods can be employed that would boost the signal. In the mean time, the red and NIR channel responses are being monitored using the on-board solar calibration system and lunar calibration. The SWIR channels, conversely, had degraded significantly before they had been turned on, hence making it difficult to relate their current response to prelaunch calibration. Further monitoring and evaluation of the SDSM data will be needed to determine whether the degradation of its component pose a risk to future calibration of VIIRS. In addition, it was realized that changes in the instrument response at NIR wavelength changed the characteristics of the out-of-band spectral response of the instrument. For instance, much of the out-of-band (OOB) light leak in the 410 nm band occurs in the NIR, thus that additional signal is decreasing with time. When viewing the top of the atmosphere over the ocean, there is very little effect to begin with because the NIR signal, relative to radiance at blue wavelengths, is very small. However, when viewing the solar reference, the effect is much larger. Therefore, a small spurious trend is introduced in the calibration, which will require some further investigation for both solar and lunar calibration measurements. This effect is less relevant in the other visible ocean bands. However, the NIR bands may be affected by the fact that their in-band responsivity is decreasing while the OOB signal in the blue, although measured prelaunch to be very small, will be increasing significantly.

---

## 1.3 CALIBRATION AND VALIDATION (CAL/VAL) ASSESSMENT

---

### 1.3.1 PRELAUNCH ASSESSMENT

---

The operational calibration of the VIIRS instrument was reviewed in two aspects. First, the calibration algorithm theoretical basis document, the calibration plan, and the operational code used to perform the count-to-radiance conversion were carefully reviewed prior to launch. A white paper was written to summarize the entire radiometric calibration process for the reflective solar bands and to identify gaps in the process that would undermine its ability to produce data products capable of meeting NASA science objectives (Eplee, 2011b). The white paper also noted a few inefficient steps in the operational algorithm. A follow up report was provided to recommend improvements to the calibration code, including addressing significant inefficiencies (Eplee, 2011a). These reports were submitted to the NASA S-NPP project scientist and, as a courtesy, forwarded to the NOAA calibration team lead. Furthermore, an improved calibration plan outline, which identified gaps in the operational calibration plan, was also drafted and shared with the project office and NOAA.

### 1.3.2 POSTLAUNCH DEVELOPMENT

---

To further support the evaluation of NPP VIIRS ocean color capabilities, an independent calibration capability was created and supported by the Ocean Product Evaluation and Analysis Tools Element (PEATE). This provided an opportunity to independently validate the operational calibration process. More importantly, this development, along with time-dependent processing of raw data records (RDR) for the sensor, facilitated a reprocessing capability that is not available in the operational processing stream and critical to producing a consistent data record. The ocean team and the NASA VIIRS Characterization Support Team (VCST) formed a joint working group for radiometric calibration of the reflective solar bands. Findings and experiences related to this independent effort were shared with VCST, and the latter provided an updated SDSM transmittance table derived from the yaw calibration maneuvers. Preparation for the lunar calibration roll maneuvers was also done collaboratively with VCST and the mission operations team. The ocean team also collaborated with NASA Science Team member, Tom Stone (USGS), in the application of the RObotic Lunar Observatory (ROLO) model. Comparison of lunar measurements to the calibration being done using the solar diffuser were shown to be in very good agreement with a residual less than 0.5%. Relative differences between the NPP science team and VCST lunar trends also were found to be within 0.5%.

Currently the lunar measurements performed for the VIIRS evaluation are showing very close agreement with evaluation solar trending of changing in instrument response. The solar and lunar trends for green, red and NIR bands (551 nm, 671 nm, 748 nm, and 865 nm, respectively) are in agreement to 0.5%. However, there is a wavelength dependent discrepancy between the solar and lunar measurements that is up to 2% for the blue bands, the worst case being at 410 nm. This discrepancy worsens over the middle to latter part of 2012, but reduces as the year closes. The effect has also been observed by the NOAA operational calibration team and VCST, and is currently under investigation. Furthermore, there appears to be a residual

fluctuation of a few fractions of a percent in these bands from the expected monotonic decay of reflectance in these bands that has been traced to artifacts in the calibrator. However, although these issues are being pursued, we are reassured that heritage mission lunar measurements often fluctuated over the year on the order of a percent, and effect that is reduced over time, and the artifacts observed in the solar trend are relatively small and appear to be periodic and correctable. So, although more should be done to improve the instrument calibration, the status is quite good compared to heritage missions after their first year.

Fig. 4 shows a comparison of the evaluation and operational solar trending of the VIIRS instrument response with time during 2012. What is apparent is that the operational calibration was not started until about 6 February, after which the trending was erratic for months, eventually stabilizing. The slight rise about three quarters of the way through the year is from the aforementioned calibrator artifact, which has been removed from the evaluation trending. It is expected that the operational calibration will continue to be refined and will likely converge at some point in the future with the evaluation trending, which is also improving. However, those improvements will never be realized across the entire record without reprocessing. Thus the evaluation trending demonstrates a superior approach for CDR production.

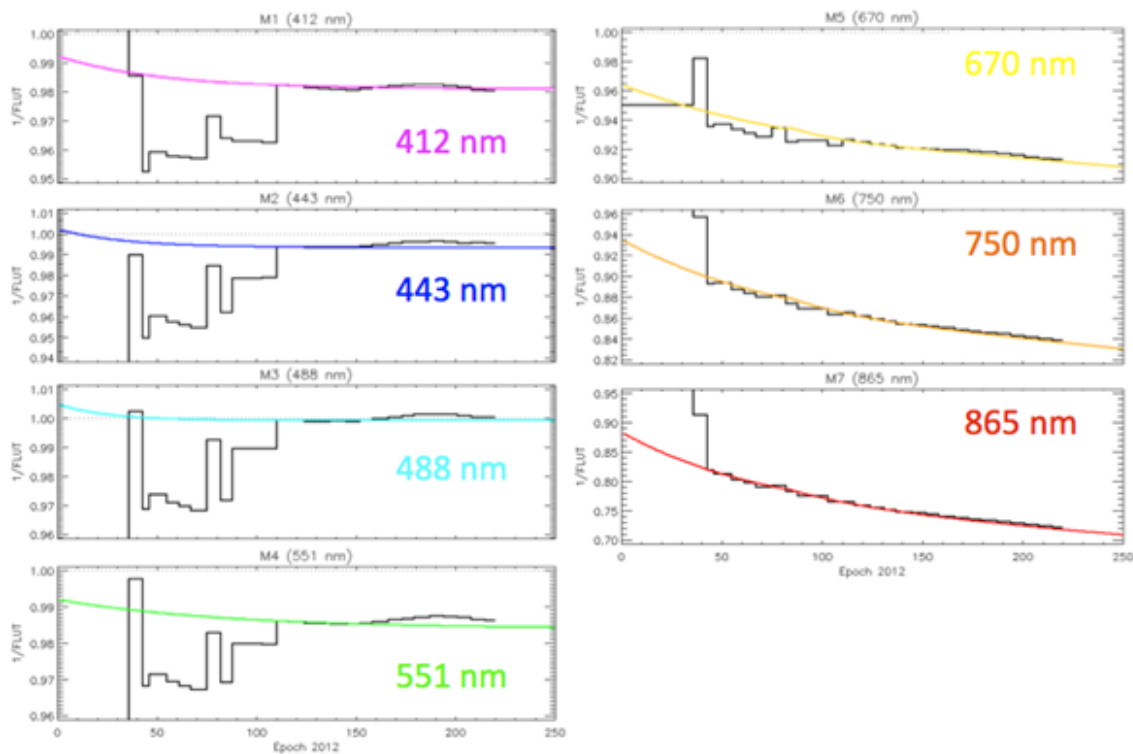


Fig. 4: Comparison of operational calibration and evaluation calibration solar trending of VIIRS responsivity for 2012. The black shows the gains used in the operational processing stream as a function of time, while the colored curves show the evaluation instrument trending for the corresponding band. The operational trends are normalized to the evaluation trends for comparison (Plots courtesy Gwyn Fireman, OBPG).

---

### 1.3.3 STRIPING AND SCAN ANGLE EFFECTS

---

Systematic variation across focal plane detectors, between the VIIRS rotating telescope half-angle mirror sides, or across scan were evaluated on orbit. Looking at the relatively uniform solar reference panel, significantly large variations were observed across detectors in some bands and also between mirror sides for others. These variations are attributed to systematic biases in the prelaunch laboratory calibration of VIIRS. Using techniques developed for MODIS, reference panel measurements were used to remove these variations. Because the operational calibration team applies an absolute calibration using the solar diffuser, these effects are also removed from the operational product. After this first-order removal of striping from the sensor, top-of-atmosphere radiance measurements were compared between the operational product from the IDPS and the NASA evaluation product. Both products showed comparable reductions in detector-to-detector and mirror side striping.

A technique had been developed for MODIS in which Level 2 (L2) surface reflectance was compared against Level 3 (L3) global composite maps. Statistics of the differences between the L2 granules and L3 maps were stratified by scan angle, detector, and mirror side to isolate any trends. Trends showed a significant residual striping effect in VIIRS surface reflectance, but no significant mirror side differences remained. Results of this analysis are shown for the three bands used to produce chlorophyll a product in Fig. 5. For comparison, the same analysis was applied to MODIS Aqua and the corresponding results are shown in Fig. 6. It is suspected that these residual striping effects made be from a mechanism that is spectrally dependent because they appear when viewing the ocean but not the solar spectrum of the calibrator, but further evaluation is needed. The variation in surface reflectance across detectors is larger than what is currently seen for MODIS, and thus this will need to be remedied. MODIS striping was removed using a statistical approach and this technique can also be applied to VIIRS also.

To a lesser degree, some systematic variation with scan angle is also noticeable in surface reflectance, but to a lesser degree. This trend with scan angle becomes significant in some bands, but mostly at scan angles too large to be useful for production of high quality data anyway. A correction was developed for MODIS to remove a similar systematic, scan-angle dependent effect and the same correction can also be applied to VIIRS.

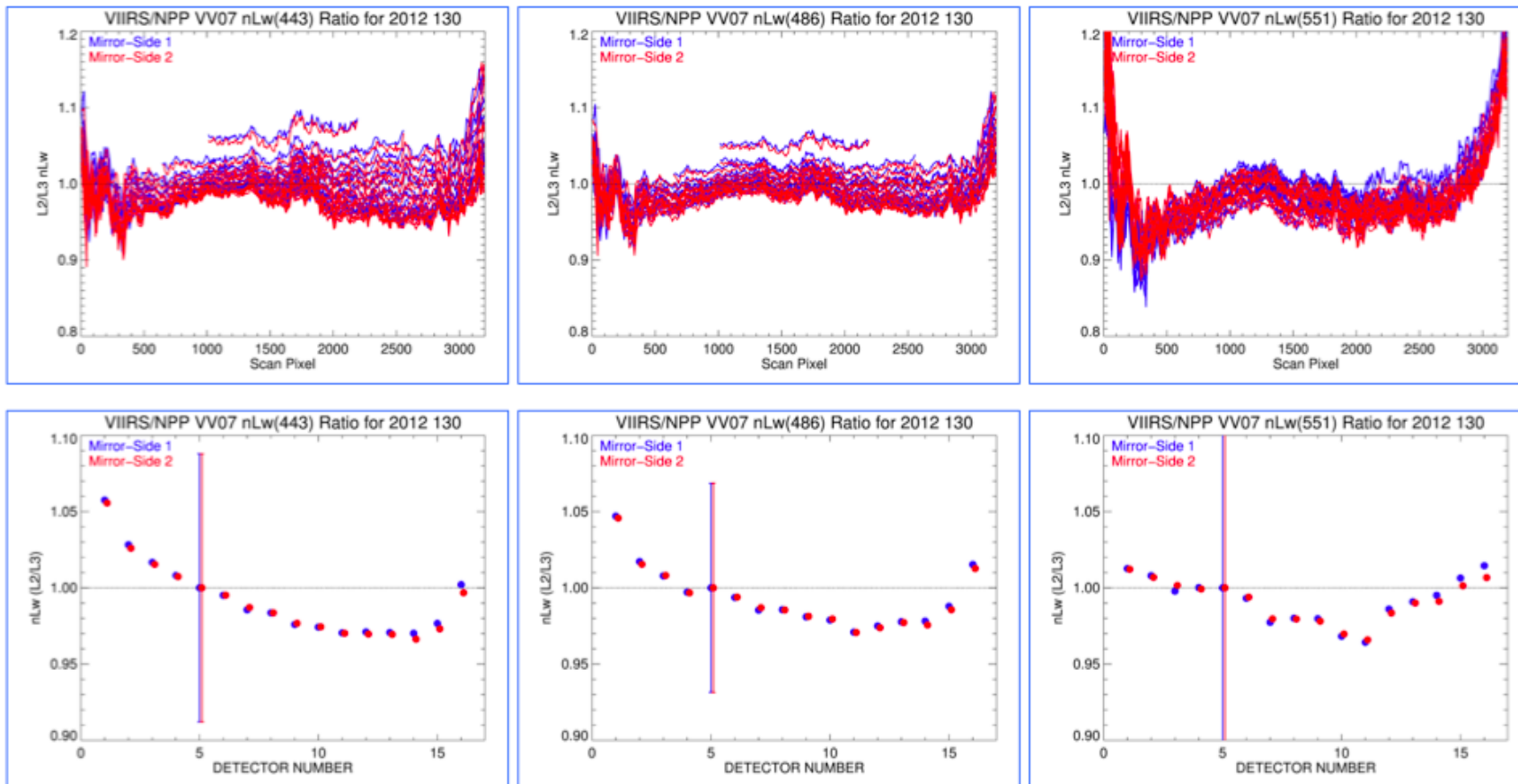


Fig. 5: Isolation of systematic spatial trends in VIIRS surface reflectance images. The top row shows scan angle trends as a function of scan pixel number for the three bands used to produce the chlorophyll *a* product. Each curve represents a different detector. Much of the variation is caused by the detector-to-detector differences, which are captured in the panels in the bottom row. The traces in the top row that float above the rest, but are limited to the middle of the scan, are the edge detectors, which are not transmitted by VIIRS outside of 32° scan angle. The pronounced difference in detectors at or near the edge of the focal plane is evident in plots on the bottom row. The green band (551 nm) does show some higher scan angle artifacts, but this is correctable.

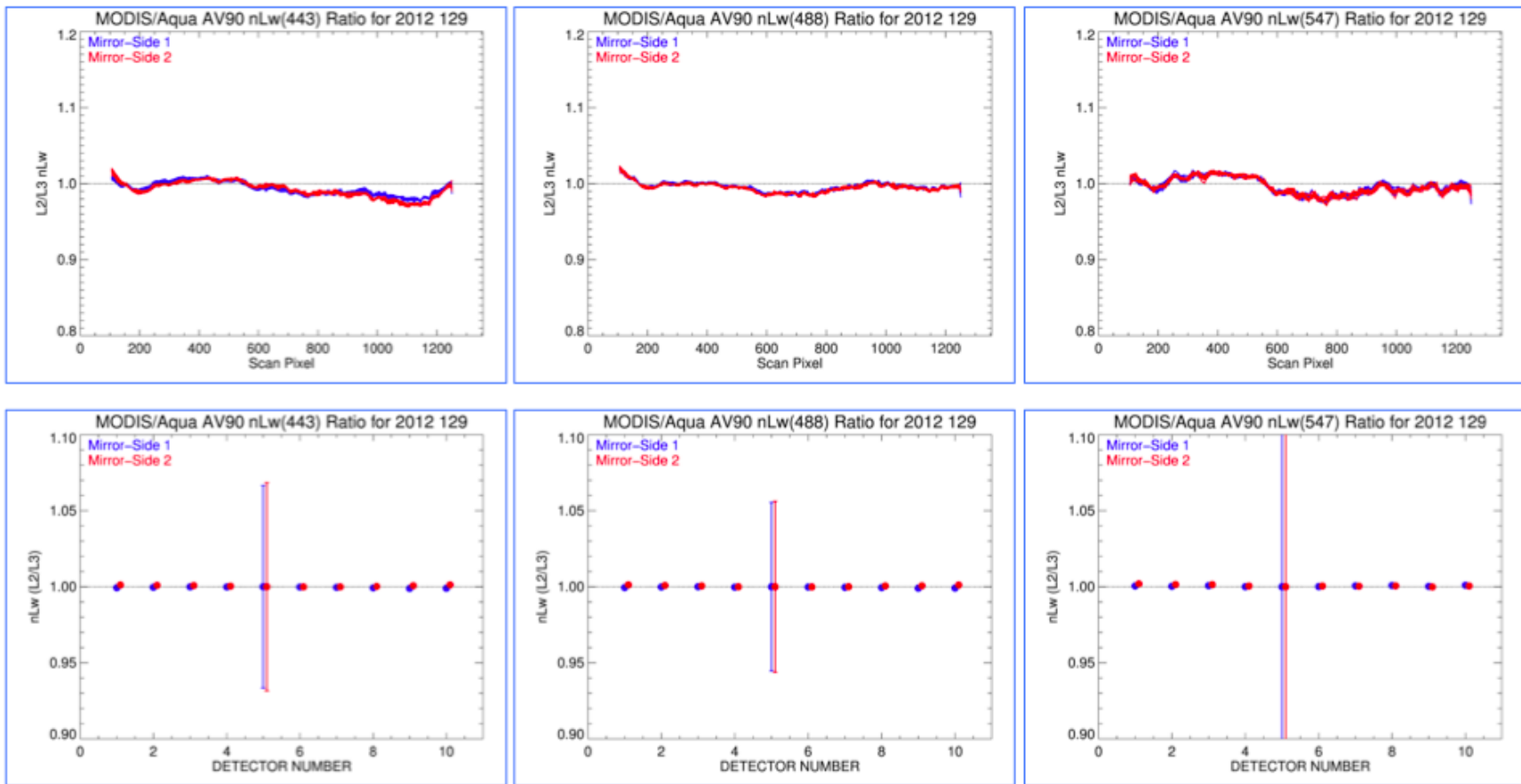


Fig. 6: Isolation of systematic spatial trends in MODIS Aqua surface reflectance images. These plots are analogous to those in Fig. 5. These shows how MODIS Aqua currently appears when this type of analysis is applied after corrections were applied. The same correction will be applied to VIIRS in the NASA evaluation products.

---

## 2. SCIENCE TEAM ASSESSMENT EFFORTS

---

### 2.1 OVERVIEW OF TEAM ACTIVITIES

---

The science teams activities for this assessment of VIIRS data products can be categorized into three areas:

- 1) **Data Collection** – This includes data collected for validation of VIIRS EDR and evaluation products and for development of new algorithms. These activities are described in Section 2.3.
- 2) **Algorithms Development** – Algorithms were developed to generate data products that were original part of the NASA EOS data record, but not supported by S-NPP. In addition, experimental algorithms were also explored. Algorithm development activities are described in Section 2.4.
- 3) **Product Evaluation** – These activities were divided into two independent efforts, one supported by investigators at NASA/GSFC (Turpie, McClain, and Franz) and one support by NOAA/NESDIS/STAR (Wang). These approaches, which are described in Section 2.5, take approaches with different emphases, offering different information. However, both approaches largely show agreement where their analyses overlap.

Although these activities were highly independent, some coordination was afforded toward production of a collaborative assessment toward latter half of the award period, which was lead by the team at NASA/GSFC under Turpie, who served as Ocean Discipline Lead. The science team activities were also heavily supported by the Ocean PEATE, which is described in the next section.

### 2.2 OCEAN PEATE SUPPORT

---

The Ocean PEATE serve NASA VIIRS evaluation products based on NASA calibration and algorithms (L2 & L3) via the ocean color website (<http://oceancolor/gsf/nasa/gov>). IDPS EDRs were collected for use of the S-NPP Science Team, but kept in an archive hidden from the public. Access is limited because these are the same products that are available through the Comprehensive Large Array-data Stewardship System (CLASS). NOAA operational products, i.e., chlorophyll *a* concentration, normalized water-leaving radiance (nLw), and Inherent Optical Properties (IOP) were publicly made available as L3 products only, and only via the Ocean Color Website (L3 browser).

SeaBASS is the primary repository for oceanic optical data collected *in situ* under NASA funding. SeaBASS provides a user interactive tool analyzed matching pairs of satellite and *in situ* measurements. This tool now provides a search and retrieval capability for only NASA evaluation VIIRS satellite products, but will not work with IDPS EDR data. Matches of *in situ* measurements with IDPS EDR satellite products were done manually by PEATE personal. Statistical analysis of paired *in situ* and satellite measurements was conducted by science team

using a Model II regression technique (i.e., one that assumes that errors are present in both the predictor and explanatory variables), which was not available as part of the SeaBASS analysis capability at the time.

As the NASA calibration matures, the Ocean PEATE is expected to reprocess of the NASA evaluation products frequently. Thus, to improve reprocessing efficiency, the Ocean PEATE switched over to producing an uncorrected L1b (also referred to as a "pseudo" L1a because it provides the same processing functionality as the SeaWiFS L1a) to bypass reprocessing of geolocation. The entire mission was reprocess in this fashion in earlier December 2012. The Ocean PEATE subsequently removed all NOAA and NASA-calibrated SDRs currently available on the ocean color website.

The Ocean PEATE supported the NASA/GSFC team by facilitating the NASA evaluation processing stream and through the distribution of evaluation products to the entire team. The Ocean PEATE also supported implementation of algorithms being development by other team members, including the PIC algorithm (Balch) and the PAR algorithm (Frouin). Algorithm development by Wang was facilitated by the NOAA evaluation processing capability. Gregg used *in situ* data and L3 data from the Ocean PEATE, but implemented processing using an external capability. All investigators making measurements at sea, either for validation or algorithm development, are required to archive their collections in SeaBASS, which is support by the Ocean PEATE.

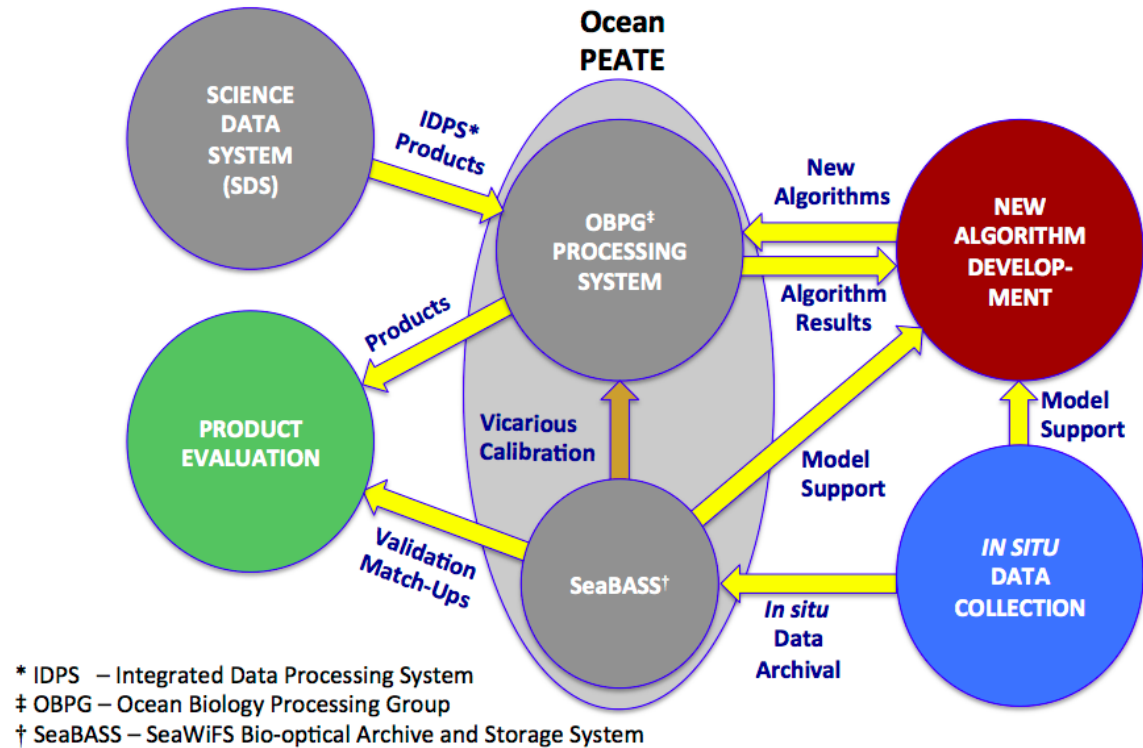


Fig. 7: Science Team / Ocean PEATE Workflow.

Fig. 7 illustrates the how the science team’s workflow relates to Ocean PEATE and other data capabilities and resources. Equipment and staff for the Ocean PEATE are provided by the Ocean Biology Processing Group (OBPG) at NASA/GSFC, which facilitates the evaluation processing stream and the SeaBASS archive. *In situ* data collected by the team are archived in SeaBASS, which also receives data from other sources, e.g., AERONET-OC or MOBY. Archived and recently collected *in situ* data also feed in the science team develop of new algorithms. Algorithms are passed to the PEATE team for implementation in the evaluation processing stream, and results are evaluate by science team members. Meanwhile, NOAA EDR are retrieved from the NASA SDS and archived in the Ocean PEATE along with NASA L2 and L3 files generated by the Ocean PEATE. The science team compares NOAA and NASA VIIRS evaluation products to MODIS products and compares the VIIRS products to *in situ* data. Details of the products and services provided by the Ocean PEATE to the science are list in Table 1. Fig 8 diagrams the processes involved in generation of SDR, EDR, and L1-L3 evaluation products in the IDPS and Ocean PEATE.

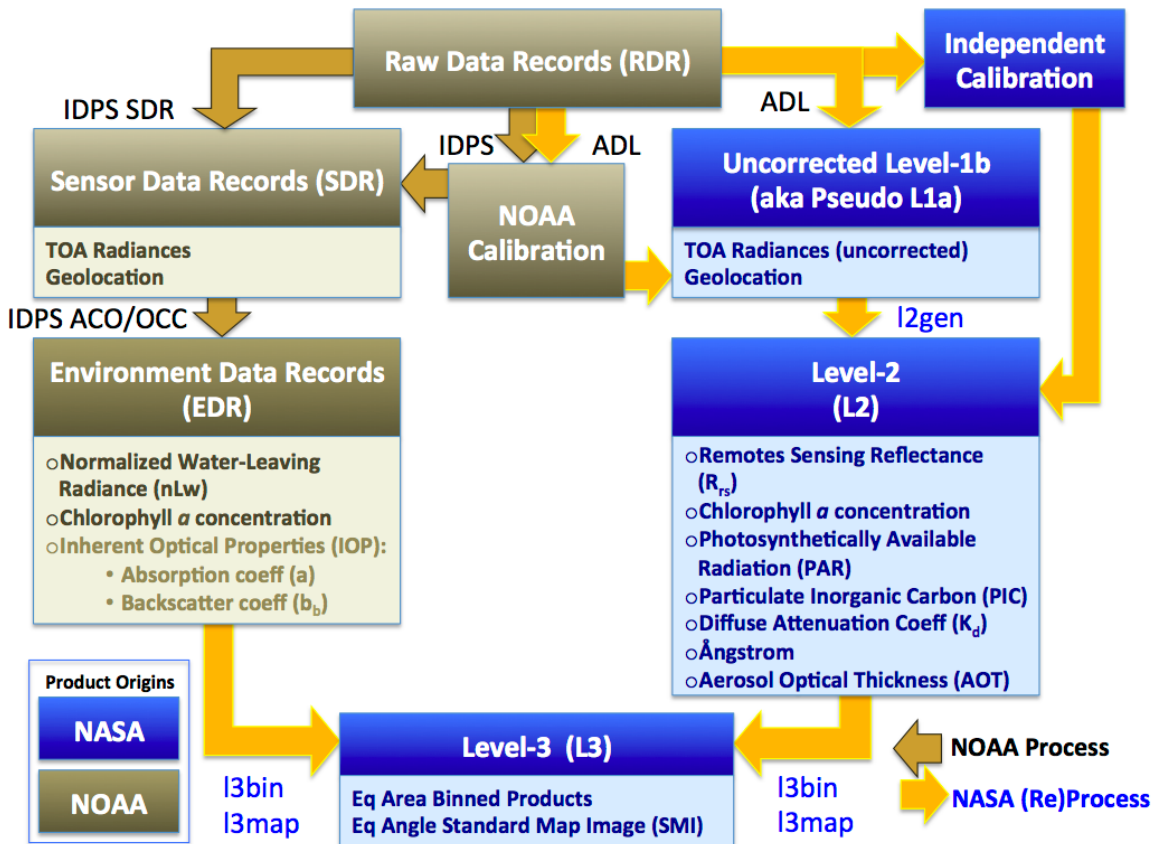


Fig. 8: Processing of EDR and NASA evaluation products. The blue boxes show the process for generating evaluation products in the Ocean PEATE. The brown boxes indicate processing that is facilitated by the IDPS. Note that NOAA calibration feeds the geo-location of the NASA product, while the radiometric calibration is done independently in off-line processing in the Ocean PEATE.

Table 1: Products and support provide by the Ocean PEATE.

TEAM	INVESTIGATION	OCEAN PEATE PRODUCTS	PROCESSING SUPPORT AND SERVICES
Balch (PI) Bowler	New Algorithm Data Collection	L2 Evaluation $R_{rs}(\lambda)$ (algorithm input)	<b>Algorithm Implementation:</b> Particulate Inorganic C (PIC) Particulate Organic C (POC) <b>New Product Generation:</b> L2 & L3 Evaluation PIC & POC <b>Services &amp; Tools:</b> SeaBASS Archival Support
Frouin (PI) Deschamps	New Algorithm Data Collection	L2 Evaluation $R_{rs}(\lambda)$ (algorithm input)	<b>Algorithm Implementation:</b> Photosynthetically Available Radiation (PAR) <b>New Product Generation:</b> L2 & L3 Evaluation PAR <b>Services &amp; Tools:</b> SeaBASS Archival Support
Gregg (PI) Casey Rousseaux	New Algorithm	L3 Evaluation Chl $a$ L3 Operational Chl $a$	<b>Services &amp; Tools:</b> SeaBASS Archive Retrievals and Match-up
Minnett (PI) Evans Turpie	SST Evaluation	L1 Evaluation (Thermal Bands)	<b>Services &amp; Tools:</b> Match-up Support
Siegel (PI) Nelson	New Algorithm Data Collection	L2 Evaluation $R_{rs}(\lambda)$	<b>Services &amp; Tools:</b> SeaBASS Archival Support
Turpie (Sci PI) McClain (PI) Franz	OC Evaluation	L2 & L3 Evaluation $R_{rs}(\lambda)$ , Chl $a$ , Angstrom, AOT L2 & L3 Operational $nLw(\lambda)$ , Chl $a$	<b>Services &amp; Tools:</b> Independent Solar and Lunar Calibration Support Regional Time Series Tool Scan Angle Artifact Detection Tool SeaBASS Match-up Tool
Wang (PI) NOAA Team	OC Evaluation New Algorithms	L3 MODIS Products	Global and regional data comparisons Satellite and in situ matchup MOBY time series

## 2.3 DATA COLLECTION

Measurements were taken at sea by three of the investigators (Balch, Siegel, and Frouin) to support algorithm development and validation. A list of data collected and used in this assessment is provided in Table 2. At the time of this report, data collections are still being processed for archival into SeaBASS, where they will add to the validation of VIIRS data products and other analyses. However, investigators who collected and analyzed the data they collected performed some direct comparisons of their data to VIIRS evaluation products generated by the Ocean PEATE and provided some interpretation of what they observed at sea. EDR comparisons with *in situ* data were carried out by the NASA GSFC and NOAA investigators on the science team, however, such analyses have been limited to radiometric parameters. Radiometric data was mostly provided by AERONET-OC, which provided about an order of magnitude more data points than was available from data collected on cruises. Data collect at the calibration buoy known as the Marine Optical Buoy (MOBY) was compared the EDR data, but not the NASA evaluation products (the NASA evaluation product was vicariously calibrated with MOBY data).

Table 2: Sources of *in situ* data used towards science team efforts. \*Data collected by source external to the Science Team but used in this report.

Who	What	When	Where
Balch	<ul style="list-style-type: none"> <li>• Temperature, Salinity, pH</li> <li>• chlorophyll fluorescence</li> <li>• fluorometric pigments</li> <li>• backscattering</li> <li>• spectral absorption</li> <li>• attenuation</li> <li>• particle size spectra (FlowCAM)</li> <li>• nutrients</li> <li>• dissolved organic carbon</li> <li>• particulate organic carbon</li> <li>• biogenic silica</li> <li>• Above water radiance</li> </ul>	Continuous underway measurements: February-March 2012 (35 d) October-November 2012 (43 d) March, June and November 2012 (18 d)	Great Belt II cruise Atlantic Meridional Transect Gulf of Maine GNATS cruise
Siegel	<ul style="list-style-type: none"> <li>• Spectral measurements of remote sensing reflectance</li> <li>• Absorption and scattering coefficient</li> <li>• Backscattering spectra</li> <li>• Nutrient</li> <li>• Fluorometric chlorophyll</li> <li>• Phytoplankton pigments (HPLC)</li> <li>• Dissolved and particulate organic carbon</li> <li>• Particulate silica concentrations</li> <li>• Particle size spectra</li> </ul>	Monthly, 1996-present	Day long cruises at 7 stations across the Santa Barbara Channel (15-550m deep)
Frouin	<ul style="list-style-type: none"> <li>• SIMBADA Measurements:               <ul style="list-style-type: none"> <li>• Marine reflectance</li> <li>• Aerosol optical thickness</li> </ul> </li> <li>• Photosynthetically Active Radiation data</li> </ul>	02/20/11-13/03/11 05/10/11-12/10/11 11/07/11-11/18/11 03/07/12-03/17/12 January 2012-January2013	Southern Atlantic SouthWest Pacific East Asians Seas Northwestern Atlantic COVE site Chesapeake Bay (North Atlantic)
*	<ul style="list-style-type: none"> <li>• <i>In situ</i> radiometric data (<math>nL_w(\lambda)</math>)</li> <li>• Water leaving radiances</li> </ul>	November 2011-Present January 2012-Present	MOBY site (Hawaii) AERONET-OC (CSI-Gulf of Mexico and USC-Newport Beach California)

---

Also, at the time of this report, only ten measurements of chlorophyll *a* concentration were matched to satellite data following the strict protocols that was established by NASA for validation of heritage mission data products. As field data continues to be delivered and processed according to NASA protocols in the coming year, the sample of chlorophyll *a* data should increase significantly. However, this is expected to still be limited as much of the data is being collected from optically complex regions of the sea (e.g., coastal water or coccolithophore blooms), which supports vital investigations that help with algorithm development and help us understand how to improve satellite remote sensing of important biological phenomena that are difficult to measure from space.

---

### 2.3.1 BIGELOW LABORATORY FOR OCEAN SCIENCES: BALCH LABORATORY

---

The Balch laboratory participated in several cruise campaigns in support of VIIRS validation of radiances, chlorophyll *a* product. These cruises were: (a) Great Belt II cruise aboard *R/V Revelle* (Feb-March 2012; 35d) between Durbin, S. Africa and Fremantle, Australia, (b) Atlantic Meridional Transect Cruise #22 aboard *RRS James Cook* (October-November, 2012; between Southampton, UK and Punta Arenas, Chile; 43d) and (c) Gulf of Maine GNATS cruises aboard *R/V Connecticut* (March, June, November, 2012; each cruise was 2d each).

Continuous underway measurements – supporting optical data for algorithm development were taken using a semi-continuous underway sampling system; it has been applied in studies of algal populations in the Equatorial Pacific, Arabian Sea and Gulf of Maine (Balch, 2004; Balch et al., 2004; Balch et al., 2001; Balch and Kilpatrick, 1996). It measured variables for a suite of properties that are related to general hydrography, optics, overall phytoplankton abundance, as well as optical properties that serve as proxies for general POC and coccolithophore PIC. Acid-labile backscattering is correlated to the PIC concentration (Balch et al., 2001) while beam attenuation is well correlated to POC (Bishop, 1999; Bishop et al., 1999; Gardner et al., 1993). Our system measured temperature, salinity, pH, and chlorophyll fluorescence. Total backscattering at 531 nm ( $b_{b\ tot}$ ) was measured inside an enclosed 2L volume using a WETLABS ECO-VSF (3 angle). Backscattering was measured by the same instrument following acidification of seawater with a weak acid to dissolve calcium carbonate ( $b_{b\ acid}$ ), and by difference, acid labile backscattering ( $bb'$ ; Balch and Drapeau, 2004; Balch et al., 2001; Balch et al., 1996). Every several hours along track, discrete water samples were collected and analyzed for chlorophyll, PIC and POC as a means to calibrate the system. Also sampled with the above underway system were measurements of absorption and attenuation at 9 wavelengths across the visible spectrum using a WETLABS ac-9 (which allowed resolution of spectral absorption and scattering across the visible spectrum), 0.2 $\mu$ m-filtered absorption and attenuation at 9 visible wavelengths (related to the amount of chromophoric dissolved organic matter in sea water) (Balch et al., 2008; Roesler and Perry, 1989).

Above-Water Radiance Measurements – In order to independently verify remotely-sensed estimates of PIC, free of atmospheric error, water-leaving radiance, sky radiance and downwelling irradiance were measured from the bow of the research vessels using a Satlantic SeaWiFS Aircraft Simulator (MicroSAS). This instrument has been an integral part of our

---

underway system since, within 2.5-3 hours of local apparent noon, the MicroSAS system allows us to evaluate apparent optical properties in real time for surface chlorophyll and PIC content without stopping the ship. This system also allowed optical derivation of these products when overhead clouds prevented synoptic satellite ocean color determinations of PIC, which was frequent in some of the environments. The radiance data (collected at 10 Hz) were used to calculate spectral, normalized water-leaving radiance that was directly applied to the merged PIC algorithm (see above) and POC algorithm (Stramski et al., 1999). Protocols for AOP measurement and calibration were according to Mueller (Mueller, 2003; Mueller et al., 2003a; Mueller et al., 2003b). A plaque calibration was performed regularly at local apparent noon using a 2% spectralon reflectance plaque. This provided a regular vicarious calibration over the duration of the cruise to track instrument calibrations.

Processing of radiance data for algorithm validation was done in several steps. The first step was that raw radiance data from the Satlantic microSAS were converted from instrument counts to calibrated radiances and irradiances using the Satlantic software "Prosoft". Next, the solar azimuth and elevation angles relative to the radiometers were calculated for each datum. The third step was to eliminate any data where solar elevation is less than 20°, where ship pitch or roll made the data unusable, or data where the radiometer view was contaminated by white caps. Next, we matched-up discrete data for PIC with appropriately processed microSAS radiance data or satellite radiance data and consolidated this into the master match-up database. The most time intensive step of PIC algorithm maintenance involved the recalculation of the coefficients for the two-band model followed by recalculation of the LUTs. In particular, the relation between the chlorophyll concentration and the particulate backscattering (from non-calcified phytoplankton) was critical since "non-PIC backscattering", by definition, affects the PIC backscattering calculation in the algorithm. This process was iterated until the error in PIC, relative to ship-derived values, was minimized. Once the best-fit coefficients were determined, then we ran the models for all combinations of chlorophyll and PIC and derived the revised look-up table.

*Analytical methods* – The technique of Fernandez et al. (1993) was used to prepare samples for CaCO<sub>3</sub> concentration analysis. Briefly, 200 ml samples were filtered onto 0.4µm pore-size polycarbonate filters and rinsed first with filtered sea water, then borate buffer (adjusted to pH=8) to remove sea water calcium chloride. This pH adjustment was critical to insure that carbonates were stable during sample storage. Later, filters were placed in trace metal free centrifuge tubes with 5 ml 0.5% Optima grade nitric acid and the Ca concentration was measured using ICP-OES (University of Maine, Sawyer Analytical Facility) (Cheng et al., 2004). Samples for chlorophyll were filtered through H/A filters and measured according to the JGOFS protocols (JGOFS, 1996).

## **Results**

### **PIC estimates**

The validation data available for analysis were from the Great Belt II cruise and Atlantic Meridional Cruise 22 (total of 892 match-ups, at varying times from the satellite overpass, up to 7h). Overall, the VIIRS PIC estimates were about 21% low from those determined optically from

the ship (using acid-labile backscattering measurements convolved with the backscattering cross-section of calcite (parallel laboratory and field measurements) (Fig. 9).

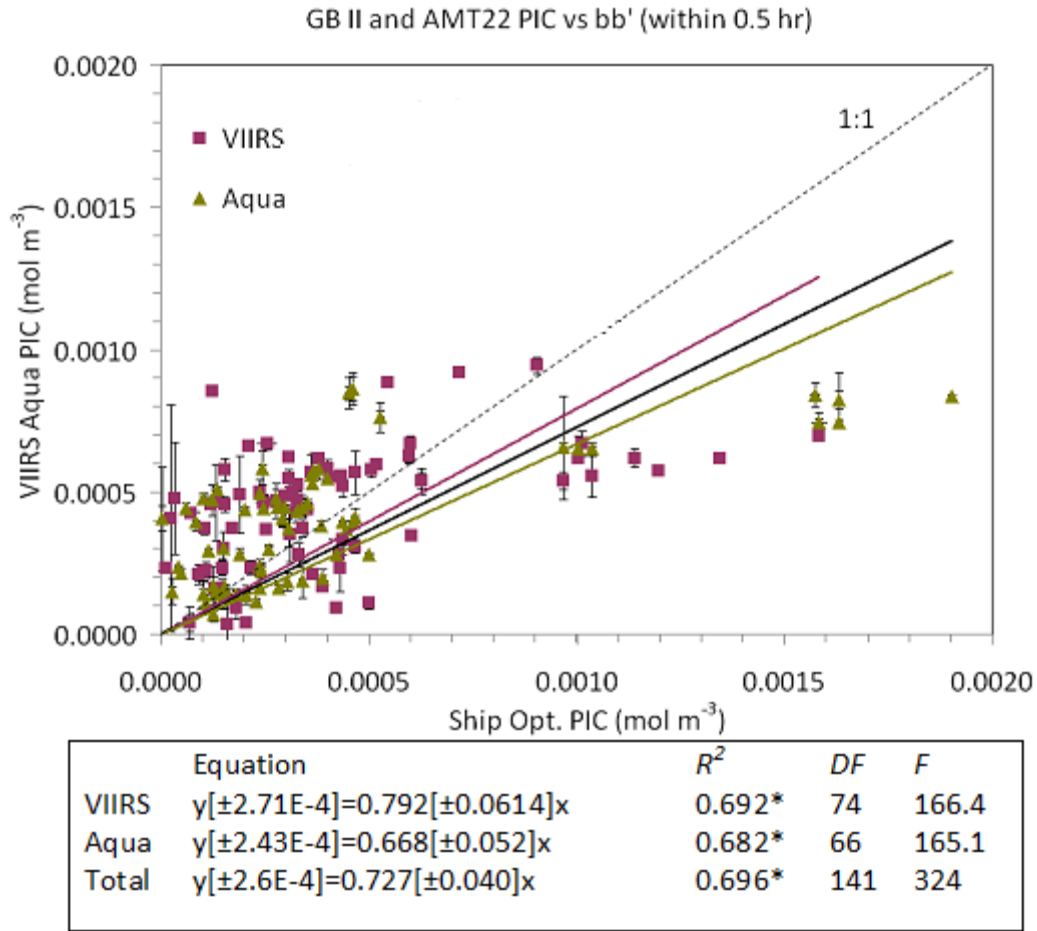


Fig. 9: Satellite-derived PIC estimates made with VIIRS and MODIS-Aqua plotted against Ship-derived estimates of PIC, made using the optical acid-labile backscattering technique. All data shown are for ship measurements made at the same location as satellite measurements, within ½ hour of each other. Least-squares linear regressions are shown for the total data set as well as the data sets from each individual satellite sensor. Regressions are driven through 0. The 1:1 line (dashed line) is shown for reference. Equations for each regression are given. Values in square brackets are the standard error for the various constants. The squared coefficient of correlation, degrees of freedom, F statistic, and probability that such a relationship could be derived by chance are also given. It can be seen that the satellites were generally underestimating PIC by about 21% for VIIRS and 33% for MODIS Aqua based on the slopes of the regressions and the value of the PIC backscattering cross-section used in the analysis. This likely is not the fault of the satellite sensor but our ability to predict the backscattering cross-section of PIC, for all the different species of coccolithophores observed across the various ocean basins that we worked in. The standard error for the satellite-derived PIC measurements was about  $2.5 \times 10^{-4}$  mol m<sup>-3</sup> (equivalent to 0.25µM or 3µg/L) and these were not different between Aqua and VIIRS. Y error bars on these plots represent the standard error of the 9 pixel measurements made by the satellite at each station. The standard errors of the ship determinations of PIC were about  $5 \times 10^{-5}$  mol m<sup>-3</sup> (which is mostly related to the error associated with the acid-labile backscattering determination. (\*) indicates statistical significance ( $p < 0.001$ ).

## Chlorophyll Estimates

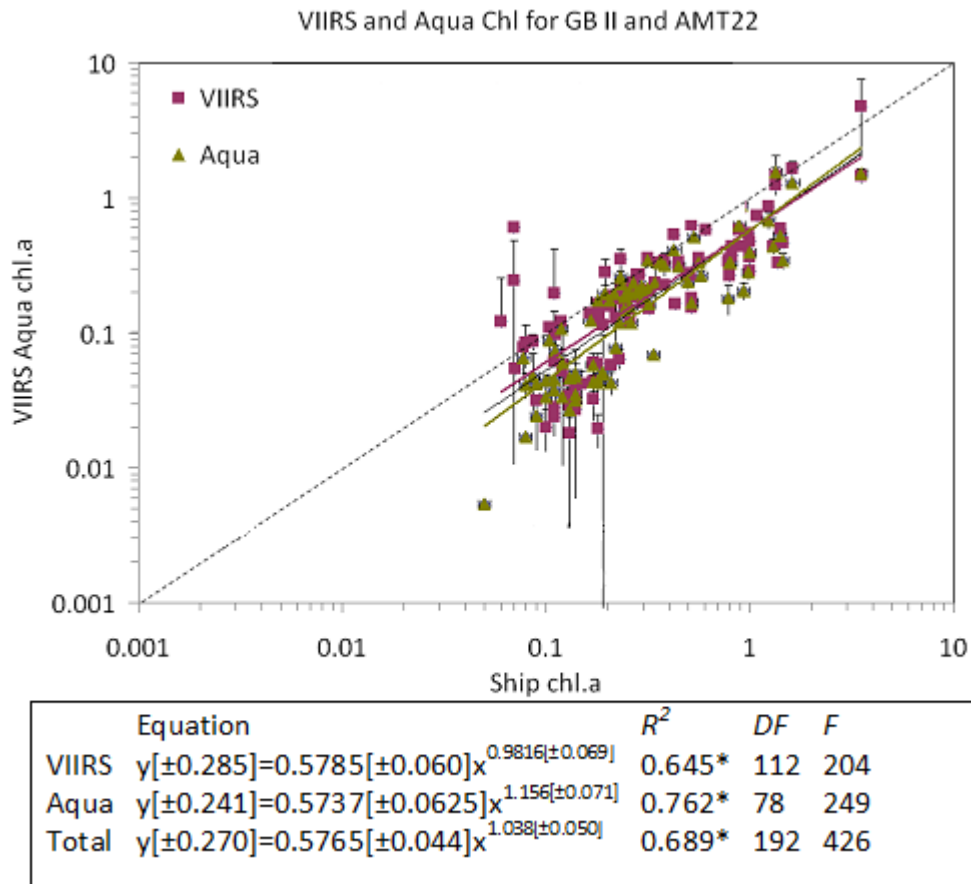


Fig. 10: Satellite-derived chlorophyll *a* estimates made with VIIRS and MODIS-Aqua plotted against Ship-derived estimates of chlorophyll *a*, made using the fluorometric technique. All data shown are for ship measurements made at the same location as satellite measurements, made on the same day. Least-squares power functions are shown for the total data set as well as the data sets from each individual satellite sensor. Equations for each regression are given. Values in square brackets are the standard error for the various constants. The squared coefficient of correlation, degrees of freedom, F statistic, and probability that such a relationship could be derived by chance are also given. The 1:1 line (dashed line) is shown for reference. It can be seen that the satellites were generally underestimating chlorophyll *a* by about 58% for VIIRS and 57% for MODIS Aqua based on the constants in the regressions. The slopes of the power functions are not significantly different from 1. The standard error for the satellite-derived chlorophyll *a* measurements was 0.285 log units for VIIRS and 0.241 log units for MODIS Aqua (about a factor of two). Y error bars on these plots represent the standard error of the 9 pixel measurements made by the satellite at each station. The standard errors of the ship determinations of chlorophyll *a* were about  $\pm 7\%$  based on the precision of triplicate measurements. (\*) indicates statistical significance ( $p < 0.001$ ).

Shipboard chlorophyll estimates were compared to satellite estimates from both VIIRS and MODIS Aqua (Fig. 10). Comparisons were included in this analysis for data from the same day of

each overpass. The results for the chlorophyll validations show that VIIRS chlorophylls were good to  $\pm 0.285$  log units (about a factor of 2). Moreover VIIRS chlorophyll estimates were 58% lower than ship-board chlorophylls (derived from triplicate fluorometric extractions). The exponent of the least-squares power fit was not significantly different from 1 (meaning that the two variables were co-varying equally). We also extracted MODIS Aqua chlorophyll data from the same data sets and show them in Fig. 10. The Aqua chlorophyll values had an accuracy of 0.24 log units and showed a bias of 57% below the shipboard values, virtually identical to what we measured for VIIRS.

### Radiometric matchups

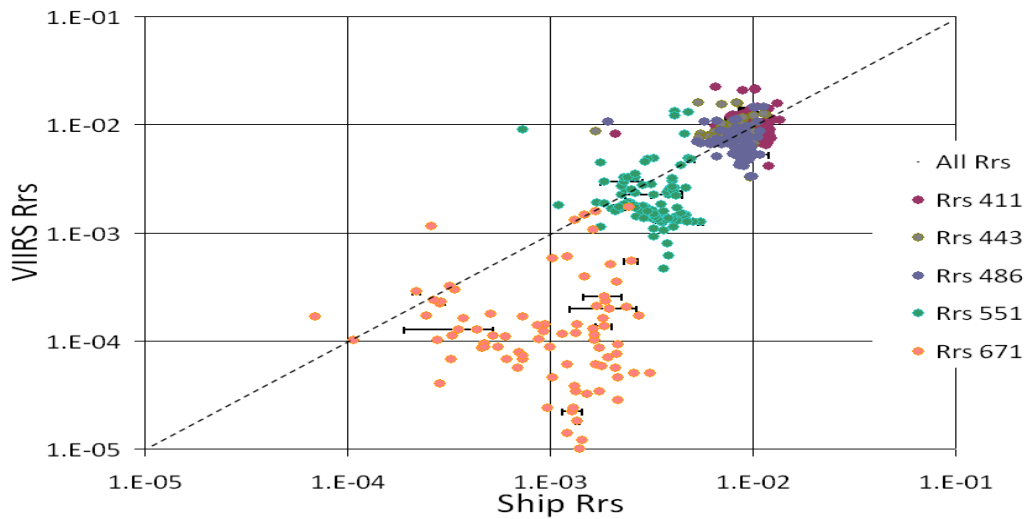


Fig. 11: Data for ship versus satellite reflectance for 5 wavelengths across the visible spectrum. Horizontal error bars reflect the standard deviation of the ship data when the ship occupied the station for a long periods of time.

VIIRS radiances were compared directly to radiances measured from the bow of the research vessels that we worked on. The results of the comparison are given in Table 3. It can be seen that at 412 and 445nm, the VIIRS and ship-derived radiances were within about 5-7% of each other. At the higher wavelengths, the VIIRS instrument underestimated the ship-derived radiances by an increasing amount. The same results are shown in Fig. 11 and Fig. 12. The PIC algorithm would be expected to be sensitive to such differences in absolute RRS, but clearly, the errors are no greater than for MODIS Aqua, given the comparisons shown in Fig. 9 and Fig. 17.

Table 3: Comparison of the ratio of VIIRS to shipboard radiance measured with the bow-mounted Atlantic radiance sensors. Other statistics (standard deviation, standard error, maximum and minimum are also provided.

wavelength (nm)	412	445	488	555	672
Average	1.069	1.063	0.870	0.866	0.323
Median	0.912	0.956	0.768	0.598	0.120
Std Dev	0.507	0.556	0.551	1.281	0.588
Count	98	98	98	98	86
Std Error	0.051	0.056	0.056	0.129	0.063
Max	3.938	5.175	5.488	12.086	4.417
Min	0.344	0.334	0.331	0.128	0.004

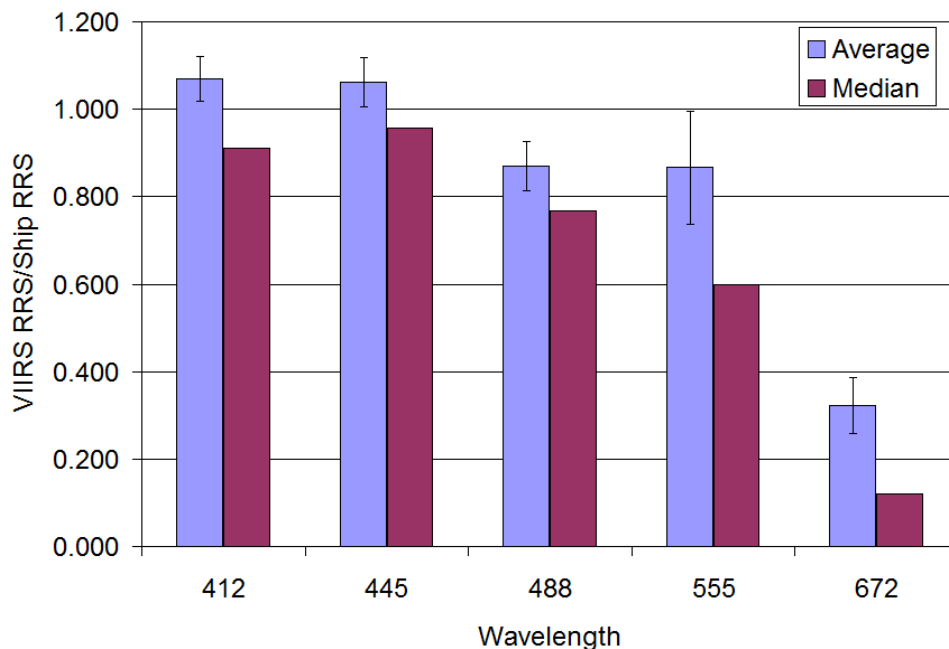


Fig. 12: Ratio of remote-sensing reflectance measured by VIIRS and ship-mounted radiometers. Both the average and median ratios are shown. The error bars on the averages reflect the standard deviation of the values.

### Summary

The comparisons between VIIRS-derived PIC and chlorophyll estimates are remarkably close to those achieved with MODIS Aqua. While there are some differences between the two sensors, they show exceedingly similar statistics in terms of the algorithm bias and RMS error. VIIRS radiance estimates in the blue end of the spectrum were within 5-7% of what we measured aboard ship. The 488nm, 555nm and 672nm bands show larger differences. Underestimates of 555nm RRS by VIIRS could impact the accuracy of the PIC algorithm (given that it is not a ratio algorithm but uses absolute radiances). The similarity of VIIRS and Aqua PIC products in this analysis could be related to the fact that the Aqua 555nm band has degraded, as well.

### 2.3.2 PLUMES AND BLOOMS – SIEGEL (UC SANTA BARBARA)

The focus of the Plumes and Blooms (PnB) program is to understand, predict and utilize changes in ocean color in complex coastal waters. The PnB study site is the Santa Barbara Channel, California where intense phytoplankton blooms (often >10 mg chlorophyll per m<sup>3</sup>) and episodic discharges from the coastal watersheds creating large sediment plumes. The core of the PnB program includes the monthly day-cruises sampling 7 stations across the Santa Barbara Channel. Water depths vary from 15 to 550 m. Field observations started in 1996 and they have continued continuously to the present. Ship support is provided by collaboration with the NOAA Channel Islands National Marine Sanctuary on their 55 foot research vessel, the R/V Shearwater.

---

A full suite of ocean optical, physical, biological and biogeochemical measurements are made at each PnB station. These include spectral measurements of remote sensing reflectance (Biospherical PRR-600 and C-OPS spectroradiometers), absorption and scattering coefficients (WETLABS AC-9), backscattering (HOBI Labs Hydrosat-6) spectra. Component absorption spectra (dissolved, particulate and phytoplankton absorption spectra) are also sampled in the laboratory. Samples are collected for nutrient, fluorometric chlorophyll, phytoplankton pigment (High Performance Liquid Chromatography, HPLC analyzed at NASA GSFC), dissolved and particulate organic carbon (measured at UCSB) and particulate silica concentrations (all except the HPLC phytoplankton pigments are measured at UCSB). Recently we have added a Sequoia Scientific LISST-100X laser particle sizer, which provides an in situ assessment of the particle size spectra (Kostadinov et al., 2009; Kostadinov et al., 2012).

The PnB in situ data set provides one of the most complete ocean optics data sets in the world enabling a wide host of ocean color science questions to be attacked. These include the assessment of phytoplankton functional types on ocean color (Anderson et al., 2008; Barrón et al., 2013), the dynamics of particle backscattering (Antoine et al., 2011; Kostadinov et al., 2007), the optical assessment of the particle size spectrum (Kostadinov et al., 2009; Kostadinov et al., 2012), an understanding of the interactions of light with colored dissolved organic matter (Nelson and Siegel, 2013; Swan et al., 2012) and the assessment of harmful algal blooms from satellite observations (Anderson et al., 2011; Anderson et al., 2009).

The monthly sampling of seven stations in a highly variable environment also make the Plumes and Blooms project an excellent site to validate satellite ocean color data products. Fig. 13 illustrates the comparison of same day match ups of spectral remote sensing reflectance (Rrs) and chlorophyll concentration created from PnB field observations and SeaWiFS, MODIS-Aqua and VIIRS-NPP satellite observations. Here the operational (NASA) algorithms are used. Relevant statistics (slope of the log-transformed regression fit and the  $r^2$  statistic) are shown in Table 4. A match up is created only when all satellite channels of reflectance are positive (negative Rrs(412) values are found about 30% of the time). The negative Rrs(412) values are thought to occur due to an over atmospheric correction through an atmosphere characterized by highly absorbing aerosols ( $SSA \leq 0.9$ ) which are not considered in the operational ocean color retrieval algorithms because this requires satellite radiance to be measured in the near-UV spectral range as is planned for the PACE mission.

The immediate thing to notice is the quality of the satellite-field data is roughly similar for all three satellite data sets. Retrievals of the Rrs(~412) (and to a lesser extent for Rrs(443)) are problematic for all three satellite data sets due to the over correction issue described above (although it is especially bad for VIIRS-NPP observations of Rrs(412) where the slope between satellite and field observations is actually negative). That said, the retrieval of Rrs(~550) and chlorophyll concentrations from all three satellites are reasonable as  $r^2$  values are roughly near 50%. However the satellite observations consistently under predict the field observations.

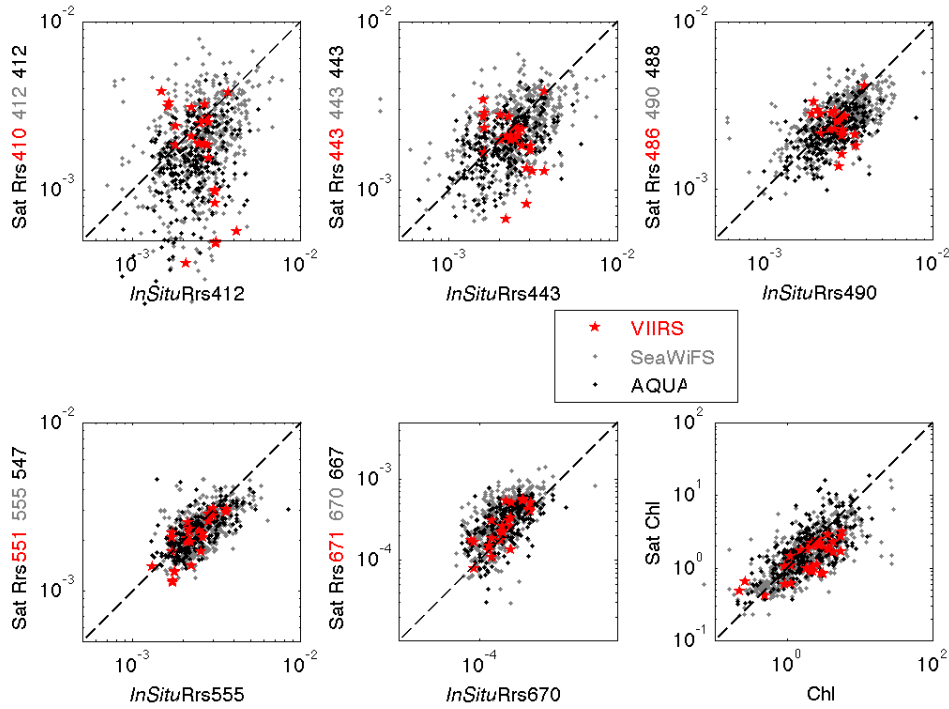


Fig. 13: Comparison of in situ Rrs and fluorometric chlorophyll observations from SeaWiFS (gray dots), MODIS-A (black dots) and VIIRS-NPP (red stars).

Table 4: Statistical comparison between PnB field and satellite data products.

seawifs (Rrs = 478; Chl = 579)

412	443	490	560	670	chl	bands
0.5147	0.4520	0.4871	0.5627	0.4888	0.5818	slope
<b>0.1110</b>	<b>0.2171</b>	<b>0.3523</b>	<b>0.3435</b>	<b>0.2754</b>	<b>0.5250</b>	r <sup>2</sup>

Aqua (Rrs = 272; Chl = 293)

0.6809	0.5424	0.5537	0.5403	0.6201	0.6488	slope
<b>0.1730</b>	<b>0.2804</b>	<b>0.3584</b>	<b>0.4094</b>	<b>0.3504</b>	<b>0.4908</b>	r <sup>2</sup>

Viirs (Rrs = 25; Chl = 35)

-1.1816	-0.4823	-0.1957	<b>0.9143</b>	<b>0.8565</b>	0.5260	slope
0.1963	0.0921	0.0229	<b>0.5795</b>	<b>0.6065</b>	<b>0.5526</b>	r <sup>2</sup>

Values that are red font are significant at the 95% confidence level.

The relatively good correspondence with the operational chlorophyll concentration is not unexpected as the NASA operational chlorophyll algorithm is a band ratio algorithm. Band ratio algorithms typically reduce the effects of noise in the Rrs retrievals on the final product. However, they are also limited as they are unable to separate covarying optical properties that often confound interpretation of satellite ocean color data (e.g. Siegel et al., in review; Siegel et al., 2005).

---

### 2.3.3 SIMBADA MEASUREMENTS – FROUIN (SCRIPPS INSTITUTE OF OCEANOGRAPHY)

---

The SIMBADA radiometer was originally developed by LOA, University of Lille to evaluate POLDER-derived ocean color. Requirements included (1) quality measurements of the basic ocean color variables, (2) low cost, and (3) capability to collect sufficient data in a wide range of environmental conditions (i.e., over the global oceans). The instrument is portable, compact, hand-held instrument that can be operated from fixed and moving platforms at sea (e.g., ship does not need to stop). It measures both marine reflectance and aerosol optical thickness in spectral bands approximately 10 nm wide centered at 350, 380, 412, 443, 490, 510, 565, 620, 670, 750, and 870 nm.

Several radiometric parameters can be measured with the SIMBADA radiometer. Aerosol optical thickness is obtained by viewing the Sun, and marine reflectance by viewing the ocean surface at a nadir angle of 45° and a relative azimuth angle of 135°. The measurements are made through a vertical polarizer which, when viewing the surface, reduces substantially sunlight reflected in the instrument field-of-view. Same optics and detectors but different electronic gains are used in Sun- and ocean-viewing modes. Field-of-view is 3°. Measurements are made simultaneously in all the spectral bands (one collimator and detector for each band), but viewing the Sun and the ocean surface is accomplished sequentially. Frequency of measurements is 10 Hz. Data is only collected in clear sky situations, i.e., when satellite ocean-color retrievals are made. The instrument also acquires data on viewing angles (inclinometer, magnetometer) and internal control parameters, i.e., time, geographical location (GPS), temperature, and atmospheric pressure. Final marine reflectance is generally close from the raw reflectance (i.e., perturbing effects are small). Uncertainty budget for marine reflectance: ±0.0015 to ±0.0010 (ultraviolet to blue), ±0.0004 (green), ± 0.0002 (red). Uncertainty budget for aerosol optical thickness: ±0.02 (ultraviolet to green), ±0.01 (red to near infrared)

Measurements of marine reflectance and aerosol optical thickness were made with SIMBADA radiometers during various campaigns of opportunity in the Southern Atlantic, Southwest Pacific, East Asian Seas, and Northwestern Atlantic. Other campaigns of opportunity have been planned (or just been conducted) in the Gulf of Mexico, Southwest Pacific, and Northwestern Atlantic. The accomplished and current/planned campaigns are listed below. The geographic location of SIMBADA measurements made during the accomplished campaigns is given in Fig. 14. During the campaigns water samples are collected for phytoplankton pigment analysis.

#### Accomplished campaigns

- MV1102, SIO, 02/20/11-13/03/11, Cape Town (South Africa) to Valparaiso (Chile).
- CALIOPE1, IRD, 05/10/11-12/10/11, New Caledonia (East Coast), 21°30S, 166°E.
- VITEL1, IRD, 11/07/11-11/18/11, North Vietnam, 20° 30N, 107°E.
- UPSEN1, LOCEAN, 03/07/12-03/17/12, Senegal, 14°20N, 17°14W.

### Current/planned campaigns

-Gulf of California, CICESE and UABC (4 cruises): 02/01-02/08 2013, 04/14-04/21 2013, 05/29-06/05 2013, 11/8-11/15 2013, 31°20N, 114°20W.

-Colorado Delta, CICESE and UABC (4 cruises): 02/16-02/21 2013, 04/29-05/04, 06/13-06/18 2013, 11/23-11/28 2013, 31°40N, 114°40W.

-CALIOPE2, IRD, 07/24-08/03, 2013, New Caledonia (East Coast), 21°30S, 166°E.

-UPSEN2, LOCEAN, 02/20-03/18 2013, Senegal, 14°20N, 17°14W.

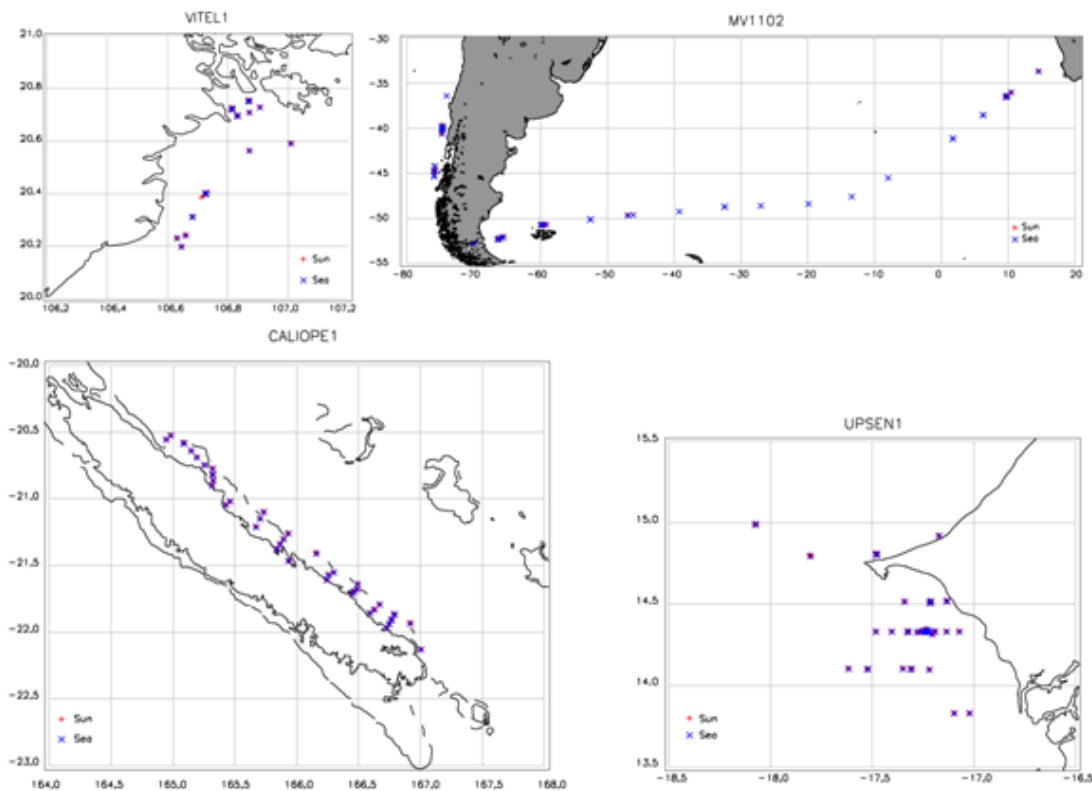


Fig. 14: Geographic location of SIMBADA data (Sea and Sun measurements) collected during MV1102, VITEL1, CALIOPE1, and UPSEN1 campaigns.

---

## 2.4 ALGORITHM DEVELOPMENT

---

### 2.4.1 DIFFUSE ATTENUATION COEFFICIENT AT 490 NM ( $K_d(490)$ )

---

The vertical diffuse attenuation coefficient,  $K_d(490)$ , is one of the most commonly determined apparent optical properties of the ocean. It provides information on the fraction of solar radiation penetrates at a given depth and hence an important parameter for ocean color research. It can be used to estimate the light field in the ocean euphotic zone, which can be used in heat budget or primary production models.  $K_d(\lambda)$  is typically formulated as

$$K_d(z, \lambda) = -\frac{1}{E_d(z, \lambda)} \frac{dE_d(z, \lambda)}{dz} \quad \text{Eqn. 1}$$

where,  $E_d$  is the planar downwelling solar irradiance in watts per square meter,  $\lambda$  is the wavelength in nanometers, and  $z$  is depth in meters. Algorithms to estimate  $K_d$  at 490nm have been devised for remote sensing applications as is a standard data product generated from SeaWiFS and MODIS data. However, this important parameter was not included in the NPP EDR suite of data products. However, both the NASA algorithm (I2gen) and the NOAA research algorithm employed by Wang (NOAA-MSL12) can produce this quantity using VIIRS surface reflectance values. Wang explore the NOAA-MSL12 output using VIIRS data and compared to the MODIS versions of data product.

Fig. 15 provides color images for global level-3 composite distributions of the VIIRS-derived water diffuse attenuation coefficient at the wavelength of 490 nm  $K_d(490)$ , compared with those from MODIS-Aqua. These are for  $K_d(490)$  global images of the daily (August 12, 2012), 8-day (August 12–19, 2012), and monthly (August of 2012). VIIRS  $K_d(490)$  data were from NOAA-MSL12 using Wang et al. (2009) algorithm, while MODIS-Aqua data were directly downloaded from NASA/OBPG website. As shown in Wang et al. (2009), for open oceans  $K_d(490)$  data should be the same as those from SeaWiFS and MODIS standard product (same empirical algorithm), while for the coastal regions Wang et al. (2009) algorithm produces significantly high values. Indeed, Fig. 15 shows that VIIRS  $K_d(490)$  data are similar to those of MODIS-Aqua over open oceans, while VIIRS has produced improved (significantly large)  $K_d(490)$  data over coastal regions, e.g., the Chesapeake Bay, China east coastal region, etc.

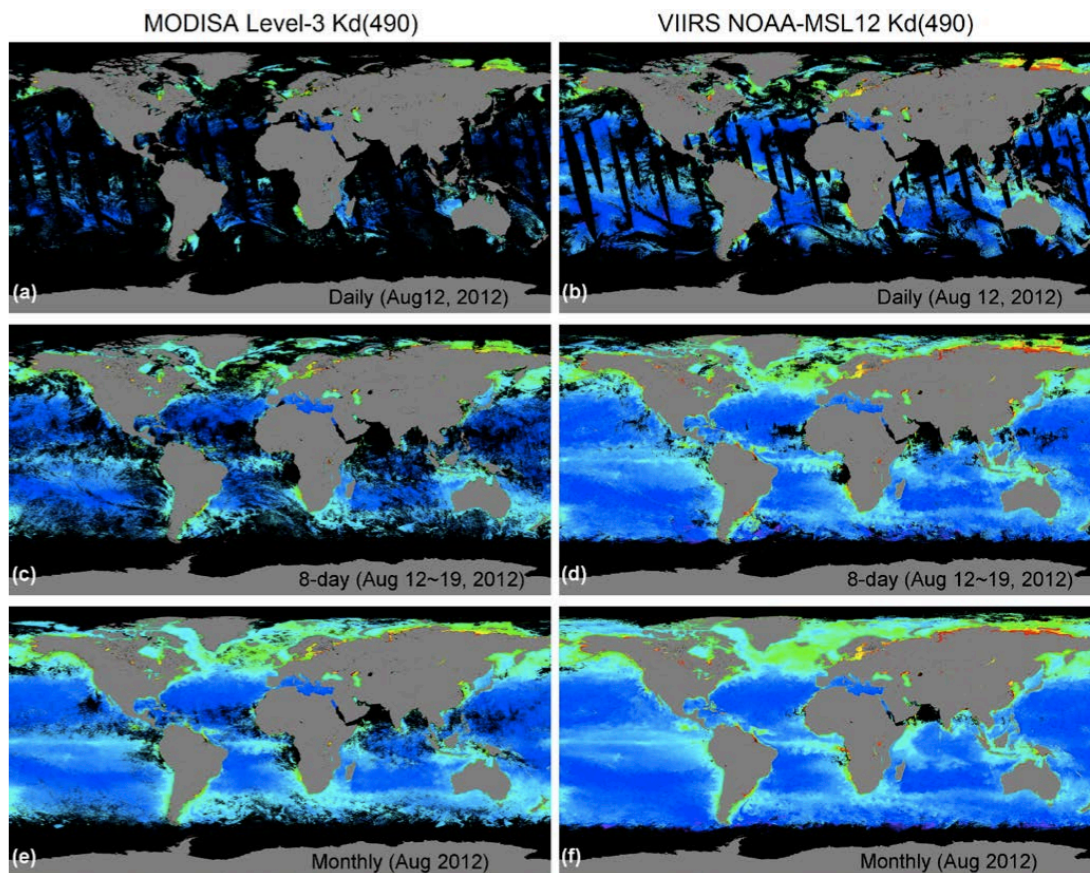


Fig. 15: Global VIIRS Kd(490) images for (a) and (b) daily (August 12, 2012), (c) and (d) 8-day (August 12–19, 2012), and (e) and (f) monthly (August of 2012). Plots (a), (c), and (e) were from MODIS-Aqua data (from NASA/OBPG), while plots (b), (d), and (f) were derived from NOAA-MSL12-produced data. Note scale for Kd(490) is log-scale  $0.01\text{--}2\text{ m}^{-1}$ .

## 2.4.2 PARTICULATE INORGANIC CARBON (PIC)

Data for the MODIS-Aqua sensor are shown for comparison and VIIRS and Aqua gave virtually identical results (Fig. 16). Aqua PIC estimates were about 33% lower than ship PIC estimates. The underestimates of PIC for both sensors is related to the current value of the PIC backscattering cross-section ( $b_b^*$ ; units of  $\text{m}^2 (\text{mol PIC})^{-1}$  which is implemented in the NASA PIC algorithm). The underestimate of PIC does not have anything to do with the VIIRS or AQUA sensors, at least that is apparent in this analysis. Indeed,  $b_b^*$  is not constant in nature but varies with coccolithophore species and this can be a significant source of error in the algorithm. Most high latitude coccolithophores are of one species, *Emiliana huxleyi* while equatorial, subtropical and subpolar populations have a much more diverse assemblage of coccolithophore species with vastly different-shaped coccoliths. We are currently formulating a latitude-dependent  $b_b^*$  computation which reflects the geographic variability in coccolithophore species observed throughout the global ocean and their associated scattering properties. This will achieve better agreement between the satellite- and ship-derived PIC values.

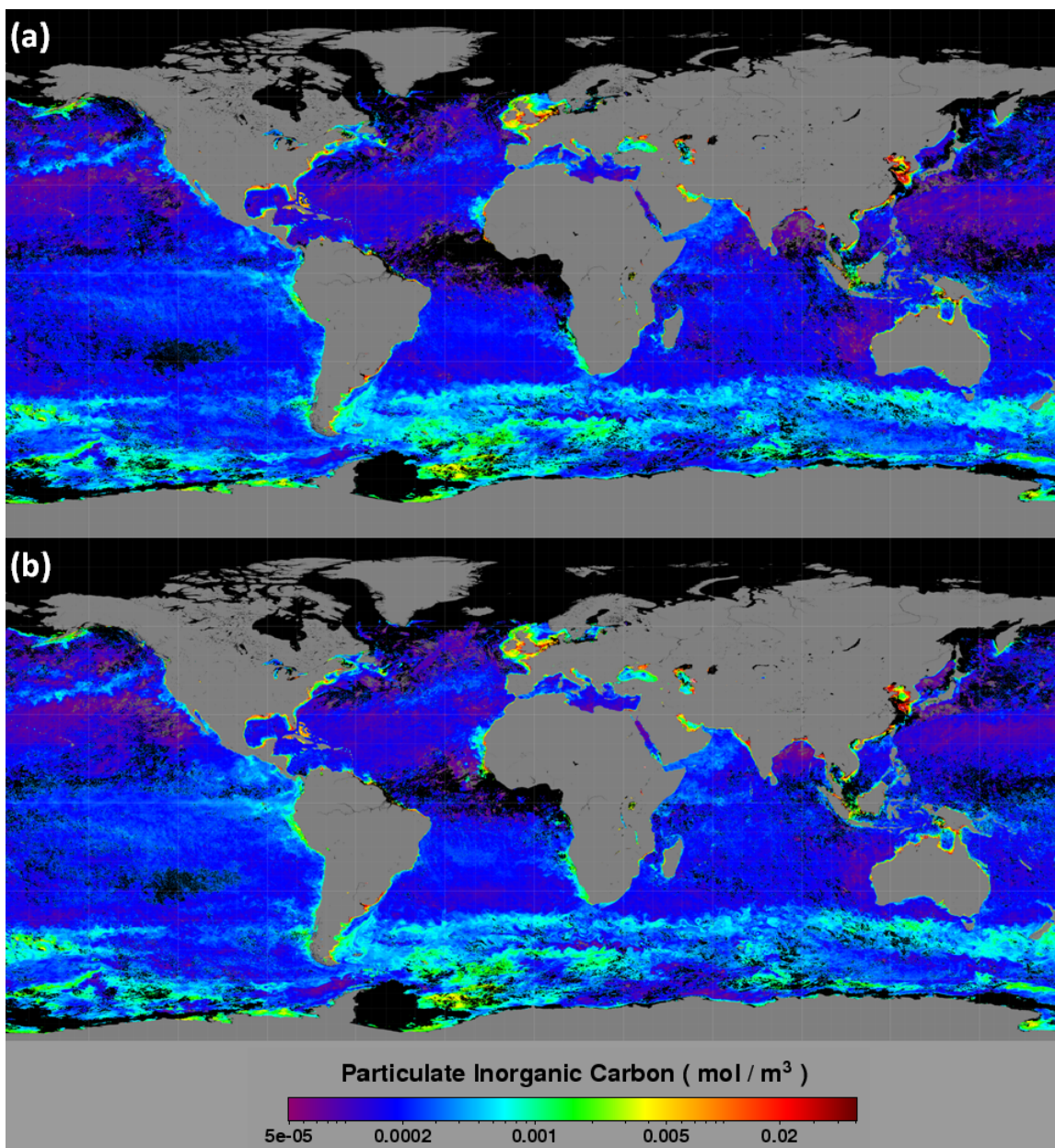
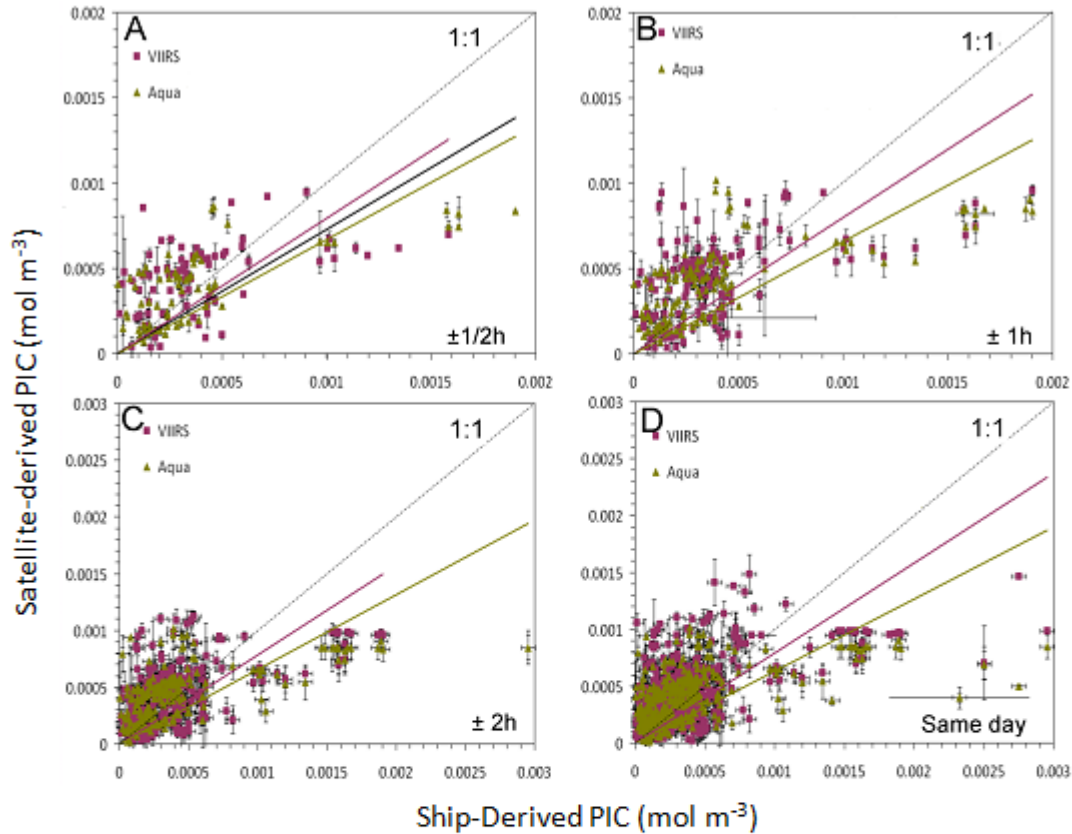


Fig. 16: Particulate Inorganic Carbon from (a) MODIS-Aqua and (b) VIIRS.

Overall, for both satellite sensors, the statistical fits between ship and satellite PIC estimates were good to within a standard error of 0.25-0.3  $\mu\text{M}$  PIC (= 3-3.6  $\mu\text{g}$  PIC/L), which is encouraging. These comparisons degraded slightly as the difference in time between ship PIC measurement and satellite overpass increased but the difference was not major (Fig. 17). The PIC validation results from both satellite sensors accounted for 60-70% of the variance in the ship-derived PIC measurements and the probability that these relationships occurred by chance,  $P$ , was  $<0.001$ , based on the F-statistic derived from these data (see statistics in each panel of Fig. 9 and Fig. 17). For PIC concentrations measured aboard ship using bow-mounted radiometers, compared to satellite-derived PIC values, however, the degradation of the statistics was much more significant as the difference between ship and satellite measurement

increased (results not shown). The reason for this is that the PIC algorithm relies on absolute radiances, not radiance ratios (like chlorophyll) and absolute radiances will vary considerably over sun angle, thus for ship PIC measurements taken by more than 30 minutes, the comparison with the satellite results was poor. Therefore these results are expected.



	Equation	$R^2$	DF	F
a	VIIRS $y[\pm 2.71E-4]=0.792[\pm 0.0614]x$	0.692*	74	166.4
	Aqua $y[\pm 2.43E-4]=0.668[\pm 0.052]x$	0.682*	66	165.1
b	VIIRS $y[\pm 2.82E-4]=0.800[\pm 0.045]x$	0.681*	147	313
	Aqua $y[\pm 2.57E-4]=0.658[\pm 0.037]x$	0.717*	123	311
c	VIIRS $y[\pm 2.92E-4]=0.785[\pm 0.033]x$	0.685*	267	582
	Aqua $y[\pm 2.82E-4]=0.658[\pm 0.032]x$	0.665*	217	430
d	VIIRS $y[\pm 3.08E-4]=0.791[\pm 0.026]x$	0.653*	501	943
	Aqua $y[\pm 2.82E-4]=0.634[\pm 0.026]x$	0.610*	387	604

Fig. 17: Performance of PIC algorithm applied to VIIRS (purple points) and MODIS Aqua (green points) for data validated within A)  $\pm 1/2h$  of an overpass, B)  $\pm 1h$  of an overpass, C)  $\pm 2h$  of an overpass and D) the same day of an overpass. Statistics for the least-squares linear fits are shown in purple and green text for VIIRS and Aqua sensors, respectively. Note, the scales on the X and Y axes are not the same on all the panels. Vertical error bars are for the standard deviation of the 9 pixels of satellite PIC taken at each sample location. The horizontal error bars represent the errors associated with the acid-labile measurements of PIC. (\*) indicates statistical significance ( $p < 0.001$ ).

---

### 2.4.3 ESTIMATE PHOTOSYNTHETICALLY AVAILABLE RADIATION (PAR)

---

An algorithm, originally developed to estimate photosynthetically available radiation (PAR) at the ocean surface from SeaWiFS data (Frouin et al., 2003), was adapted for use with VIIRS data. The algorithm estimates daily PAR, i.e., the average quantum energy flux from the Sun in the spectral range 400-700 nm during 24 hours, expressed in Einstein/m<sup>2</sup>/day. A code to compute PAR from VIIRS data was delivered to NOAA and NASA, implemented by NASA's OBPG as part of their ocean color processing line, and used to produce operationally a global 4-km time series of daily, weekly, and monthly PAR since the NPP launch, January 2012 until present.

In the algorithm, daily PAR is estimated for each instantaneous pixel, assuming that the cloud/surface system is stable during the day and corresponds to the satellite observation. Daily PAR is obtained as the difference between the incident solar flux between 400 and 700 nm (known) and the reflected flux (measured), taking into account atmospheric absorption (modeled). Knowledge of pixel composition is not required, eliminating the need for cloud screening and arbitrary assumptions about sub-pixel cloudiness. The daily PAR estimates obtained separately from different orbits are binned using a simple, linear averaging scheme (arithmetical mean).

The PAR model uses plane-parallel theory and assumes that the effects of clouds and clear atmosphere can be decoupled. The planetary atmosphere is therefore modeled as a clear sky atmosphere positioned above a cloud layer, and surface PAR is expressed as the product of a clear-sky component and cloud transmittance. The strength of such a decoupled model resides in its simplicity. Importantly, it is not necessary to distinguish between clear and cloudy regions within a pixel. The solar flux reaching the ocean surface is given by

$$PAR = PAR_{clear}(1 - A)(1 - A_s)^{-1} \quad \text{Eqn. 2}$$

where  $A$  is the albedo of the cloud-surface system and  $A_s$  the albedo of the surface, and  $PAR_{clear}$  is the solar flux that would reach the surface if the cloud/surface system were non reflecting and non absorbing.  $A$  is expressed as a function of the radiance measured by the satellite sensor in the PAR spectral range. Details about the model are provided in Frouin and Chertock (1992), Frouin et al. (2003) and Frouin et al. (2012).

The VIIRS PAR estimates were compared with MODIS-A estimates on daily, weekly, and monthly time scales. The 4-km time series from January to December 2012 was used. Fig. 18 display scatter plots of VIIRS versus MODIS-A estimates, and Table 5 gives the comparison statistics. The VIIRS values are higher than the MODIS-A values by about 5%, and RMS differences are 17%, 11%, and 7% on daily, weekly, and monthly time scales, respectively. Fig. 19, Fig. 20 and Fig. 21 display examples of PAR products, July 3, 2012 (Fig. 19), July 3-10, 2012 (Fig. 20), and July 2012 (Fig. 21). The MODIS-A maps are displayed on top, the VIIRS maps in the middle, and the differences (VIIRS - MODIS-A) at the bottom. The VIIRS and MODIS-A maps exhibit similar latitudinal gradients and features associated with cloud systems. Differences do not have a regional dependence in the daily products, but they are more variable in the low and

---

middle latitudes of the summer hemisphere in the weekly and monthly products, due to instrument-dependent gaps in the estimates. The gaps in the daily products are filled in the weekly and monthly products. Note that the present PAR products do not cover regions with low solar zenith angles (ocean-color products are not generated in those regions), but the algorithm works over the entire range of solar zenith angle.

The VIIRS PAR estimates were compared with in situ measurements made routinely at the COVE site off Chesapeake Bay in the North Atlantic. The comparison included data collected during the period January 2012 - January 2013. Only the data collected concomitantly with the 2 PAR sensors were used in the evaluation, which allowed good quality control of the data and efficient elimination of outliers. Fig. 22 displays the scatter plots of estimated versus measured values on daily, weekly, and monthly time scales, and Table 5 gives the performance statistics. Compared with in situ measurements, the VIIRS estimates are higher by 1.4 to 1.9 E/m<sup>2</sup>/d (4 to 6%), depending on the time scale. The higher values may be explained by the fact that satellite overpass occurs when cloudiness is generally reduced and/or by modeling errors. RMS differences are significantly decreased when going from daily to monthly estimates, from 5.8 to 2.3 E/m<sup>2</sup>/d (17 to 7%). These biases and RMS differences are slightly higher than those obtained in the VIIRS/MODIS-A comparisons above, made over the global ocean. Variability during the course of the year is generally well described at the COVE site, especially at the monthly time scale (Fig. 23). The results, even though preliminary, suggest that the VIIRS PAR estimates are suitable for studies of aquatic photosynthesis.

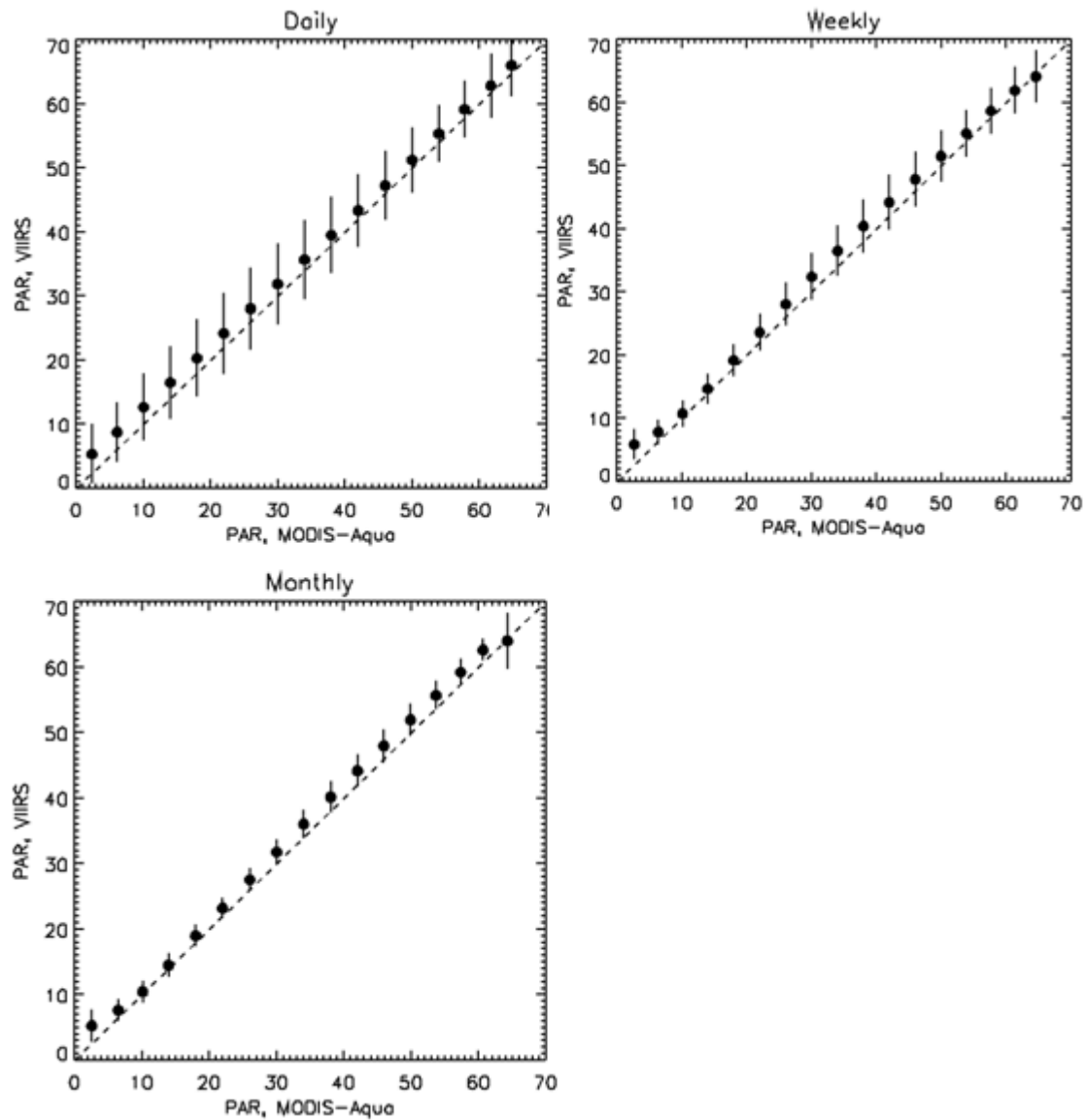


Fig. 18: Comparison of PAR estimated by VIIRS and MODIS-A on daily, weekly, and monthly time scales. Units are  $E/m^2/d$ . The 4-km time series, January to December 2012, is used. VIIRS values are higher by about 5% on average. RMS difference is reduced by a factor of more than 2 (to 7%) from daily to monthly estimates.

Table 5: VIIRS/MODIS-A PAR comparison statistics (January-December 2012, global).

$r^2$	Bias ( $E/m^2/d$ )	RMS ( $E/m^2/d$ )
0.889	1.79 (5.1%)	5.83 (16.6%)
0.938	1.74 (4.6%)	4.02 (10.7%)
0.983	1.67 (4.6%)	2.54 (7.0%)

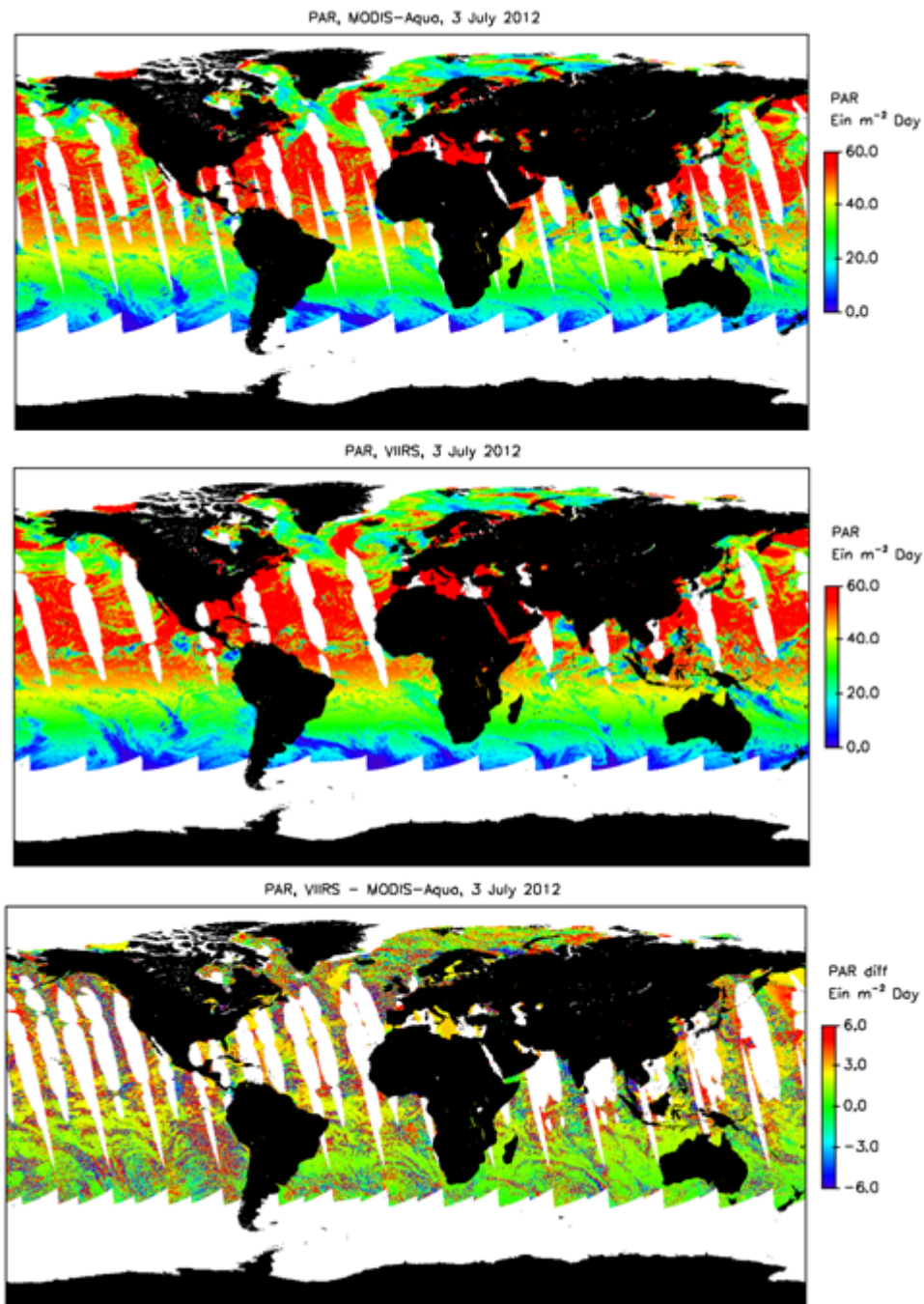


Fig. 19: Global 4-km daily PAR products from MODIS-A (top), VIIRS (middle), and difference (bottom). July 3, 2012.

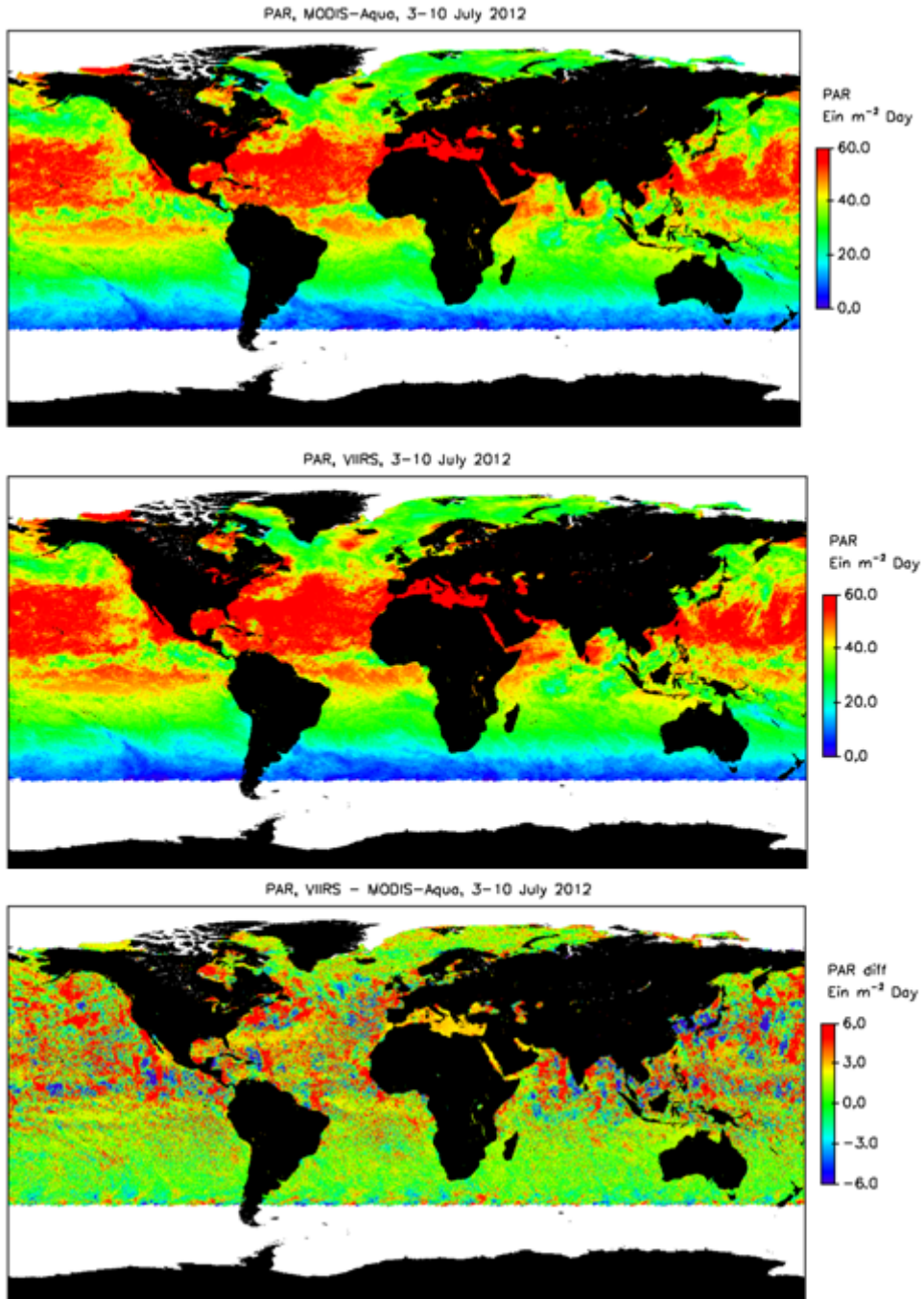


Fig. 20: Global 4-km 8-day PAR products from MODIS-A (top), VIIRS (middle), and difference (bottom). July 3-10, 2012.

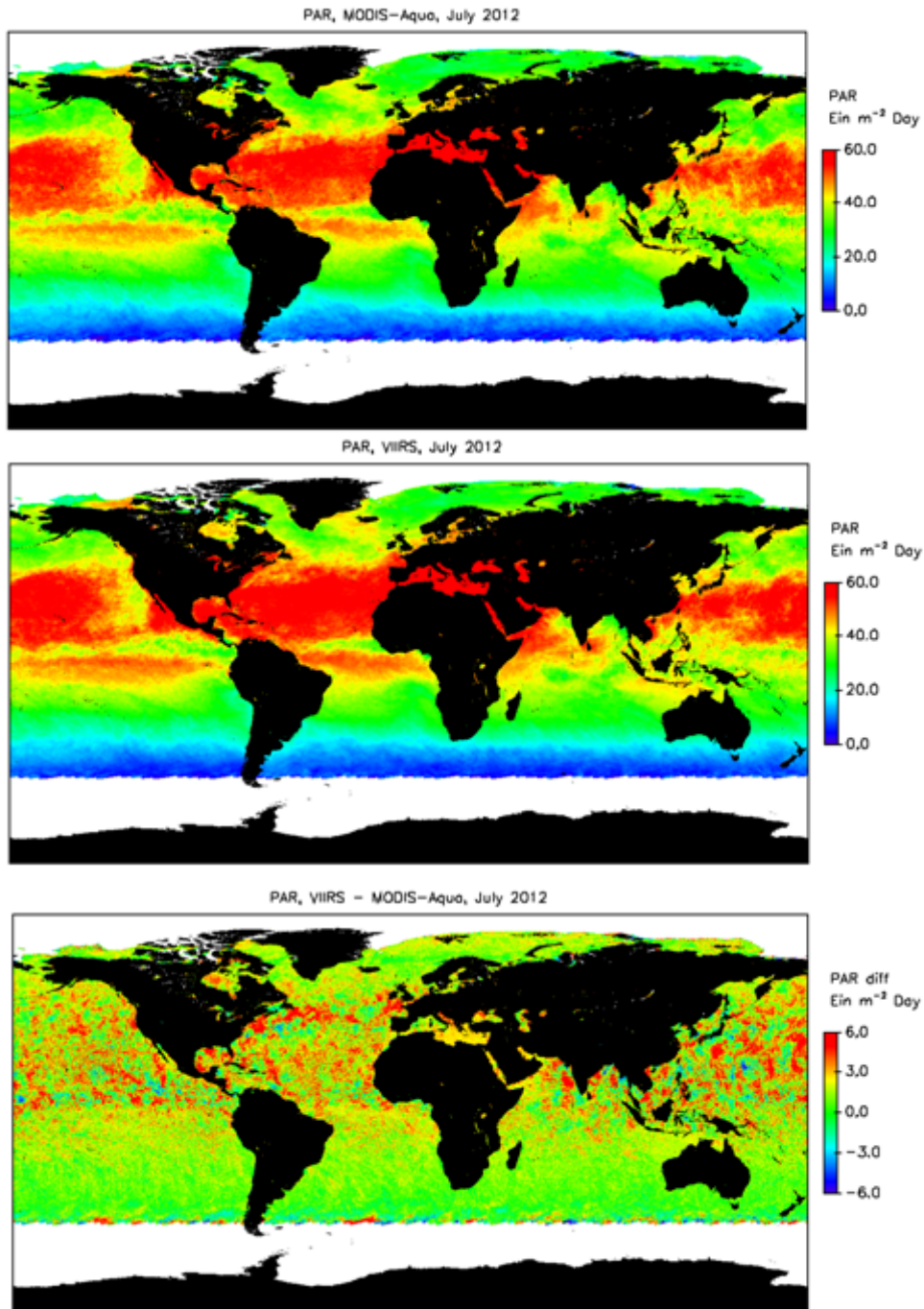


Fig. 21: Global 4-km monthly PAR products from MODIS-A (top), VIIRS (middle), and difference (bottom). July 2012.

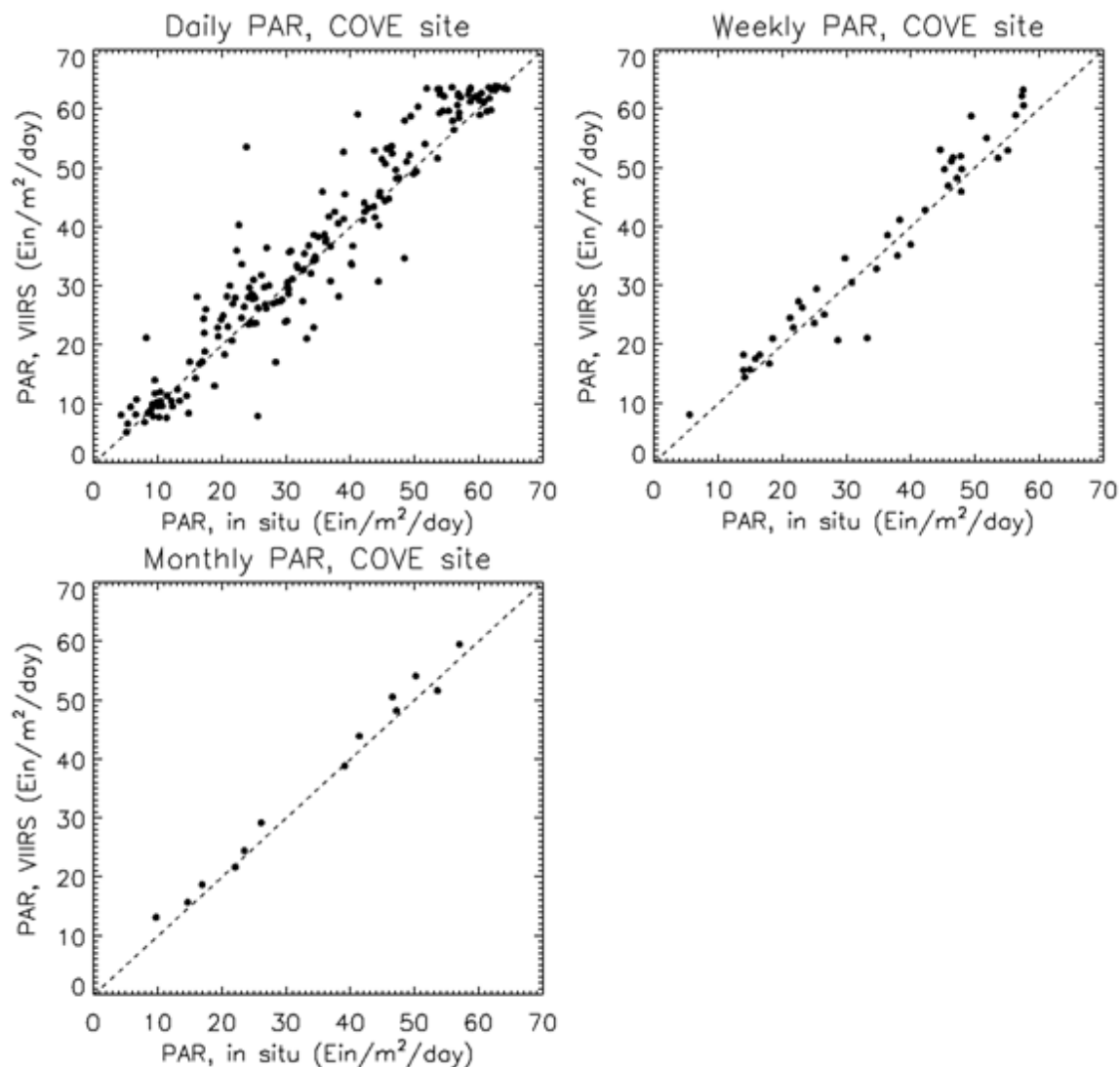


Fig. 22: Comparison of PAR estimated from VIIRS data with in situ measurements on daily, weekly, and monthly time scales. Time period is January 2012-January 2013. The in-situ data were collected at the COVE site, off Chesapeake Bay.

Table 6: VIIRS/In-Situ PAR comparison statistics, January 2012-January 2013, COVE site.

$r^2$	<i>Bias</i> ( $E/m^2/d$ )	<i>RMS</i> ( $E/m^2/d$ )
0.910	1.93 (5.6%)	5.81 (16.8%)
0.949	1.43 (4.2%)	4.05 (11.8%)
0.990	1.46 (4.5%)	2.32 (7.2%)

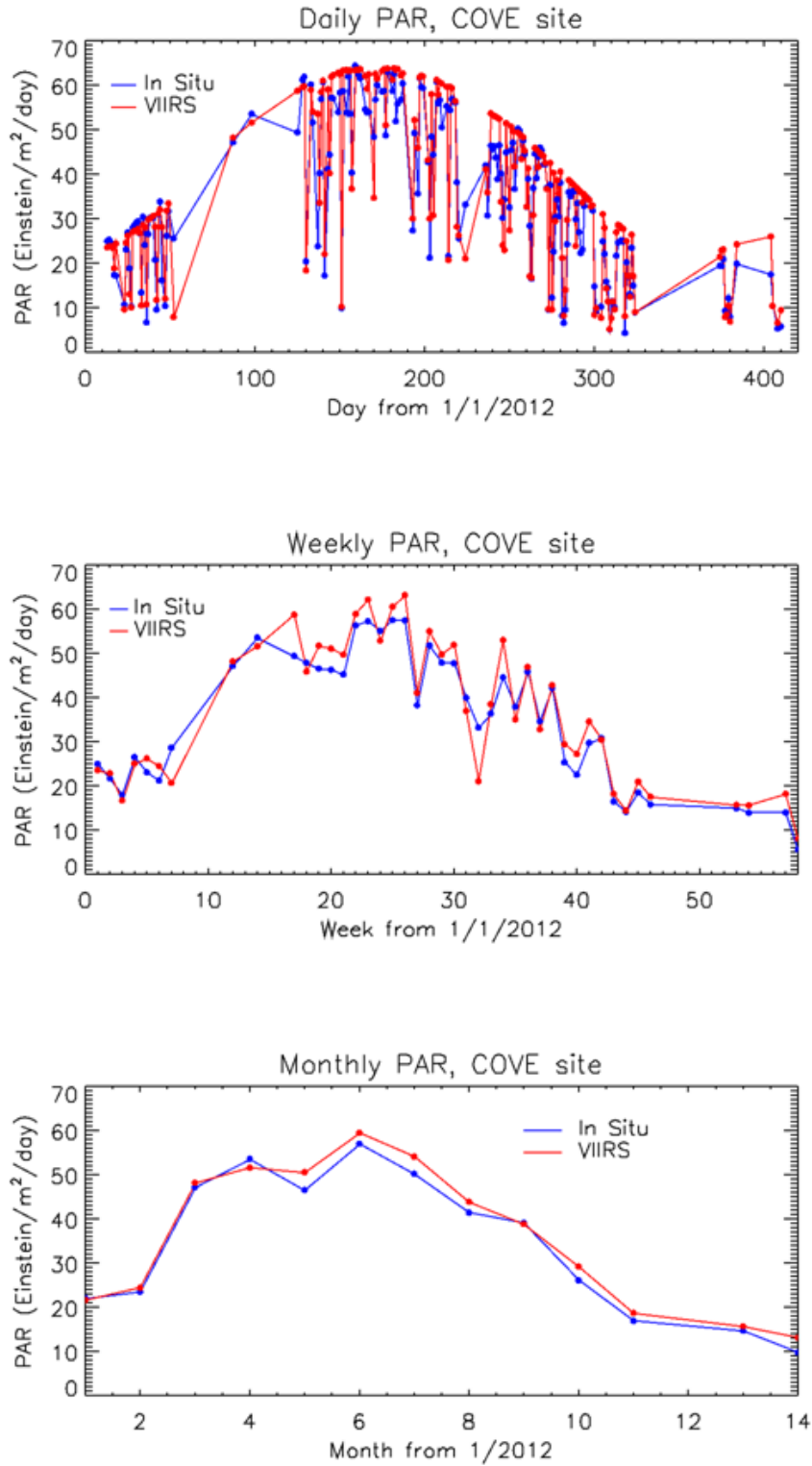


Fig. 23: Time series of PAR estimated from VIIRS data and measured at the COVE site on daily, weekly, and monthly time scales.

---

#### 2.4.4 CHLOROPHYLL CONCENTRATIONS AND INHERENT OPTICAL PROPERTIES

---

Semi-analytic ocean color algorithms tease apart competing optical properties that influence ocean color spectra (Kostadinov et al., 2007; Maritorena et al., 2002; Siegel et al., 2005). The UCSB group has developed and applied a semi-analytical algorithm, the Garver-Siegel-Maritorena (GSM) model, to simultaneously retrieve values of chlorophyll concentrations (Chl-a), the absorption coefficient for colored dissolved and detrital materials at 443 nm (CDM) and the particulate backscattering coefficient at 443 nm (BBP). The GSM model was optimized using a global data set of field observations of Rrs and Chl-a, CDM and BBP (Maritorena et al., 2002). We have also optimized the GSM model using PnB data (Kostadinov et al., 2007).

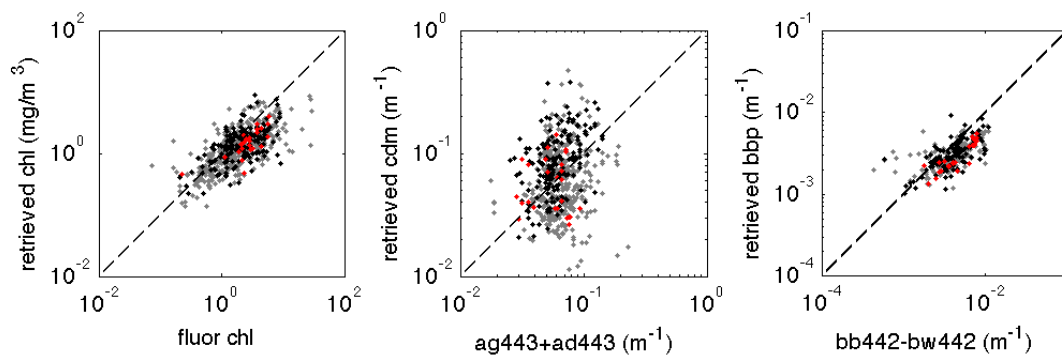


Fig. 24: Matchup comparison between field and satellite estimates of Chl-a, CDM and BBP from the locally optimized version of the GSM algorithm (Kostadinov et al. 2007).

The comparison between PnB-optimized GSM model retrievals is very encouraging for Chl-a and BBP for all three satellite data products (Fig. 24; regression slope and  $r^2$  for each parameter are given in Table 7). However the performance is not acceptable for CDM, especially for the S-NPP VIIRS matchups where a statistically insignificant relationship is found (Table 7). The poor performance for CDM is expected based upon the comparison of the Rrs(412) matchups. Note also that the regression slopes are always less than unity, showing again that the satellite observations are under predicting the field observations. As mentioned already, the performance for Chl-a and BBP is pretty good from the PnB-optimized GSM model independent of the satellite data source.

In summary the performance of the VIIRS-NPP data set as processed using the NASA algorithm (Dec 2012) is not far out of line with performance seen from MODIS-A or SeaWiFS. This is true for comparison of the Rrs, operational Chl-a and the locally optimized GSM model. The performance in the violet is poor for all three satellite data sources and is particularly bad for VIIRS-NPP. One hopes that this will improve as our knowledge of the instrument improves. However, the CDM retrievals remain troubling and advances will only come from satellite instrumentation advancements that will allow us to account for absorbing aerosols.

Table 7: Matchup Statistics for the Locally Optimized Version of the GSM Ocean Color Algorithm for the PnB Data Set

<b>SeaWiFS</b>	Chl	CDM	BBP
# matchups	369	332	166
Regression Slope	<b>0.57</b>	<b>0.21</b>	<b>0.40</b>
r <sup>2</sup>	<b>0.63</b>	<b>0.40</b>	<b>0.48</b>

<b>MODIS-A</b>	Chl	CDM	BBP
# matchups	164	168	120
Regression Slope	<b>0.49</b>	<b>0.69</b>	<b>0.53</b>
r <sup>2</sup>	<b>0.60</b>	<b>0.92</b>	<b>0.64</b>

<b>VIIRS-NPP</b>	Chl	CDM	BBP
# matchups	25	25	25
Regression Slope	<b>0.60</b>	-0.07	<b>0.76</b>
r <sup>2</sup>	<b>0.84</b>	0.56	<b>0.93</b>

Bold values are significant at the 95% c.i. level.

#### 2.4.5 EARLY RESULTS FROM THE SWIR METHOD OF ATMOSPHERIC CORRECTION

The traditional atmospheric correction over the ocean involves the Gordon and Wang (1994) algorithm, which assumes the contributions to the top-of-atmospheric signal from the ocean is negligible. With this assumption, the VIIRS NIR bands at 745 and 862 nm are used to determine aerosol reflectance estimation and correction (Gordon and Wang, 1994). However, the assumption that the ocean is completely dark at these wavelengths is often violated in regions of turbid or productive water, such along coasts, in estuaries, and in inland waters. To overcome the problems that arise, an alternative algorithm was developed (Wang, 2007) that uses the Shortwave Infrared (SWIR) bands in place of the NIR bands. The SWIR-based atmospheric correction algorithm (Wang, 2007) has been developed and implemented in the NOAA-MSL12 package for VIIRS ocean color processing with the VIIRS SWIR bands of 1238, 1610, and 2250 nm, and some preliminary results from Wang are presented in the report.

Results derived using the SWIR-based atmospheric correction algorithm are shown in Fig. 25 and Fig. 26. Fig. 25 provides global VIIRS ocean color products on September 25, 2012 derived from the NOAA-MSL12 using the SWIR bands 1238 and 2250 nm for Chl-a (Fig. 25(a)),

$nL_w(443)$  (Fig. 25(b)),  $nL_w(551)$  (Fig. 25(c)), and  $nL_w(671)$  (Fig. 25(d)), respectively. We found these global daily images are comparable to those from the NIR algorithm. In coastal regions, however, results from the SWIR algorithm are improved compared with those from the NIR algorithm. For example, Fig. 26 shows histograms of the VIIRS-derived  $nL_w(412)$  on Sep. 25, 2012 over highly turbid waters in China's east coastal region for cases of using the NOAA-MSL12 with the NIR algorithm (Fig. 26(a)) and the SWIR 1238 and 2250 nm algorithm (Fig. 26(b)). It shows that results from the SWIR algorithm have been significantly improved with much less negative  $nL_w(412)$  data. However, this work is on going.

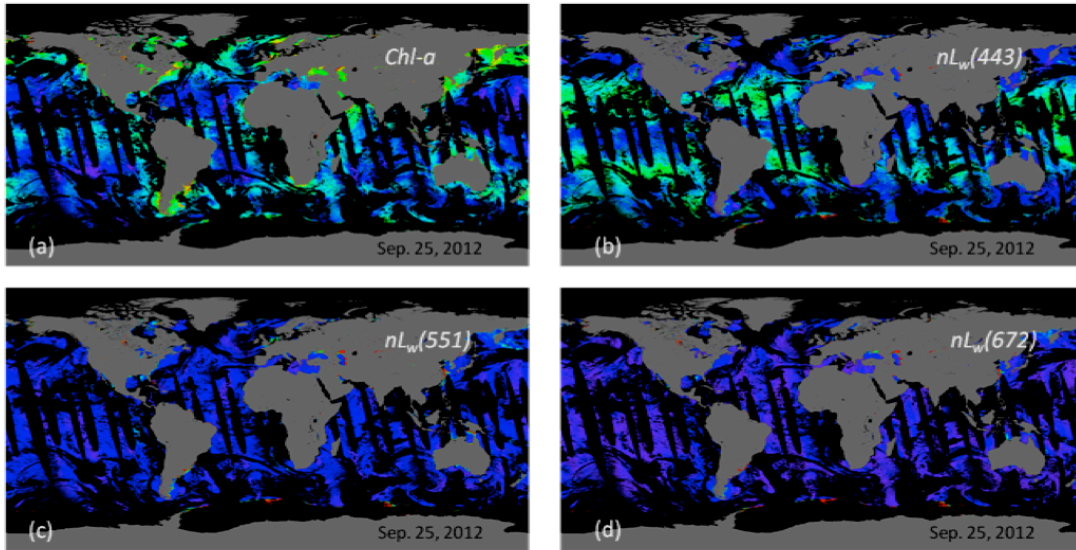


Fig. 25: Global VIIRS ocean color products on Sep. 25, 2012 derived from the NOAA-MSL12 using the VIIRS SWIR 1238 and 2250 nm bands for (a) Chl-a, (b)  $nL_w(443)$ , (c)  $nL_w(551)$ , and (d)  $nL_w(671)$ . Note scales are the same as in Figs. 1-3.

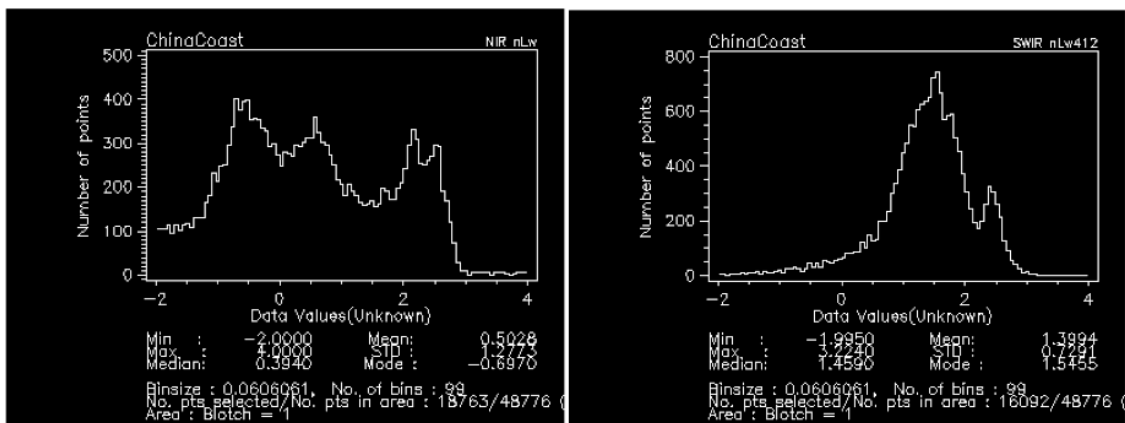


Fig. 26: Histograms of the VIIRS-derived normalized water-leaving radiance at the wavelength of 412 nm  $nL_w(412)$  on Sep. 25, 2012 over highly turbid waters in China's east coastal region for cases of using (a) NOAA-MSL12 with the NIR algorithm and (b) NOAA-MSL12 with the SWIR (1238 and 2250 nm) algorithm.

---

## 2.4.6 ASSIMILATING GLOBAL OCEAN CHLOROPHYLL FROM SUOMI NPP-VIIRS: PROSPECTS FOR EXTENDING THE OCEAN COLOR TIME SERIES

---

The Suomi NPP mission is intended to continue the time series of global ocean color data. It follows the succession of OCTS (1996-1997), SeaWiFS (1997-2010) and MODIS-Aqua (2002-present). As with all new ocean color sensors, VIIRS was expected to exhibit discrepancies with previous and concurrent missions, including SeaWiFS and MODIS-Aqua. We initially evaluate the first 12 months of global ocean data from VIIRS and compare with MODIS-Aqua data.

Level-3 9KM VIIRS global chlorophyll data compares favorably with MODIS-Aqua for 2012. There is divergence in the seasonal cycle, but the mean difference is -3.5% (VIIRS lower). In coastal waters (<200m), chlorophyll concentration from VIIRS are 7.5% higher than those from MODIS-Aqua (Table 8). Similarly, the uncertainty of chlorophyll data is slightly higher in the coastal waters compared to the open ocean.

Table 8: Point comparisons of 9 km VIIRS and MODIS-Aqua for 2012.

	Global	Open Ocean (>200m)	Coast (<200m)
Bias	-3.5%	-3.7%	7.5%
Uncertainty	12.7%	12.8%	16.4%
Correlation	0.979	0.962	0.943
N	123745	108058	14301

The distribution of differences shows that VIIRS modestly overestimates chlorophyll in the tropics (Fig. 27). The differences are much larger in the northern high latitudes and alternate between overestimates by VIIRS and a very large underestimate along the western sides of both the North Pacific and North Atlantic. In the Southern regions, VIIRS is always within 10% of MODIS. In the northern latitudes, chlorophyll concentrations from VIIRS are always within 8% of that of MODIS. The distribution of the differences is shown in Fig. 28.

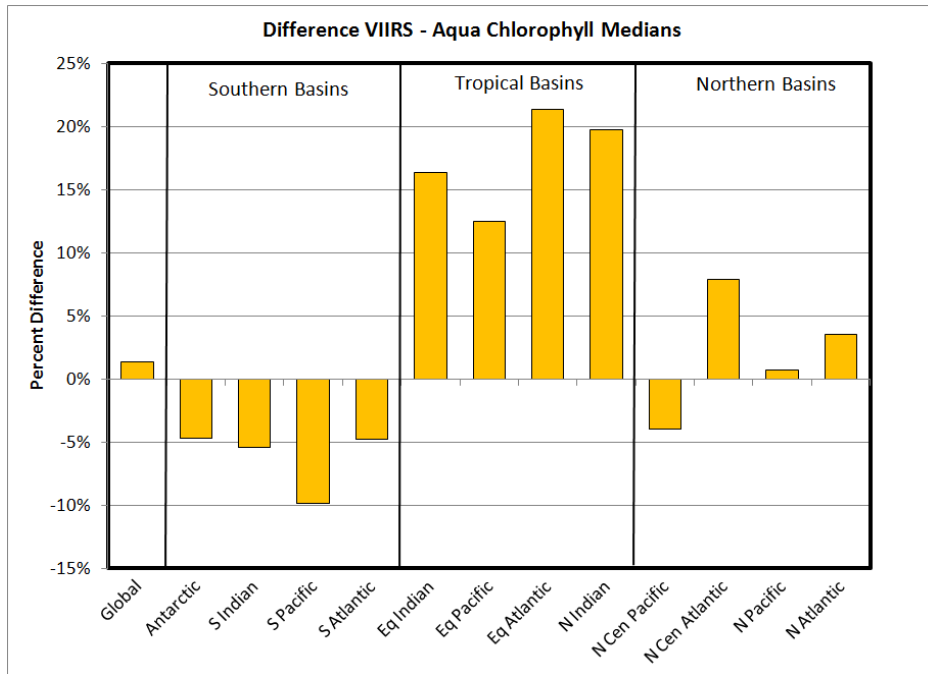


Fig. 27: Percentage difference in chlorophyll between the regional medians for the 14 major oceanographic basins between VIIRS and MODIS Aqua.

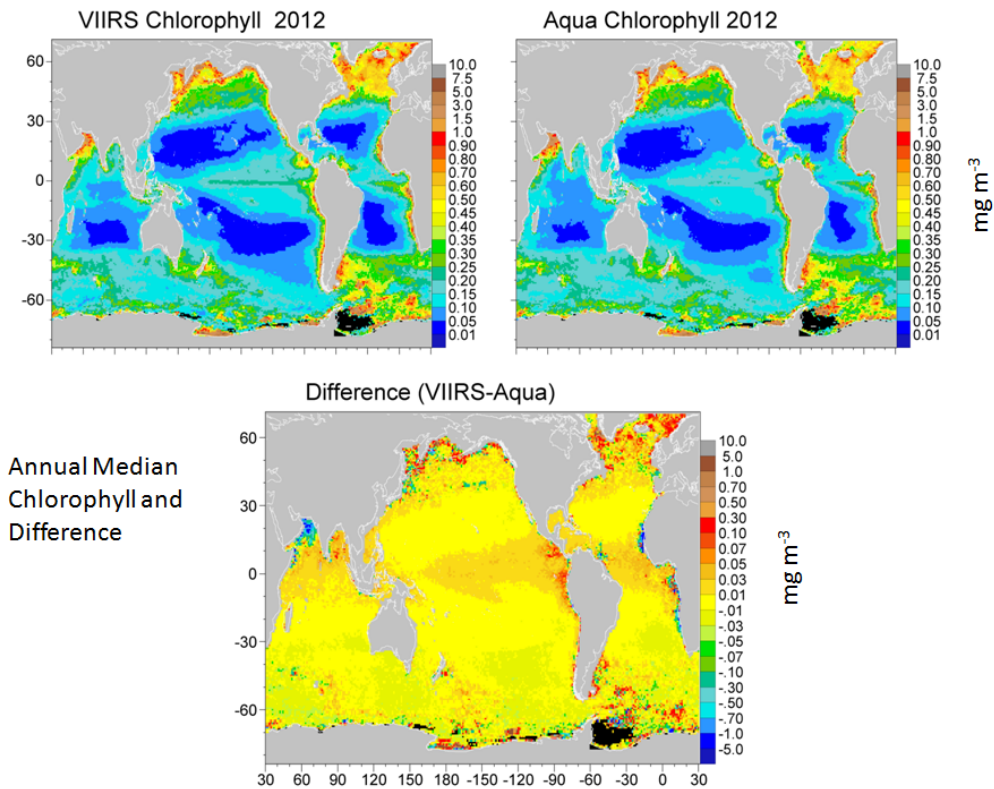


Fig. 28: VIIRS chlorophyll annual median (top left) and MODIS-Aqua (top right). The difference is shown at the bottom.

One source of discrepancies between chlorophyll concentration from MODIS and VIIRS originates from the gaps in sampling. Ocean color missions typically observe only about 15% of the ocean per day, due to inter-orbit gaps, insufficient light for detection at high latitudes, sun glint, clouds, and aerosols. Data assimilation rectifies these problems, and removes biases associated with these data gaps by producing complete daily coverage (Gregg and Casey, 2007). The biases caused by the sampling are considerable (Fig. 29).

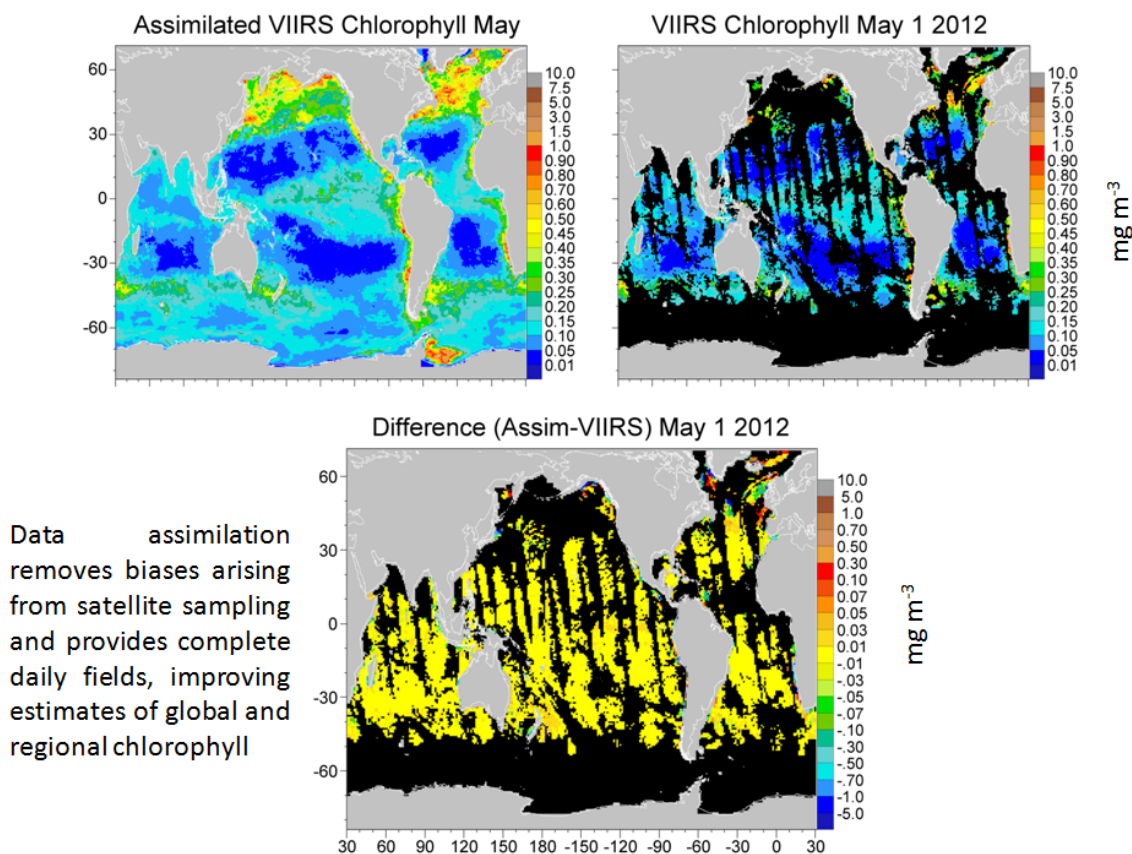


Fig. 29: The effects of data assimilation on one-day ocean coverage of chlorophyll. Top left: assimilated VIIRS chlorophyll for May 1 2012. Top right: VIIRS chlorophyll for the same day. Bottom: difference.

Data assimilation of both MODIS-Aqua and VIIRS reduces the differences in the high latitudes and the Indian Ocean (Fig. 30). Unfortunately, however, the differences in the tropical Pacific and Atlantic are actually increased (Fig. 30). Fig. 31 shows the differences between the assimilation and the satellite data on maps and quantitatively in a bar graph. We note that the problems observed in the tropics is not new to the December re-processing, and was apparent in the one of the other versions that predated December (Table 9).

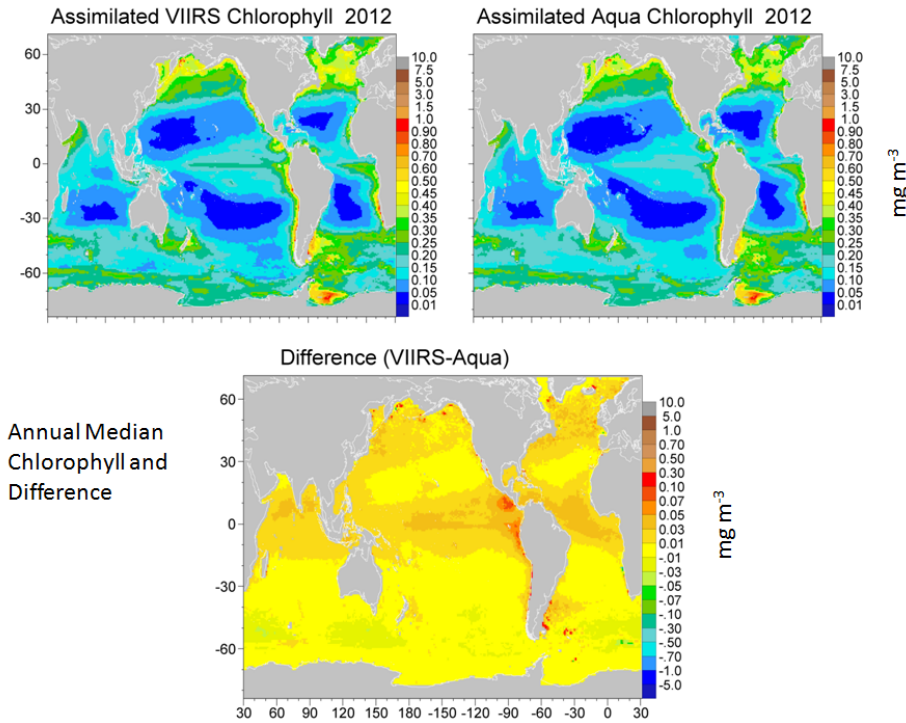


Fig. 30: Assimilated VIIRS chlorophyll annual median (top left) and assimilated MODIS-Aqua (top right). The difference is shown at the bottom.

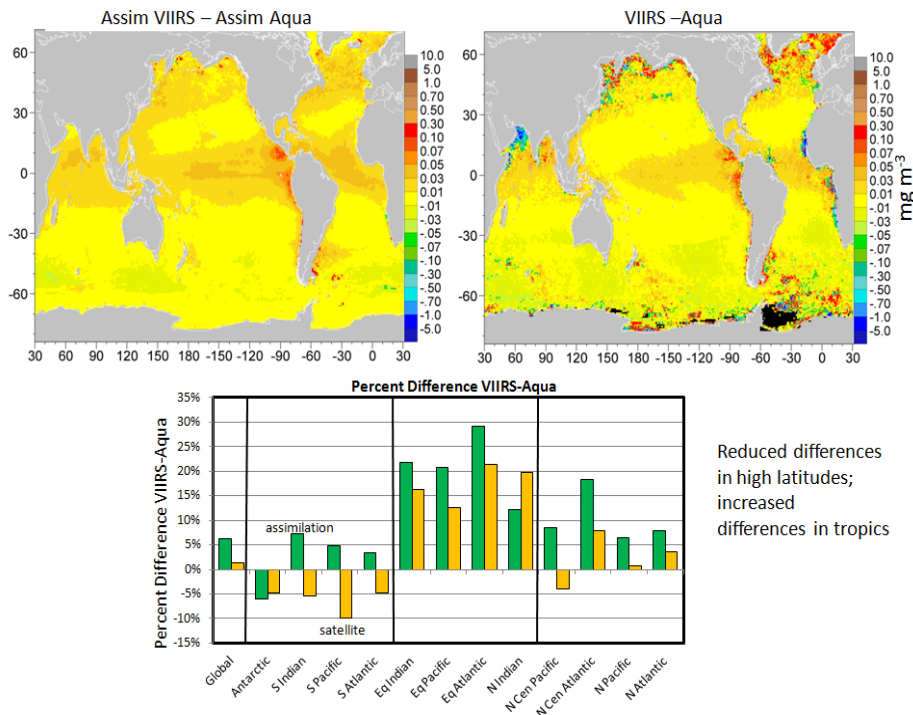


Fig. 31: Differences in VIIRS-MODIS in the assimilation and in the data, as annual medians. Note that the differences in high latitudes are reduced by the assimilation, but accentuated in the tropics, especially the Pacific. The differences are quantified in the bar graph at bottom.

The results suggest promise for extending a consistent ocean color time series but there is more work to be done. Perhaps application of our bias-correction method (Gregg and Casey, 2010; Gregg et al., 2009) can reduce the differences even more. However, this requires substantial amounts of in situ data that were not available in time for the production of this report. An additional possibility is the lack of masking for cloud shadows in the NASA VIIRS data products. These unmasked cloud shadows are consistent with the geographical distributions of the differences. This hypothesis is currently being tested by comparing the flagged values from the EDR (mapped by OBPG) with those from the NASA reprocessing and these results will be available for the next report.

Table 9: Previous results: Global Mean Differences VIIRS-Aqua. Previous versions of VIIRS processing, approximate dates, and results. We did not address the tropics in the first version, so it is listed as not available.

	Data	Assimilation	Bias-corrected Assimilation	Tropics Problem?
May 2012 Version	2.0%	16.9%	9.0%	N/A
Oct 2012 Version	3.6%	15.7%	9.8%	Yes
Dec 2012 version	2.8%	6.8%	6.4%	Yes

---

## 2.5 PRODUCT EVALUATION

---

A two-pronged approach was taken in the evaluation of the NOAA EDR products. In the first presented here, Wang (NOAA) examines the ocean color EDR parameters to MODIS Aqua, in situ data, and NOAA research software based on NASA algorithms. In the second, Turpie and McClain focus on whether NOAA EDR products can continue the NASA CDR. The latter approach is referred to by the authors as *constructive*, in that it builds a research processing capability on existing NASA computational infrastructure and management. In both approaches, the question as to whether VIIRS raw data have the potential to meet NASA or NOAA science requirements is addressed.

---

### 2.5.1 NOAA EFFORT

---

The NOAA effort includes some initial evaluations and assessments of VIIRS ocean color data products, or ocean color Environmental Data Records (EDR) (Level-2 data), including normalized water-leaving radiance spectra  $nL_w(\lambda)$  at VIIRS five spectral bands (M1 to M5) and chlorophyll *a* concentration (Chl-*a*). Specifically, VIIRS ocean color products derived from VIIRS operational data processing, i.e., Interface Data Processing Segment (IDPS), are evaluated and compared with those from the NOAA-MSL12 (Multi-Sensor Level-1 to Level-2) ocean color data processing system, as well as from in situ measurements. In addition, VIIRS Sensor Data Records (SDR) (Level-1B data) have been evaluated. In particular, VIIRS SDR and ocean color EDR have been evaluated with a series of in situ data from the Marine Optical Buoy (MOBY) in the waters off Hawaii (Clark et al., 1997). It is noted that in this report MOBY in situ radiance data have been used as an independent data set, i.e., vicarious gains derived from MOBY measurements have not been applied for deriving VIIRS IDPS ocean color data product.

#### 2.5.1.1 DATA AND METHOD

##### 2.5.1.1.1 VIIRS IDPS-SDR/EDR Data

The Suomi NPP VIIRS SDR (Level-1B) and IDPS-produced EDR (Level-2) data are downloaded routinely from the NPP central technical support infrastructure GRAVITE and the NOAA Comprehensive Large Array-data Stewardship System (CLASS). The IDPS-produced EDR data files contain chlorophyll *a* concentration, normalized water-leaving radiance spectra ( $nL_w(\lambda)$ ) and IOPs (absorption and backscattering coefficients) from VIIRS bands M1 to M5 (at nominal center wavelengths of 410, 443, 486, 551, and 671 nm, respectively), as well as relevant quality flags. The VIIRS SDR data include the VIIRS-measured top-of-atmosphere (TOA) radiance/reflectance from M1 to M11, geo-location data, cloud mask intermediate product, and on-board-calibration intermediate products. The VIIRS shortwave infrared (SWIR) bands include M8, M10, and M11 at wavelengths of 1238, 1610, and 2250 nm, respectively. The SDR, geo-location data, various intermediate products, and on-board-calibration data are required for processing VIIRS SDR (Level-1B) to EDR (Level-2) using the IDPS-like data processing software, i.e., the Algorithm Development Library (ADL). All VIIRS data started from November 21, 2011 to present have been downloaded to generate VIIRS EDR products.

---

### 2.5.1.1.2 NOAA-MSL12 Level-2 Ocean Color Products

The NOAA-MSL12 ocean color data processing package is developed based on the NASA SeaDAS version 4.6, which has been used to process various satellite ocean color data from the level-1 to level-2, e.g., SeaWiFS, MODIS. It has been enhanced to include the function to process ocean color data for Suomi-NPP-VIIRS at the NOAA Center for Satellite Applications and Research (STAR) Ocean Color EDR Team. NOAA-MSL12 has been used to process IDPS SDR data to ocean color EDR (Level-2) data from the start of the VIIRS mission. The input data of NOAA-MSL12 include VIIRS SDR data from M1 to M7, geo-location data, and the on-board-calibration intermediate product. The ancillary input data include ozone concentration, surface atmosphere pressure, sea surface wind speed, and water vapor, which are obtained from the NCEP definitive ancillary data. The NCEP definitive ancillary data set is an assimilated data product from Global Forecast System (GFS). For near-real-time data processing, ancillary data from the GFS model are used (Ramachandran and Wang, 2011). The NOAA-MSL12 output products include chlorophyll *a* concentration,  $nL_w(\lambda)$  for VIIRS M1 to M5 bands, diffuse attenuation coefficient at the wavelength of 490 nm  $K_d(490)$ , etc., as well as various level-2 data quality flags.

*The NIR Method* In the NOAA-MSL12 software package for current VIIRS ocean color data processing, the atmospheric correction uses the Gordon and Wang (1994) algorithm, which uses two VIIRS NIR bands at 745 and 862 nm for aerosol reflectance estimation and correction (Gordon and Wang, 1994). The chlorophyll *a* concentration algorithm for VIIRS is OC3V, which is similar to OC3M for MODIS (O'Reilly et al., 1998; O'Reilly et al., 2000), but with different coefficients tuned for VIIRS spectral bands.

*The SWIR Method* Furthermore, the SWIR-based atmospheric correction algorithm (Wang, 2007) has been developed and implemented in the NOAA-MSL12 package for VIIRS ocean color processing with the VIIRS SWIR bands of 1238, 1610, and 2250 nm, and some preliminary results are presented in the report.

*VIIRS Data Processing* In addition, at NOAA/STAR, we have developed a global near-real-time VIIRS ocean color data processing system, in which the NOAA-MSL12 software is embedded for VIIRS Level-1B (SDR) to Level-2 (EDR) data processing. The system automatically downloads global VIIRS IDPS SDR data and ancillary data in near-real-time, and then processes them into ocean color Level-2 (EDR) data using the NOAA-MSL12 software, and stores the level-2 (EDR) output data in a designated area in the system for analysis and evaluation. There are ~550 incoming VIIRS daytime granules per day, and it takes less than ~two hours to process. For the timeliness, there is currently less than about one week time-delay for global data processing, and it can be improved to 24-hour delay when the data flow becomes stable. The system is also flexible for reprocessing VIIRS ocean color data from VIIRS Raw Data Records (RDR) (Level-0) to SDR (Level-1B), and from SDR to EDR (Level-2) data, for future VIIRS ocean color algorithm development and testing.

It should be noted that the NOAA-MSL12 is used to evaluate and understand the VIIRS IDPS-produced ocean color products. Furthermore, the NOAA-MSL12 package can be used to improve the IDPS-produced ocean color data products.

---

We are currently working on the vicarious calibration for the IDPS data processing using the MOBY in situ data. In fact, some tests with vicarious calibrations have been done. However, the IDPS level-2 data used in this study are processed without applying the vicarious calibration gains. Thus, MOBY in situ data can be used as an independent data set for evaluation and assessment of VIIRS-derived ocean color products.

#### **2.5.1.1.3 IDPS and NOAA-MSL12 Level-3 Data**

The global near-real-time VIIRS ocean color data processing system in NOAA/STAR is also processing the NOAA-MSL12 level-2 and IDPS EDR data into global Level-3 data. It should be noted that the IDPS does not produce global Level-3 products. For effective evaluation of global VIIRS ocean color data quality, VIIRS ocean color global Level-3 data products are necessary. The Level-3 data processing algorithm is essentially the same as the one used for producing SeaWiFS and MODIS global Level-3 ocean color products (Hooker et al., 1995). Specifically, in the level-3 data processing, pixels containing valid level-2 data are mapped to a fixed spatial grid with resolution of  $9 \times 9 \text{ km}^2$ . The grid elements or bins are arranged in rows beginning at the South Pole. Each row begins at  $180^\circ$  longitude and circumscribes the Earth at a given latitude. Within each bin, statistics of mean or median are accumulated for periods of one day, eight days, and one month.

Currently, both NOAA-MSL12 level-2 and IDPS EDR are processed routinely into global level-3 data with 9-km spatial resolution. For daily spatial binning, the mathematical mean is calculated for all valid pixels within a bin; and for 8-day and monthly temporal binning, a median is calculated based on the daily mean, so that freckles and outliers can be removed from the global image. Before the binning process, all standard flags in the IDPS data processing (e.g., sun glint, high sensor-zenith angle, high solar-zenith angle, atmospheric correction failure, snow/ice, etc.) are applied to remove these flagged data in the IDPS level-2 product data, while three flags (high sun glint, high sensor-zenith angle, and high solar-zenith angle) are applied to the NOAA-MSL12 level-2 data. In the IDPS ocean color EDR products, however, the sun glint flag is from IDPS ocean color EDR inherited from cloud mask intermediate product, and its high sun glint area is much wider than that from the NOAA-MSL12. In addition, for the IDPS products, Horizontal Reporting Interval (HRI) flag is used as the high sensor-zenith angle. The HRI flag is equivalent to  $53^\circ$  of sensor-zenith angle, which is less than NOAA-MSL12 high sensor-zenith angle of  $60^\circ$ . Thus, some significant amounts of data are missing in the IDPS global level-3 data.

For time series analyses of VIIRS ocean color products, daily mapped VIIRS IDPS EDR and NOAA-MSL12 data at 1-km spatial resolution are used.

#### **2.5.1.1.4 In Situ Data**

In situ radiometric data were obtained from the MOBY site moored off the island of Lanai in Hawaii (<http://moby.mlml.calstate.edu/MOBY-data>) to evaluate VIIRS SDR and ocean color EDR products. The in situ  $nL_w(\lambda)$  measurements at the VIIRS-spectral-weighted wavelengths from November of 2011 to present are used to assess and evaluate the VIIRS-derived ocean color products. It is particularly noted that in this study the MOBY in situ data were used as an independent data set for IDPS ocean color products, i.e., vicarious gains derived from the MOBY measurements were not applied to derive IDPS-measured ocean color radiance

---

products. With this purpose for MOBY data application, MOBY in situ data are also extremely useful to evaluate IDPS SDR performance as well as its data quality.

In addition, some AERONET-OC in situ data are used for evaluation of VIIRS-measured normalized water-leaving radiance spectra  $nL_w(\lambda)$ .

## 2.5.1.2 RESULTS

### 2.5.1.2.1 Global Images

*Results of Chl-a and  $nL_w(\lambda)$ .* Fig. 32, Fig. 33 and Fig. 34 provide color images for global level-3 composite distributions of the VIIRS Chl-a,  $nL_w(443)$ , and  $nL_w(551)$  derived from IDPS and NOAA-MSL12 data processing for the daily (August 12, 2012), 8-day (August 12–19, 2012), and monthly (August of 2012). Fig. 32(a), Fig. 32(c), and Fig. 32(e) are color images of Chl-a for VIIRS IDPS-derived daily, 8-day, and monthly composite image, respectively, while Fig. 32(b), Fig. 32(d), and Fig. 32(f) are those from NOAA-MSL12 data processing. Composite images of VIIRS Chl-a data derived from both IDPS and NOAA-MSL12 data processing provide reasonable and similar spatial distribution in August, showing low Chl-a data in mid-Atlantic and South Pacific gyre, highs in high latitude of the Northern hemisphere and equatorial region. However, there are considerably large data missing in IDPS-derived Chl-a images, compared with those from NOAA-MSL12. In the monthly composite images of August of 2012, large gaps of IDPS-derived Chl-a data are shown (e.g., the central North Pacific ocean, eastern boundary of Pacific ocean, western ocean of Africa, Arabian sea and Indian Ocean), while most of areas are covered in the NOAA-MSL12 Chl-a image except Arabian Sea. Noticeably, data in all inland lakes are masked out in IDPS-derived Chl-a, while there are retrievals in these regions from the NOAA-MSL12, e.g., the Great Lakes. In addition, Chl-a values are slightly high in IDPS Chl-a image compared with those from NOAA-MSL12 data processing.

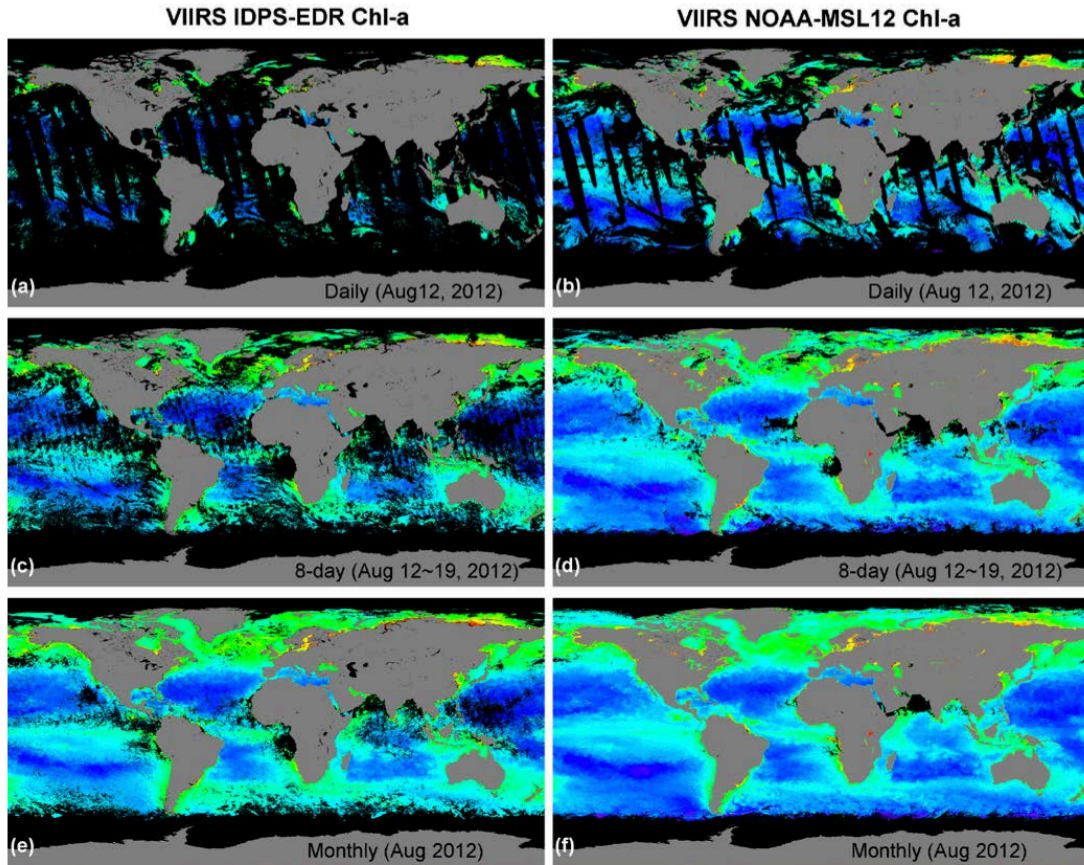


Fig. 32: Global VIIRS chlorophyll  $a$  composite images for (a) and (b) daily (August 12, 2012), (c) and (d) 8- day (August 12–19, 2012), and (e) and (f) monthly (August of 2012). Plots (a), (c), and (e) were derived from IDPS-EDR data, while plots (b), (d), and (f) were derived from NOAA-MSL12-produced data. Note scale for Chl- $a$  is in log-scale from 0.01 to 64  $\text{mg}/\text{m}^3$ .

Fig. 33 and Fig. 34 are color images of VIIRS  $nL_w(443)$  and  $nL_w(551)$ , respectively. The general spatial distribution patterns of the VIIRS  $nL_w(443)$  and  $nL_w(551)$  are similar to those of the Chl- $a$  images, and again more missing data in IDPS-derived  $nL_w(443)$  and  $nL_w(551)$  global images. The  $nL_w(443)$  and  $nL_w(551)$  values of IDPS data are relatively lower than those of NOAA-MSL12 data.

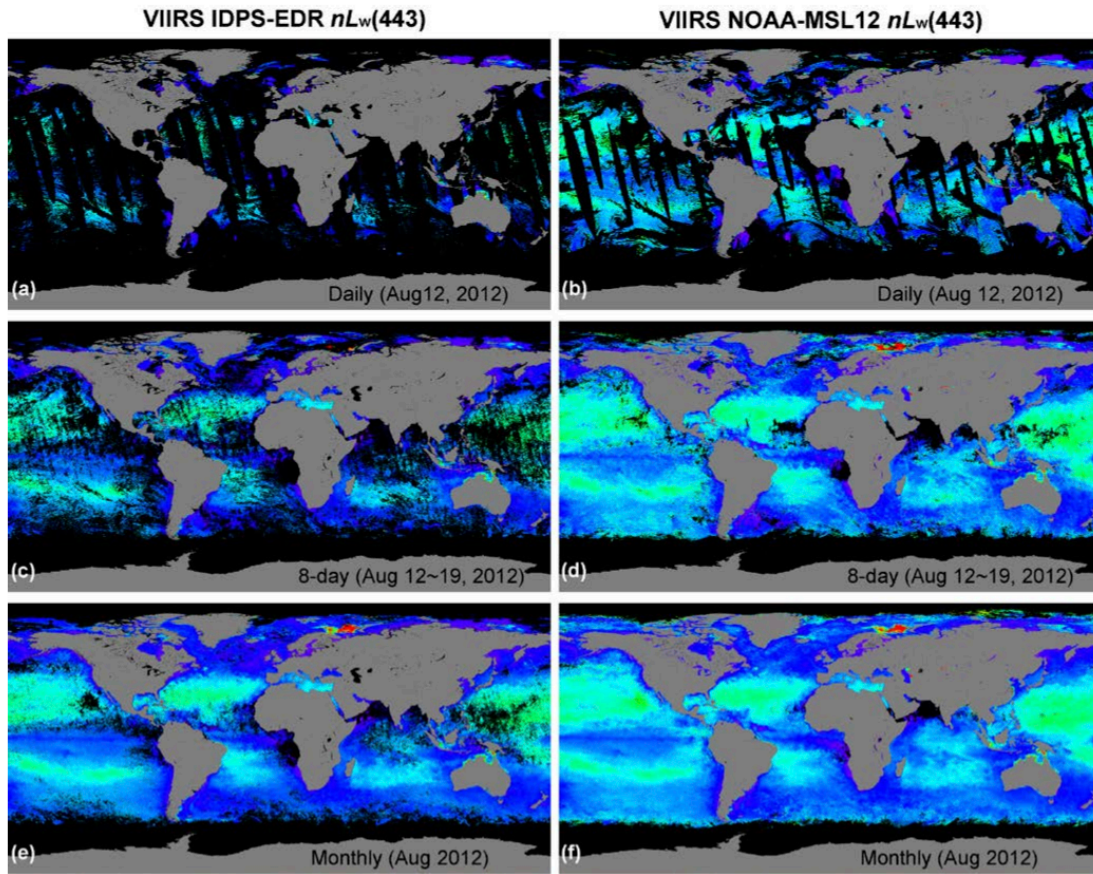


Fig. 33: Global VIIRS nLw(443) images for (a) and (b) daily (August 12, 2012), (c) and (d) 8-day (August 12– 19, 2012), and (e) and (f) monthly (August of 2012). Plots (a), (c), and (e) were derived from IDPS-EDR data, while plots (b), (d), and (f) were derived from NOAA-MSL12-produced data. Note scale for nLw(443) is  $0\text{--}5 \text{ mW cm}^{-2} \mu\text{m}^{-1} \text{ sr}^{-1}$ .

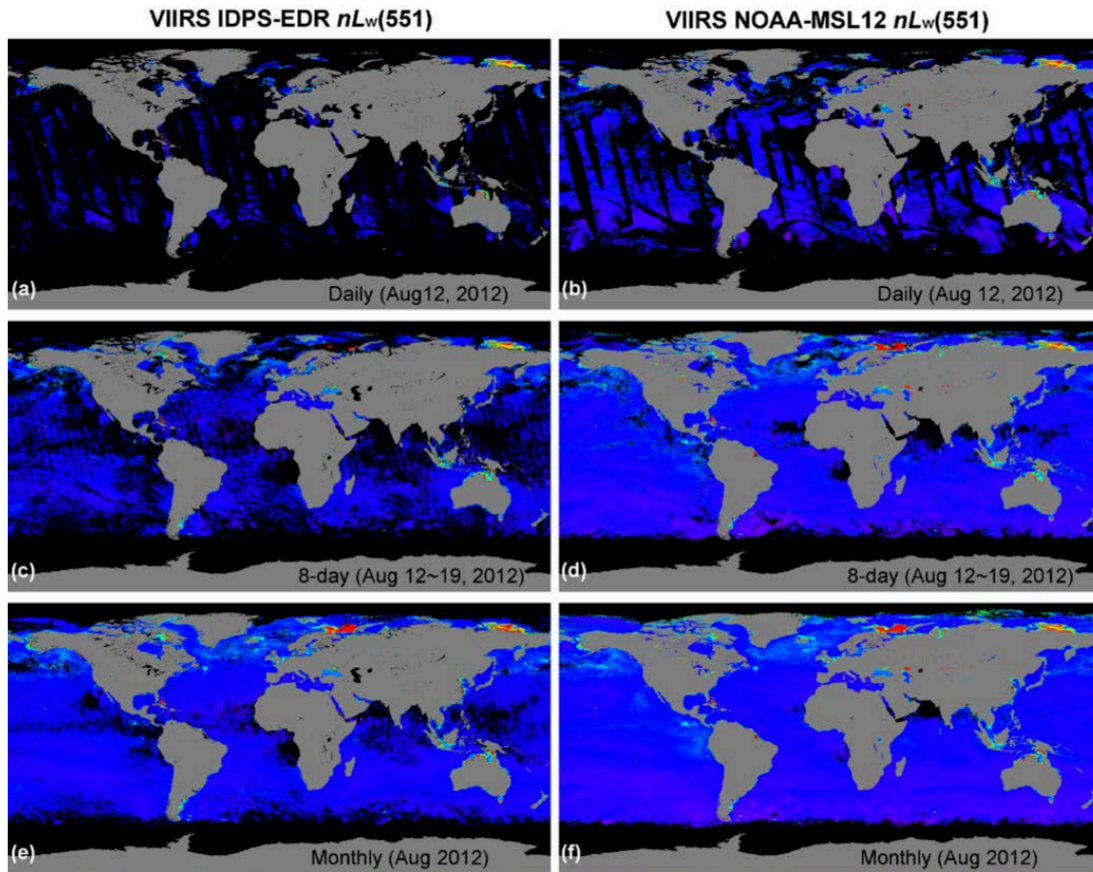


Fig. 34: Global VIIRS  $nL_w(551)$  images for (a) and (b) daily (August 12, 2012), (c) and (d) 8-day (August 12– 19, 2012), and (e) and (f) monthly (August of 2012). Plots (a), (c), and (e) were derived from IDPS-EDR data, while plots (b), (d), and (f) were derived from NOAA-MSL12-produced data. Note scale for  $nL_w(551)$  is  $0\text{--}3 \text{ mW cm}^{-2} \mu\text{m}^{-1} \text{ sr}^{-1}$ .

The reasons for IDPS data missing issue have been identified, and the data missing issue is being worked on and will be resolved soon.

*VIIRS IDPS Results Compared with MODIS-Aqua.* Fig. 35 shows color images for global level-3 monthly (August of 2012) composite distributions of the VIIRS Chl-a,  $nL_w(443)$ , and  $nL_w(551)$  derived from IDPS and MODIS-Aqua. MODIS-Aqua data were from NASA/OBPG. These results show that IDPS produces similar global ocean color distributions as compared with those from MODIS-Aqua. It is noted again data missing over coastal and inland waters from IDPS products.

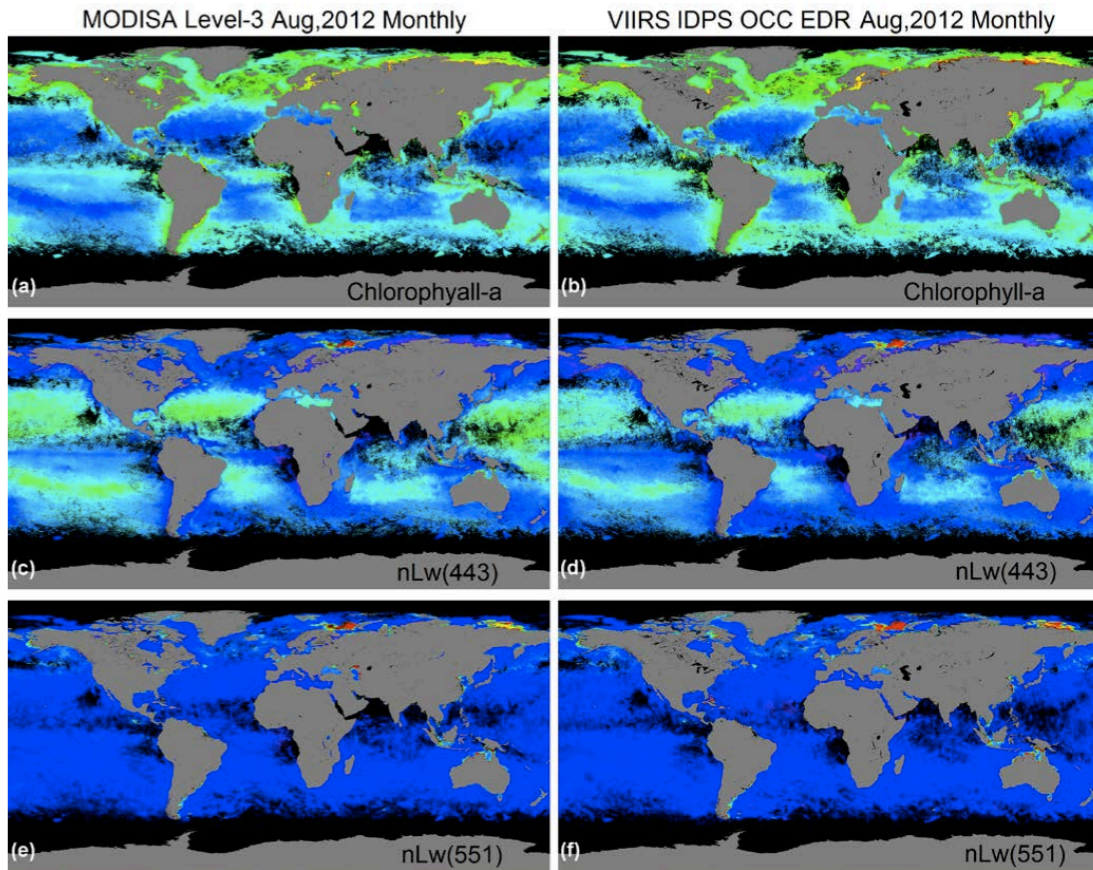


Fig. 35: Global monthly (August of 2012) VIIRS IDPS ocean color images compared with those from MODIS-Aqua for (a) and (b) chlorophyll *a*, (c) and (d)  $nL_w(443)$ , and (e) and (f)  $nL_w(551)$ . Plots (a), (c), and (e) were from MODIS-Aqua data (from NASA/OBPG), while plots (b), (d), and (f) were derived from IDPS- produced EDR data. Note scales are the same as in Fig. 32, Fig. 33 and Fig. 34.

#### 2.5.1.2.2 Time Series

Time series of the daily VIIRS  $nL_w(\lambda)$  data at wavelengths of 410, 443, 486, 551, and 671 nm derived from IDPS and NOAA-MSL12 data processing are constructed for the Hawaii MOBY site (20.5°N–21.5°N and 157.5°W–156.5°W), and compared with those of  $nL_w(\lambda)$  measurements obtained at the MOBY site (Fig. 36) for assessment of VIIRS EDR data quality. Fig. 36 shows time series of the VIIRS ocean color products from IDPS (black triangles) and NOAA-MSL12 (red circles) data processing from November 22, 2011 to August 31, 2012. In addition, the time series of the in situ  $nL_w(\lambda)$  measurements from the MOBY site are compared with the VIIRS data. The VIIRS  $nL_w(\lambda)$  values derived from NOAA-MSL12 data processing have significant noise caused by low data quality issue before February 6, 2012 due to errors in SDR calibration look-up-table (LUT). Most of  $nL_w(\lambda)$  values are highly biased compared with the in situ  $nL_w(\lambda)$  measurements at the MOBY site, and some values of VIIRS  $nL_w(410)$  from NOAA-MSL12 are low. However, there are no valid data in IDPS-produced  $nL_w(\lambda)$  before February 6, 2012 due to very strict flag masking in IDPS data processing.

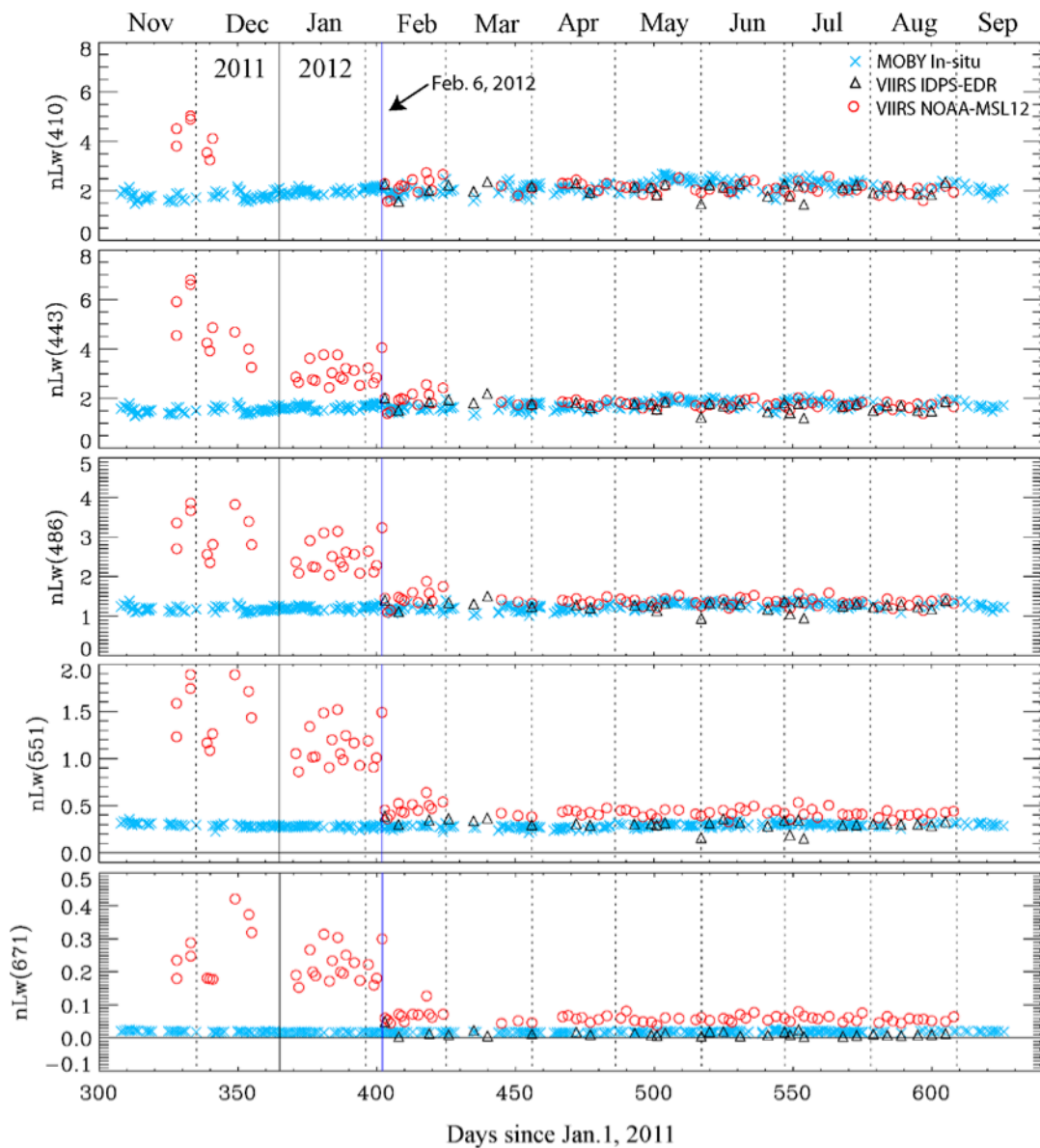


Fig. 36: Time series of the daily VIIRS  $nL_w(410)$ ,  $nL_w(443)$ ,  $nL_w(486)$ ,  $nL_w(551)$ , and  $nL_w(671)$  data derived from IDPS-EDR (black triangles) and NOAA-MSL12 (red circles) data processing in the South Pacific gyre from November 2011 to August 2012. In situ MOBY  $nL_w(\lambda)$  measurements are indicated as light blue x. Note IDPS data are significantly less than those from NOAA-MSL12. No vicarious calibrations were applied to both IDPS and NOAA-MSL12 data processing.

After using the correct/improved SDR LUTs (since February 6, 2012), noise and bias errors in VIIRS  $nL_w(\lambda)$  values from NOAA-MSL12 data processing are significantly reduced and the values are quite reasonable. However, there are still some slightly high anomalies in VIIRS NOAA-MSL12-derived  $nL_w(\lambda)$  data in February 2012. In general, the VIIRS  $nL_w(\lambda)$  values from both IDPS and NOAA-MSL12 data processing are well corresponding to the in situ  $nL_w(\lambda)$  values from the MOBY site in most of wavelengths. Some bias errors in  $nL_w(\lambda)$  are observed. Obviously, vicarious calibration is needed to resolve the bias error.

---

Time series of the daily VIIRS  $nL_w(\lambda)$  at wavelengths of 410, 443, 486, 551, and 671 nm derived from IDPS and NOAA-MSL12 ocean color data processing are also compared in the South Pacific gyre (25.5°S–24.5°S and 119.5°W–118.5°W), where ocean water is most clear and stable, to investigate performance of VIIRS data quality (Fig. 37). Fig. 37 shows time series of the VIIRS ocean color products from IDPS (black triangles) and NOAA-MSL12 (red circles) data processing from November 22, 2011 to August 31, 2012. Similar to the results from the Hawaii MOBY area, in the South Pacific gyre, before February 6, 2012 VIIRS  $nL_w(\lambda)$  values derived from NOAA-MSL12 data processing have significant errors, while  $nL_w(\lambda)$  values from IDPS are all masked out. Most of NOAA-MSL12-derived  $nL_w(\lambda)$  values are biased high, but  $nL_w(410)$  values are apparently lower in December 2011 and January 2012. Since February 6, 2012, however, errors in the VIIRS  $nL_w(\lambda)$  from NOAA-MSL12 data processing are significantly reduced and the values are quite stable. Again, significantly less data are available in IDPS-derived  $nL_w(\lambda)$  products, compared to those from NOAA-MSL12. The decreasing trends from May 2012 and increasing trends in August 2012 in VIIRS  $nL_w(\lambda)$  at blue bands (410 and 443 nm) indicate seasonal variability in the South Pacific gyre, which can also be found in the MODIS-Aqua data. The VIIRS  $nL_w(\lambda)$  values from both IDPS and NOAA-MSL12 data processing are quite similar and within a similar data ranges. However, IDPS  $nL_w(\lambda)$  values are systematically lower than those from the NOAA-MSL12.

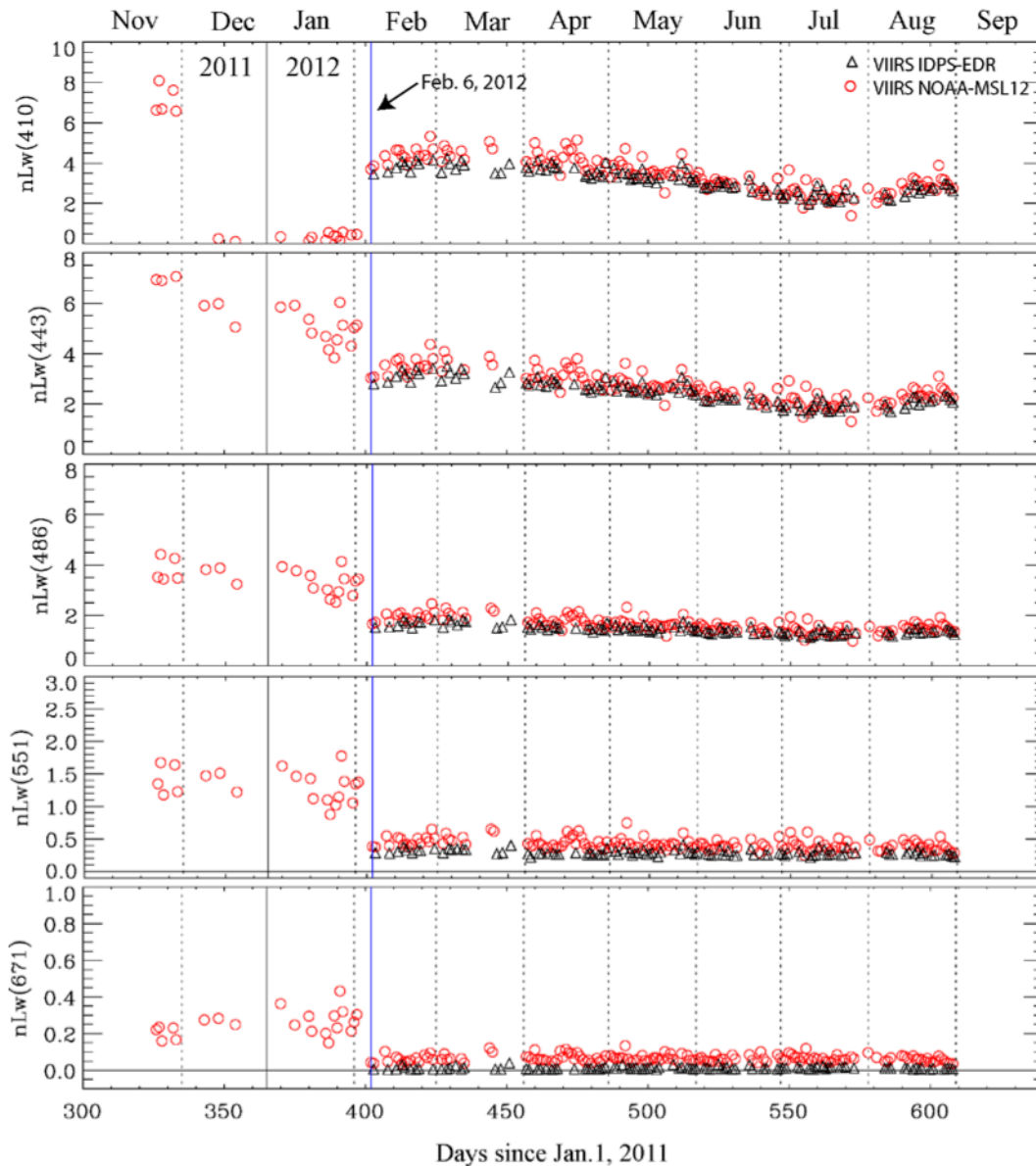


Fig. 37: Time series of the daily VIIRS  $nL_w(410)$ ,  $nL_w(443)$ ,  $nL_w(486)$ ,  $nL_w(551)$ , and  $nL_w(671)$  data derived from IDPS-EDR (black triangles) and NOAA-MSL12 (red circles) data processing in the South Pacific gyre from November 2011 to August 2012. No vicarious gains were applied to both data sets.

### 2.5.1.2.3 In Situ Matchup Comparisons

Fig. 38 shows results for matchup comparisons between VIIRS IDPS ocean color products and MOBY in situ measurements. The in situ-derived Chl-a data were obtained using the MOBY in situ  $nL_w(\lambda)$  data with the same bio-optical algorithm (OC3V). It is noted that IDPS-derived  $nL_w(\lambda)$  data have not been vicariously calibrated. Thus, results in Fig. 38 show valid validation from MOBY in situ data. Results in Fig. 38 show that IDPS-derived ocean color products are quite reasonable. However, IDPS-derived Chl-a data are biased high ( $\sim 10\%$ ) compared with those from MOBY in situ-derived data.

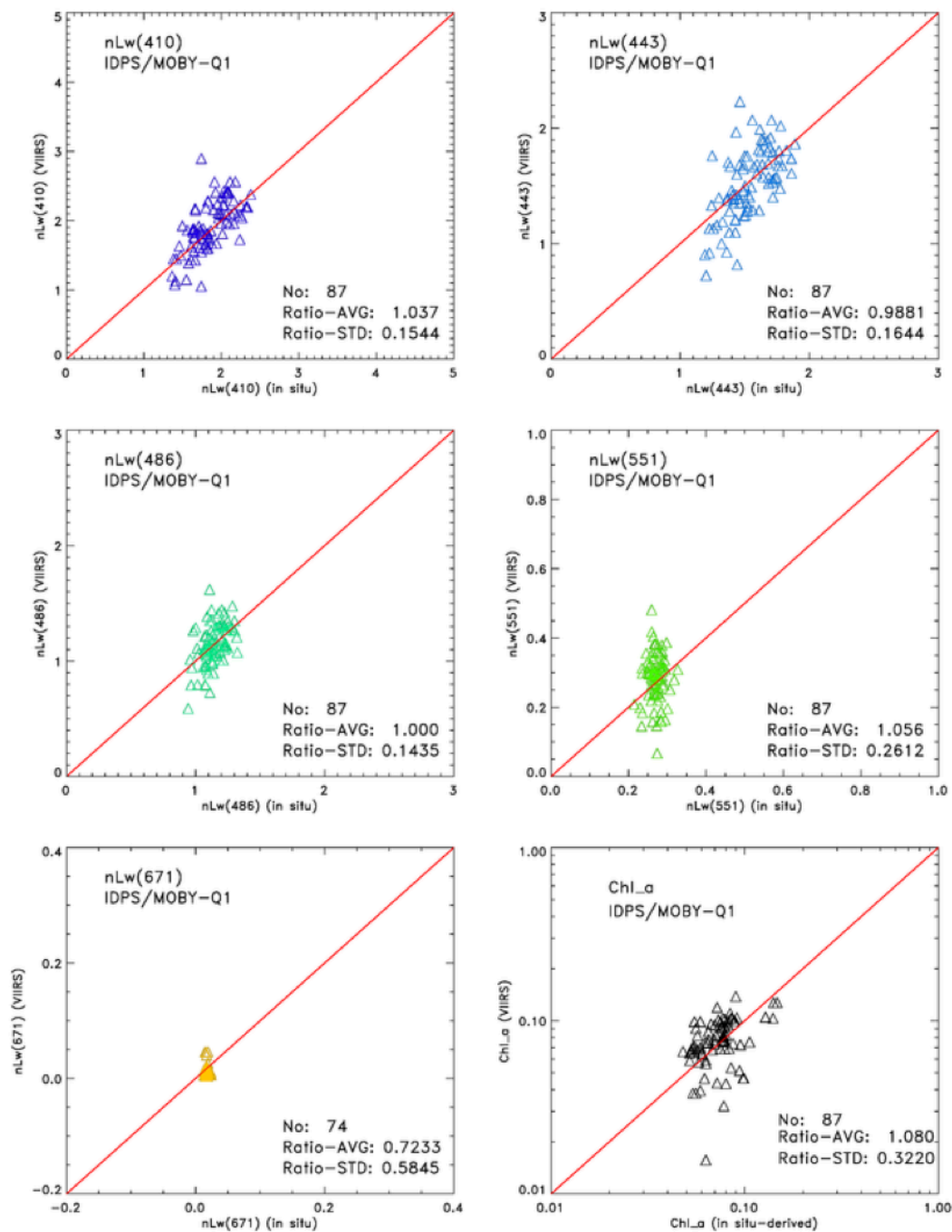


Fig. 38: Scatter plot of IDPS VIIRS Ocean color data and in situ MOBY data for nLw(410), nLw(443), nLw(486), nLw(551), nLw(671) and Chl-a. Note that the MOBY Chl-a data were derived from MOBY in situ nLw( $\lambda$ ) data. No vicarious gains were applied to IDPS data.

In addition, IDPS-derived  $nL_w(\lambda)$  data are compared with in situ measurements from AERONET-OC CSI station (Gulf of Mexico) (Fig. 39) and USC station (Newport Beach, California) (Fig. 40). For these coastal sites, IDPS-derived  $nL_w(\lambda)$  data are generally biased low (as expected).

However, there are some quite good correlations between IDPS-derived and in situ-measured  $nL_w(\lambda)$  data.

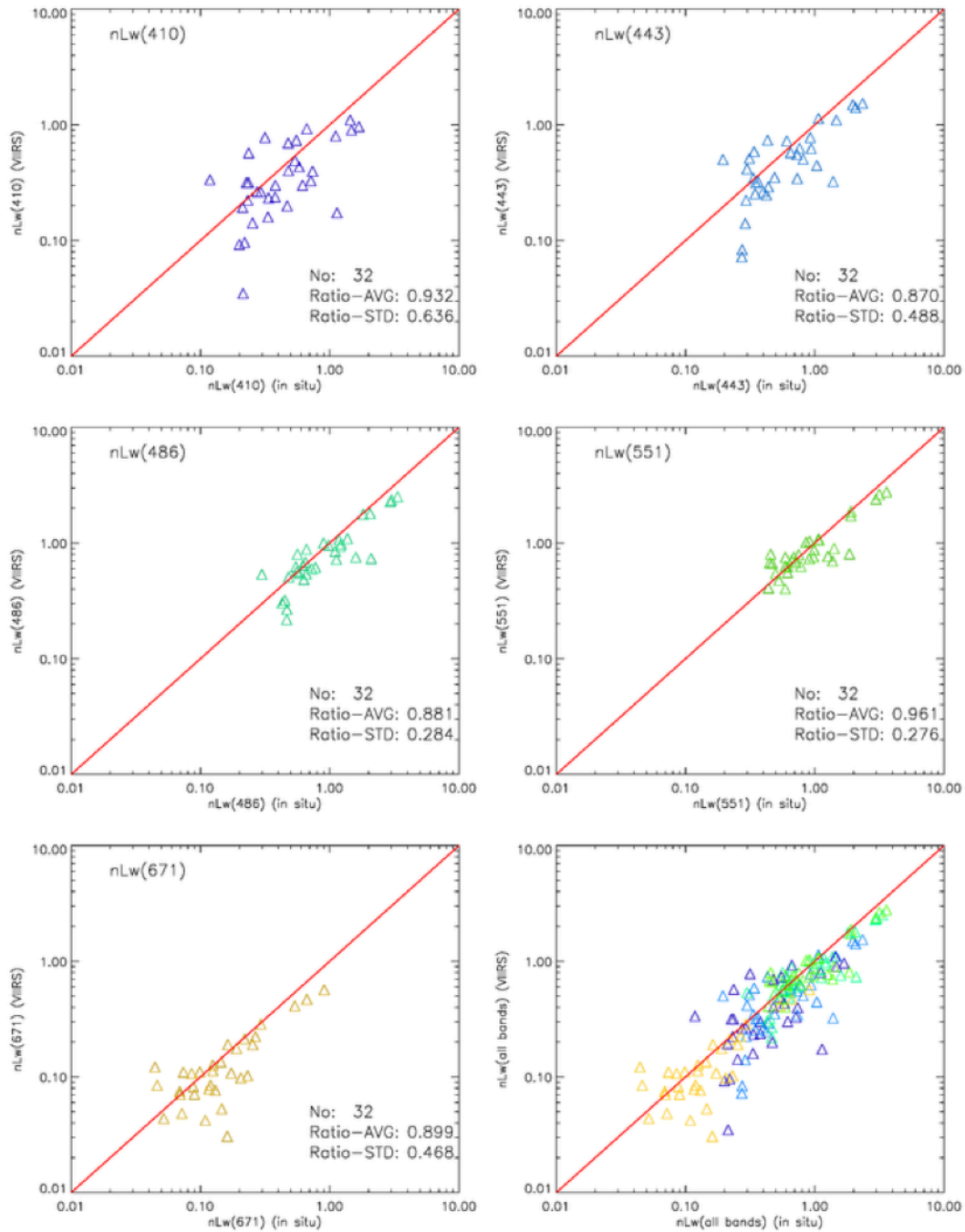


Fig. 39: Scatter plot of IDPS VIIRS Ocean color data and in situ measurements at AERONET-CSI station (Gulf of Mexico) for  $nL_w(410)$ ,  $nL_w(443)$ ,  $nL_w(486)$ ,  $nL_w(551)$  and  $nL_w(671)$ . No vicarious gains were applied to IDPS data.

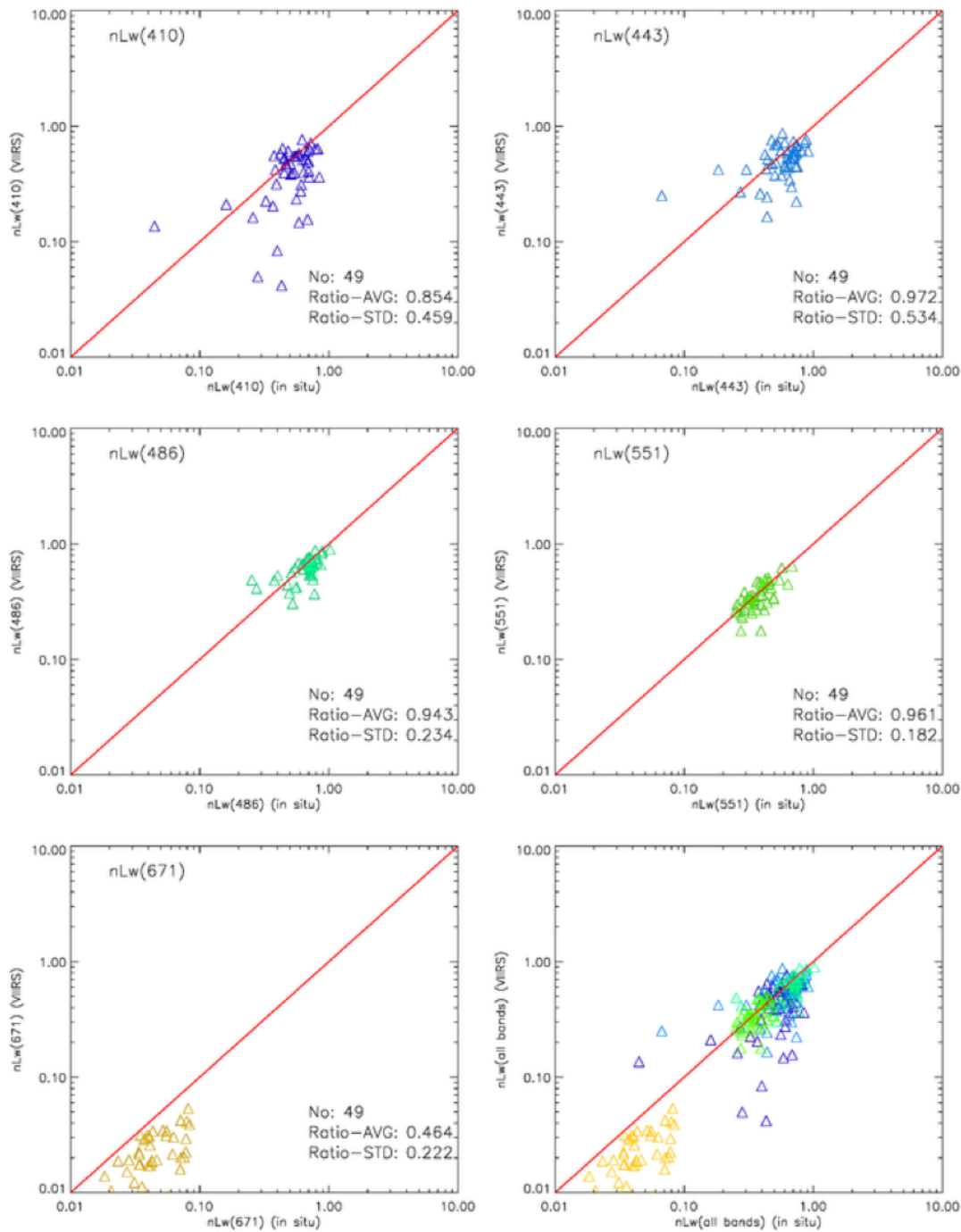


Fig. 40: Scatter plot of IDPS VIIRS Ocean color data and in situ measurements at AERONET-USC station (Newport Beach, California) for nLw(410), nLw(443), nLw(486), nLw(551) and nLw(671). No vicarious gains were applied to IDPS data.

### 2.5.1.3 DISCUSSION

The VIIRS ocean color products have been derived from IDPS and NOAA-MSL12 ocean color data processing for the global ocean. The spatial patterns of Chl-a and  $nL_w(\lambda)$  from both IDPS and NOAA-MSL12 data processing are similar and well corresponding to results from other

---

satellite ocean color remote sensing data such as MODIS and SeaWiFS. Currently, there are considerably large missing data in IDPS-derived ocean color products in the global ocean, compared with those from NOAA-MSL12-derived products. The causes for the IDPS missing data issue have been identified, and will be resolved.

Time series results of the daily VIIRS  $nL_w(\lambda)$  data show that the VIIRS level-2 ocean color products have significant errors before February 6, 2012 due to errors in SDR calibration LUTs. After using improved SDR LUTs and algorithms from February 6, 2012, VIIRS ocean color products are quite reasonable from both IDPS and NOAA-MSL12 data processing. Thus, VIIRS IDPS-derived ocean color products before February 6, 2012 have significant data quality issue and should not be used. Vicarious calibration for both IDPS and NOAA-MSL12 data processing is needed and will certainly improve VIIRS ocean color data quality.

Further VIIRS data improvement can be achieved by using daily calibration F-LUTs for producing improved SDR. Currently, IDPS SDR data have been produced using the weekly F-LUTs. Preliminary results using daily calibration F-LUTs for VIIRS SDRs show significant improved  $nL_w(\lambda)$  over MOBY site, compared with MOBY in situ data (Fig. 41). Again, vicarious calibration has not been applied for these results (Fig. 41). In particular, with reprocessed SDR (Level-1B) data before Feb. 6, 2012, VIIRS EDR  $nL_w(\lambda)$  data are now quite reasonable in that period. This shows that VIIRS data reprocessing is necessary for both SDR and EDR

In summary, our initial evaluation results show that VIIRS is potentially capable of providing high-quality global ocean color products in support of the science researches and various operational applications although there are still some important issues to be resolved, e.g., improving VIIRS SDR calibration with both solar and lunar data. Some specific conclusions are again outlined here:

- (1) VIIRS-IDPS-derived normalized water-leaving radiance spectra  $nL_w(\lambda)$  are quite reasonable in open oceans, compared with the MOBY in situ data measurements (no vicarious calibration). Vicarious calibration will be applied and will further improve VIIRS ocean color products.
- (2) VIIRS-IDPS-derived chlorophyll  $a$  data are biased high, e.g., in the MOBY site, Chl- $a$  is overall  $\sim 10\%$  biased higher compared with those derived from the MOBY in situ  $nL_w(\lambda)$  data.
- (3) Preliminary VIIRS ocean color results derived from the SWIR method are promising.
- (4) VIIRS SDR (or Level-1B) data quality has a significant impact on the VIIRS ocean color EDR. VIIRS IDPS ocean color data before February 6, 2012 are not reliable and should not be used because SDR data were poorly calibrated.
- (5) Data reprocessing for both SDR and ocean color EDR is required to meet the requirement of producing consistent and highly accurate VIIRS ocean color products, e.g., CDR.
- (6) VIIRS IDPS EDR has been declared as the Beta Status for ocean color data from Feb. 6, 2012. Thus, VIIRS ocean color EDR data are available to public from CLASS.

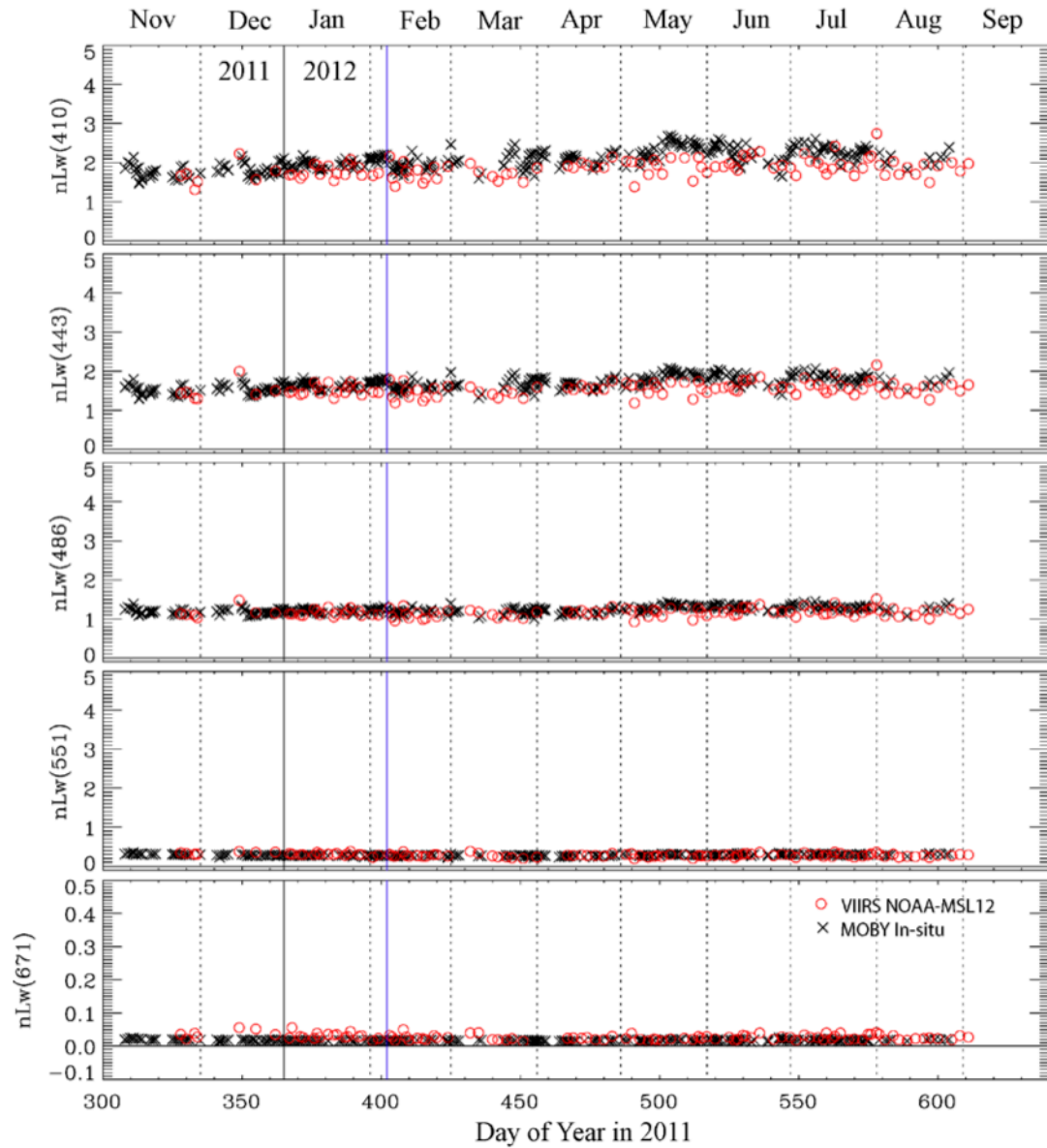


Fig. 41: Time series of in situ MOBY (black x) and daily VIIRS-derived nLw(410), nLw(443), nLw(486), nLw(551), and nLw(671) data from NOAA-MSL12 (red circles) data processing in the Hawaii MOBY area from November 2011 to August 2012. The daily F-LUTs were used for re-generating improved VIIRS SDR for VIIRS ocean color data processing using NOAA-MSL12. Note a significant data improvement in the period of before Feb. 6, 2012.

---

## 2.5.2 NASA EFFORT

---

In the NASA approach, the NASA VIIRS evaluation ocean color data products were generated based on two key capabilities. First, existing computation infrastructure (i.e., machines, storage, algorithms, support software, and manpower) were used to run VIIRS data through the NASA-selected algorithms used in generating current NASA CDR. Second, independent calibration techniques based on those applied heritage NASA ocean color sensors were applied to VIIRS (as described in Section 1.3). These two capabilities were key to providing a constructive assessment of the VIIRS data products.

Because quality of ocean color data products is highly dependent on the quality of the instrument calibration, the calibration needs of VIIRS were carefully evaluated. To that end, an independent validation was established to verify the operational calibration and to applied lessons learned from heritage missions to VIIRS. The NASA approach applied a linearized count-to-radiance conversion based on prelaunch characterization of the instrument and on-orbit measurements of the onboard calibration reference panel, using the sun to track changes in instrument responsivity. Monthly measurements of the moon were also used to trend changes in the instrument. Currently, the lunar trend is being used to verify the solar trend, and to identify, diagnose, and possibly correct anomalies in the onboard calibration system. Unlike the solar reference panel, which is constantly changing with cumulative exposure to ultraviolet radiation, the moon is a very stable reference. Over long periods of time, the lunar trend can conceivably replace the solar trending.

Another important benefit of the independent calibration is that it facilitates a time-dependent record of changes the instrument response. This record is a key component required for a reprocessing capability. During each reprocessing of the data record, the calibration record provides the processing system with information regarding the state of the instrument for any particular time. Thus, any trend in the instrument radiometric response can be effectively removed from the data record for measurements of the ocean.

The NASA evaluation processing capability offered several the advantages during this evaluation. First, it was able to facilitate full-mission reprocessing, i.e., reprocessing every data file for the entire mission. This approach produced a consistent data set, even during a time when calibration techniques were frequently changing to accommodate new information about on-orbit instrument and calibration system behavior. Furthermore, to see how well VIIRS could continue the NASA data record, the algorithms applied to VIIRS measurements were the same used to generate the record established with SeaWiFS and MODIS. Also, the evaluation processing capability provided a longer time series during the early mission, thus accelerating evaluation of VIIRS potential to support NASA ocean color science objectives by about a month. In addition, the evaluation processing capability facilitated the production of both heritage and new data products not supported by the operational data processing system. Finally, the evaluation processing capability facilitates generation of tradition EOS Level-3 data products (i.e., global composites of Level-2 data), which are also not supported by the operational processing stream.

A significant discrepancy has been observed between the lunar and solar trend, as was described in Section 1.3. This effect has also been observed by the VCST and operational

---

calibration teams. The solar trend and lunar trend curves appear to be divergent and non-monotonic during the latter half of 2012, but currently appear to be converging. It is currently suspected that the variation in the lunar trend is typical for the short-term uncertainty in lunar measurements. Lunar trends for SeaWiFS and MODIS showed fluctuations of a similar magnitude on the scale of one year. These variations rapidly decrease in significance to the trending process over the periods of multiple years. The small non-monotonic variation in the solar trend continues to be studied intensely, but it is currently suspected to be an artifact of the calibration system itself, and does not represent the behavior of the sensor.

As with heritage missions, we need the Moon to trend VIIRS, or at least identify and correct inaccuracies in the solar trend (low frequency noise). The solar trend is very precise, frequently measured, but can be inaccurate because of biases that arise when measuring a changing reference. Conversely, the Moon is a very stable reference, provided it is measured at a fix phase angle, and thus the lunar trend can be very accurate. **However, with only eight to ten lunar observations per year, up to two to three years of lunar observations may be required to fully realize the stability of the lunar time series, and by extension the solar calibration trend. Thus, as was true for the SeaWiFS and MODIS missions, the calibration gradually improves with time and refinement of the instrument trending to meet heritage standards could take at least two years.**

With the evaluation processing and independent calibration, a full suite of ocean color products could be generated using algorithms more consistent with the established ocean color data record. Products generated in geolocated satellite swath format are referred to as NASA Level-2 (L2) data products and are analogous to the NOAA EDR data products. The EDR ocean color product suite, as previously defined in Section 1.1, is essentially a small subset of the standard NASA L2 data product suite generated for the science community for other missions. The NASA suite of products also includes heritage products not being continued by the NOAA EDR (e.g., PIC and PAR). The NASA L2 production capability also could facilitate experimental products, which cannot be generated by the operational NOAA system. However, only PIC and PAR were produced for this study. The diffused attenuation coefficient at 490 nm ( $K_d(490)$ ) was also produced by the NASA evaluation processing stream, but the evaluation in this report was done using the NOAA-MSL12 algorithm by Wang. Application of GSM by Siegel, the SWIR algorithm by Wang, and the data assimilation techniques employed by Gregg, were all facilitated by other processing resources.

With some adjustment to accommodate NOAA EDR data products, the same NASA processing system provides the ability to generate global composites of NASA L2 and EDR data in Platte Carre projection, yielding what are referred to as Level-3 (L3) Standard Mapped Images (SMI), and in Integerized Sinusoidal Equal Area Grid (ISEAG) projection, creating what are called L3 binned data products. Both of these are crucial to understanding geographic and temporal trends of the data on synoptic and global scales. L3 production, however, required a careful look at data flags and masks to determine which data from the EDR or NASA L2 were to be aggregated into the L3 data products.

---

### 2.5.2.1 INITIAL PRODUCT EXAMINATION – STRUCTURE, FLAGS, AND MASKS

As data first became available early in 2012, the GSFC team began its focused on product characteristics that might affect product usability. This included the overall file structure (more specifically how the data is divided up and formatted) and the general state of the EDR flags and masks used by the NOAA EDR data products and the NASA L2 evaluation products was examined. Many aspects of the NOAA EDR products were known well before launch and multiple teams have reported deficiencies in the product file characteristics that could adversely affect their use. These issues included concerns regarding the lengthy naming convention used for data files, the ineffectual use of the HDF5 format, or the limits of data accessibility via the Comprehensive Large Array-data Stewardship System (CLASS). These issues were clearly recognized by the GSFC team as being a little more than inconvenient for the greater research community. However, the lengthy naming convention was viewed to be merely a nuisance. In effectual use of HDF5 did not render the data unusable in anyway or even affect the scientific quality of the data. Although acquiring large orders of data from CLASS could be difficult for the general community, it is assumed that NASA would continue to acquire its VIIRS data through the SDS. However, the size of an 86-second VIIRS granule (compared to an EOS 5-minute granule) breaks up a daily acquisition into a 1000 granules, which is somewhat unwieldy for climate research. Moreover, the calibrated operational product (i.e., the Sensor Data Record, or SDR) is output into one file for each band, further multiplying the number of files to be managed by a user. Because the granule size is much smaller than those of heritage missions, the chances of needing more than one granule to study and single area on the planet are greater.

Flags and masks can have a more direct affect on the scientific quality of the data. A flag is a group of one or more digital bits associated with each pixel in an EDR or L2 product. Each flag indicates the state of certain conditions that could pertain to the quality of the pixel's data value. There are 32 possible flags for the L2 product, 25 of which are directly ocean related, and there are 47 flags for the EDR, some with up to 8 states. A detailed mapping of the EDR flags to the L2 flags based on their functionality and how well they currently operate can be found in Turpie et al. (2012). Researchers can use flags, for instance, to selectively filter data by specific conditions that might affect their particular study. The evaluation of EDR flags by the GSFC team and Ocean PEATE helped determine which EDR pixels could be aggregated into EDR L3 products that would be comparable to the NASA L3 products. The flag map in Turpie et al. (2012) and repeated testing by the Ocean PEATE were used to determine which EDR flags that would be best to use for generating EDR L3 products.

Early analysis of EDR flags and masking was limited by the early state of the instrument calibration. For instance, problems during the first several months of thermal band calibration adversely affected the determination of whether clouds were the present. Thus, the VIIRS cloud mask algorithm was subject to ongoing improvements to its performance during the early stage of the mission, which also limited some the conclusions that could be drawn about future performance of that mask. Therefore, the performance of some flags and masks were observed throughout the first year of the mission, and should continue to be monitored.

Masks are different than flags in that no geophysical data is given for the EDR or L2 pixel. Instead, each masked pixel contains a special numerical value, also known as a *fill value*,

---

which indicates that the pixel has been masked. Pixels are masked when an actual quantity could not be computed from the instrument measurements. A single fill value is used in the NASA L2 files, while there are 8 different numbers used in the NOAA EDR, each indicating some additional information about the failure to compute a value. Furthermore information as to why an EDR or L2 pixel was masked can often also be deduced from information in the flags associated with that pixel.

The analysis involved examination of flags and masks for several granules over the open ocean and coastal regions. All granules showed similarities in flag performance. The L2 flags created by NASA algorithms all behaved mostly as expected (i.e., similar to heritage products). Whereas this was often also true for the EDR flags, many of the EDR flags were found to be extremely aggressive, appearing to extraneously mark more data as poor quality than expected. In fact, a significant portion of randomly scattered pixels were marked as poor quality for no apparent reason.

Most of the sporadic losses of data in the EDR data products appeared to be associated with false positive and negative indications of the presence of clouds, and probably reflected the maturing status of associated flagging algorithms. Some of the masked data also had flags set indicating confidently clear sky or could be seen to occur over relatively clear water. In the clear water cases, many masked pixels had coccolithophore or high Dissolved Organic Matter (DOM) flags set. The density of the random data loss also appeared to rise toward the end of scan with abrupt increases coincident with the transition from the 3:1 to 2:1 aggregation zone, and likewise with the 2:2 to 1:1 transition. It was also observed that all pixels corresponding to inland water are masked in the EDR data products. Thus, the EDR data products currently contain no geophysical values for areas like the Great Lakes of North America. NOAA scientists recognized this problem during 2012 and a correction has been formally requested. **However, because the IDPS does not facilitate reprocessing, the EDR for these regions are permanently lost, e.g., the EDR will never provide a chlorophyll  $a$  record for the Great Lakes for all of 2012 and whatever period afterwards that is required to insert a correction to the operational processing stream.** Conversely, although similar production errors have occurred with SeaWiFS or MODIS Aqua data products, they were corrected and removed from the data record through reprocessing.

Similarly, whenever any normalized water-leaving radiance becomes less than zero in a pixel, all EDR values associated with that pixel are masked. Therefore, in regions like the gyres, where the red band (671 nm) can become negative, potentially valid values are not calculated for either chlorophyll  $a$  concentration or for normalized water-leaving radiances and IOP coefficients in the other bands. This historically stems from the fact that the earlier version of the algorithm required all bands to compute the IOP values and the chlorophyll  $a$  concentration. However, chlorophyll  $a$  as currently computed does not depend on the red band surface reflectance. NOAA recognized this extraneous data loss and a request to change this masking behavior in the EDR data products was documented internally.

The EDR stray light flag was observed to be a significant contributor to the reduction in data in the EDR L3 products. A stray light flag is used in both the EDR and L2 products and is necessary to cull regions around clouds, land, and other bright targets when selecting data for aggregation into L3 products. NOAA EDR and NASA L2 algorithms set these flags differently. The

NASA L2 stray light flag algorithm used for VIIRS is analogous to the one used for SeaWiFS and MODIS and appeared to be performing as expected. Unfortunately, the EDR stray light flag removed a significantly larger amount of data in the clear regions around bright targets and many pixels spuriously are marked as contaminated with stray light. However, if the EDR version of the flag was not used, then too much contaminated data gets included in the corresponding L3 products. A similar situation arises with other EDR flags, but not as pronouncedly. For instance, the flagging of pixels with sensor zenith angle greater than  $53^\circ$  causes a significantly larger data cull than the  $60^\circ$  threshold used for the NASA L2 data products. It was found that the EDR flag that corresponds to the NASA L2 flag indicating a poor chlorophyll *a* data value (CHLWARN) was too conservative. In particular, chlorophyll *a* concentration can frequently fall below the EDR flag criterion of  $0.05 \text{ mg m}^{-3}$  in the gyres, thus it was not used in selecting EDR data for L3 data product generation. The combined effect of the more aggressive flagging criteria and masking results causes L3 products that are created from the NOAA EDR data to include a much smaller measurement sample compared to the L3 products based on NASA L2 data products.

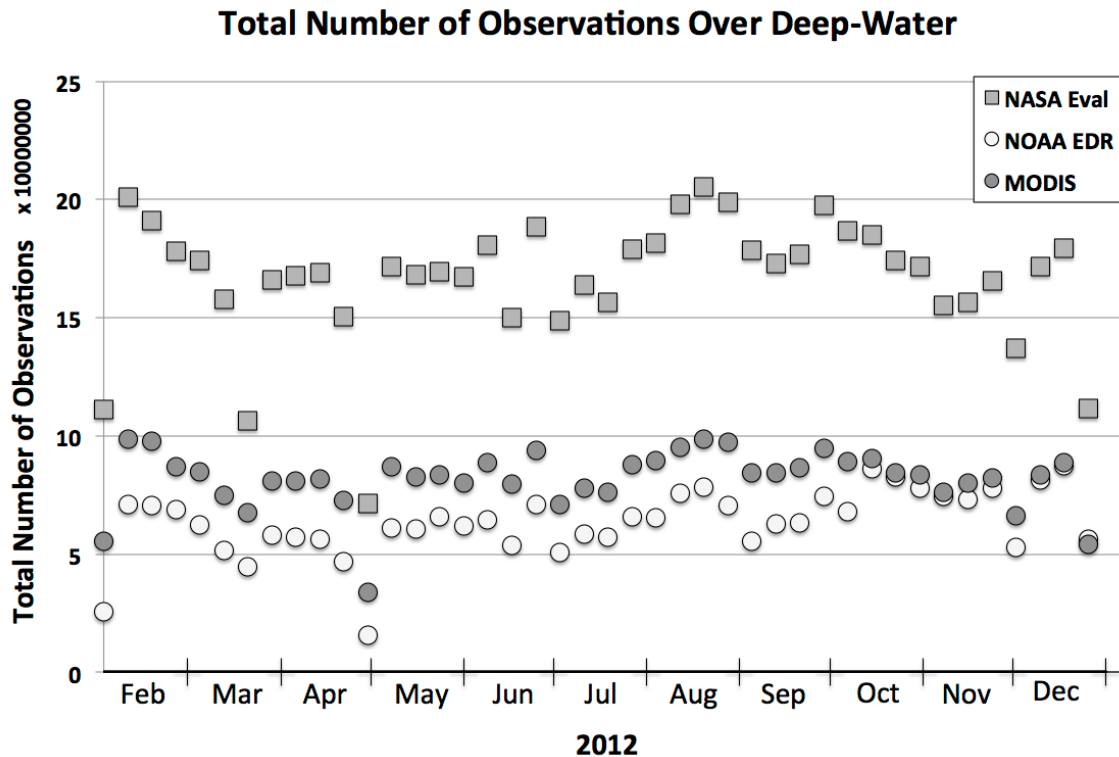


Fig. 42: Comparison of number of observations between VIIRS EDR, NASA evaluation product, and MODIS Aqua 8-day Level 3 composites. Each symbol indicates the number of observations for Level-3 bins common to all three data sets over waters with depth >1000m.

There are many other EDR flags that were considered that do not have NASA L3 selection flag analogs. There are general EDR flags that correspond to the ocean color quality in the visible bands (i.e., bands at 410, 443, 486, 551, and 671 nm). These all appear to flag significant amounts of the retrieved normalized water-leaving radiance in the EDR. The absorption (IOP\_A) quality flags were relatively benign, but still could sporadically mark large

---

regions as poor quality. The scattering (IOP\_S) flag currently culls almost all the valid retrieved data in the EDR. Hence, both of these were not used in the generation EDR L3 products.

The land/water flag in the EDR was examined. The EDR land/water flag has four states: open sea, coastal water, inland water and land. The coastal water state affected a relatively small area, supposedly flagging waters immediately against coastlines. However, the indication of coastal water showed anomalies along the western coasts of landmasses (e.g., the Californian coast). In such cases, the coastal water state frequently appeared inside regions marked as land, making a landward progression of open water, land, coastal water, and then land again. Thus, the coastal water state appeared to be offset eastward along scan from the correct location. Other than this behavior, the land and other water conditions appear to be accurate.

In creating L3 data products from NASA L2 data, it was found that the standard NASA flag for indicating a problem in the atmospheric correction algorithm (ATMWARN) was not performing optimally and so was not used in forming L3 products. The NASA ATMWARN flag was tending to be triggered by the NIR radiance ratios falling out of the expected range (i.e., 0.85 – 1.35), which was probably a result of the still immature status of the instrument calibration. As the calibration improves, the NASA L3 data products can be reprocessed with this flag in use. The corresponding EDR flag, for similar reasons, was also not performing well, and was also omitted from L3 product generation. However, the EDR data products will never be reprocessed following current NOAA mission requirements, thus generation of EDR L3 will likely continue to not use this flag, or the CHLORWARN flag, for the period where they have poor performance.

Otherwise, the current translation of the EDR flags to NASA L3 selection flags analogs appears to work reasonably. However, Fig. 42 shows that when comparing common L3 bins, the number of observations included in the EDR L3 bins was greatly reduced compared to the corresponding NASA L3 data. The number of EDR observations, in fact, was less than MODIS, which collects few samples than VIIRS (with MODIS having less spatial coverage and larger pixels). Fig. 42 also shows significant drops in the number of observations during data outages that occurred in late March and late April 2012 (note that these outages appear to affect the MODIS values because only common bins are being considered in these counts). In conclusion, the aggressive nature of the EDR flags and masks caused large portions of data to be unavailable for regional analysis.

### **2.5.2.2 LEVEL 3 COMPARISONS**

To evaluate VIIRS data products on a large spatial and temporal scale, separate L3 products derived from NOAA EDR products and NASA L2 products were processed into 9 km resolution ISEAG projections. For each eight-day period, a corresponding eight-day MODIS Aqua L3 dataset was acquired at the same spatial resolution. Regional averages of the NOAA EDR and NASA evaluation surface reflectance trends were comparable, differing only within several percent. However, the chlorophyll *a* concentration data quality is dependent on the quality of the retrieved water-leaving radiometry at 443, 486, and 551 nm. A bias of several percent can have significant effects on the derived products.

To examine the performance of the chlorophyll parameter on large scales, L3 binned data products for chlorophyll *a* concentration data taken over eight-day intervals from February 2012 to January 2013 were collected for large-scale trending analysis. Because the calibration tables were not inserted into the operational processing stream until 6 February, the EDR data prior to that date are of extremely poor quality, and were excluded from this study. Chlorophyll *a* concentration averages were taken over the deep-water region of the open ocean (i.e., waters with depth > 1000 m). The same method for taking averages was also applied to MODIS Aqua chlorophyll *a*. Only equal-area bins that were common to all three products are included in each average. Fig. 43 shows that the EDR and NASA evaluation differ greatly, while the NASA evaluation product matches remarkably well to MODIS Aqua. Note again that all three averages are using the same bin sampling, so influence of data gaps (e.g., clouds, orbital gaps, etc.) are identical between averages.

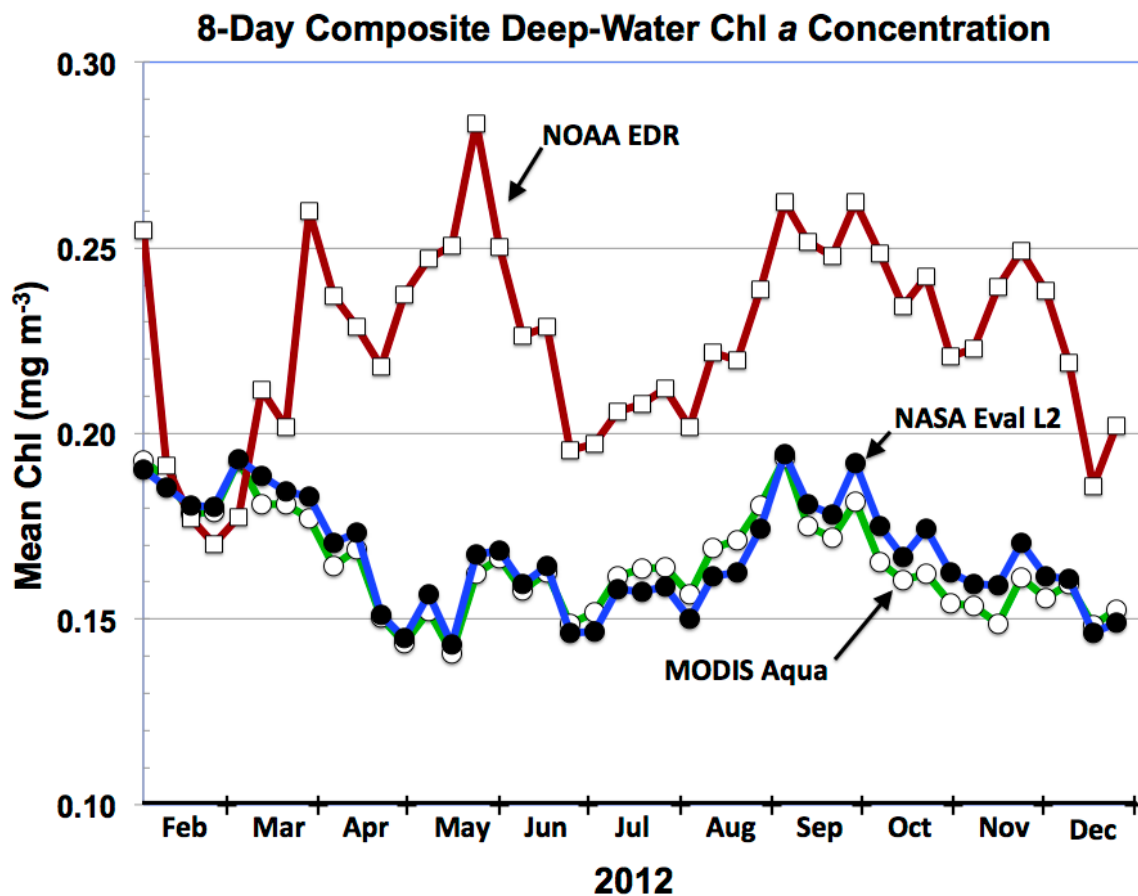


Fig. 43: Chlorophyll Mean Time Series since start of EDR production. 8-day composites of chlorophyll *a* concentration composites were averaged over waters with depth > 1000 m. The red curve is from the NOAA EDR using VIIRS data. The blue curve is from the NASA evaluation product, while the green curve is from MODIS Aqua data. Clearly, during 2012, the NASA evaluation product for VIIRS and the MODIS Aqua product are in very close agreement, while the NOAA VIIRS EDR appears inaccurate and unstable.

To put this result into a broader context, Fig. 44 shows the SeaWiFS deep-water chlorophyll time series for monthly composites overlaid with that of MODIS and the two versions of VIIRS products. Unlike the averages in Fig. 43, these are not based on common bins,

so some difference can arise from different sampling. However, these differences appear to be relatively small. The SeaWiFS and MODIS curves agree fairly well over their seven-year overlap. The NASA evaluation product also tracks the MODIS curve reasonably. The EDR chlorophyll *a* average is starkly higher than the NASA evaluation product and the difference appears similar to the finer temporal resolution time series in Fig. 43. More importantly, the EDR is likewise higher than both SeaWiFS and MODIS.

This raises a question: if the EDR surface reflectance averages over the same regions are reasonable, how could the chlorophyll *a* average be in such poor agreement? This result seems counterintuitive because it is often expected that chlorophyll *a* concentration, which is estimated from band ratios, should tend to be more robust to small errors in surface reflectance. To help understand this result, the SMI maps were taken to identify what part of the deep-water region is being affected and by how much. Relative differences were computed between the VIIRS EDR SMI and MODIS Aqua and then between the VIIRS NASA evaluation SMI and MODIS Aqua. Fig. 44 shows the global spatial distribution of the relative differences between the NASA evaluation chlorophyll *a* concentration and MODIS Aqua and the relative differences between the NOAA EDR and MODIS Aqua. The 8-day composite chosen corresponds to the maximum difference between the EDR and NASA evaluation product seen in Fig. 43.

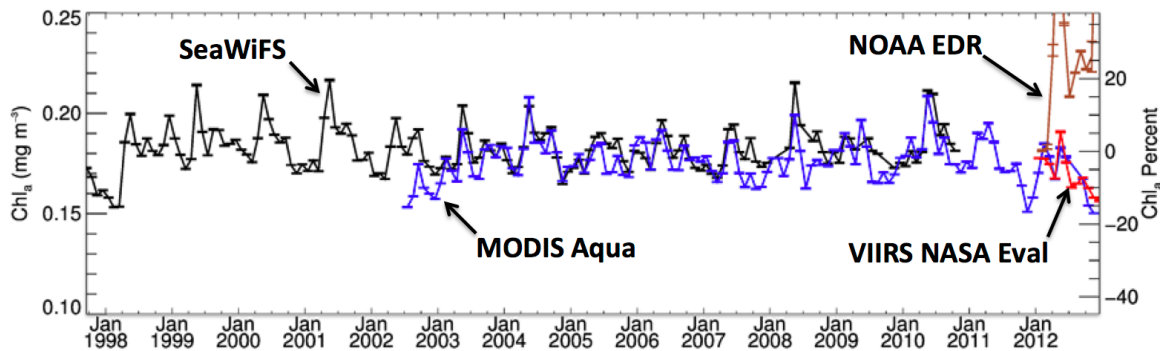


Fig. 44: Comparison with Deep-Water Chlorophyll *a* long-term time series. The black curve covers the 13 years of the SeaWiFS mission and the blue does likewise for MODIS Aqua. Both SeaWiFS and MODIS Aqua Deep-Water Chlorophyll averages are comparable. Likewise, the red curve shows the NASA evaluation Chlorophyll *a* average, which agrees well with MODIS Aqua. Conversely, the brown curve representing the EDR clearly deviates from the NASA data record. Averages are not based on common bins (Plot courtesy of B. Franz).

The resulting difference maps show that the EDR is clearly higher than MODIS Aqua over most of the world, compared to the NASA EDR, which depending on the region is only slightly higher or low. What is more notable is that the greatest relative difference occurs where high chlorophyll values exist. In short, higher the concentrations yield greater the differences.

---

### 2.5.2.3 LEVEL 2 COMPARISONS

Given the flag and mask analysis results described in Section 2.5.2.1, one might suspect that perhaps the high chlorophyll *a* concentrations in the EDR L3 arose from a preferential selection of high values from the original L2 files when aggregated into L3 products. To illustrate what is happening in the source L2 data, a L2 scene was selected in an area of high and low concentrations during the week of greatest difference. Fig. 46 shows a cutout area of the scene near the coast of Namibia on 26 May 2012. This cutout was selected to show both waters with relatively high and low concentrations. There are three prominent differences between the EDR and NASA evaluation L2. First, the EDR chlorophyll *a* concentration is universally, markedly higher than that of the NASA L2. The size of this difference suggests that it is the concentration values that mostly contribute to the difference in the L3 averages, not spurious, high values in the EDR not being properly flagged. It is also clear that there is considerably more data loss (white = no data) in the EDR in the bloom, which likely stems from algorithmic masking. It is noted that high chlorophyll *a* concentrations are being lost in this case, however, over the ocean gyres, very low concentrations could also be subject to selective exclusion. Finally, it can be seen that the pixels lost along the edges of each scan line is extended in the EDR (longer horizontal white lines). This pixel trimming is by design, although the reason for it is not clear. However, this exclusion of data is independent of data value and should have little influence in the regional EDR average.

To see if the high EDR values are sufficiently large enough to account for the peak difference seen in Fig. 43, the chlorophyll *a* concentration for the EDR was compared to the NASA evaluation in a density scatter plot, as shown in Fig. 47. The result shows that for low concentrations, the EDR is a few tens of a percent higher than the NASA evaluation product and for higher values from 1.0 to 10.0 mg m<sup>-3</sup>, the relative difference increases onward to a factor of two or three. This appears to be the right order of magnitude to account for the maximum differences seen in Fig. 43. Further analysis of surface reflectance for the three bands used to compute chlorophyll *a* concentration show differences of several percent, such that the 551 nm band is higher for the EDR and the two blue bands (443 and 486 nm) are lower. This would significantly lower the band ratios and cause higher concentrations. Moreover, sensitivity analysis showed that the band ratio algorithm is highly sensitive to band ratio errors for concentrations of 1.0 mg m<sup>-3</sup> and higher, and continues to increase in sensitivity as the concentration gets higher (or rather, the band ratio goes lower). The EDR concentrations were reproduced using the EDR surface reflectance values and NASA evaluation chlorophyll *a* algorithm, so EDR and NASA L2 algorithm are essentially identical.



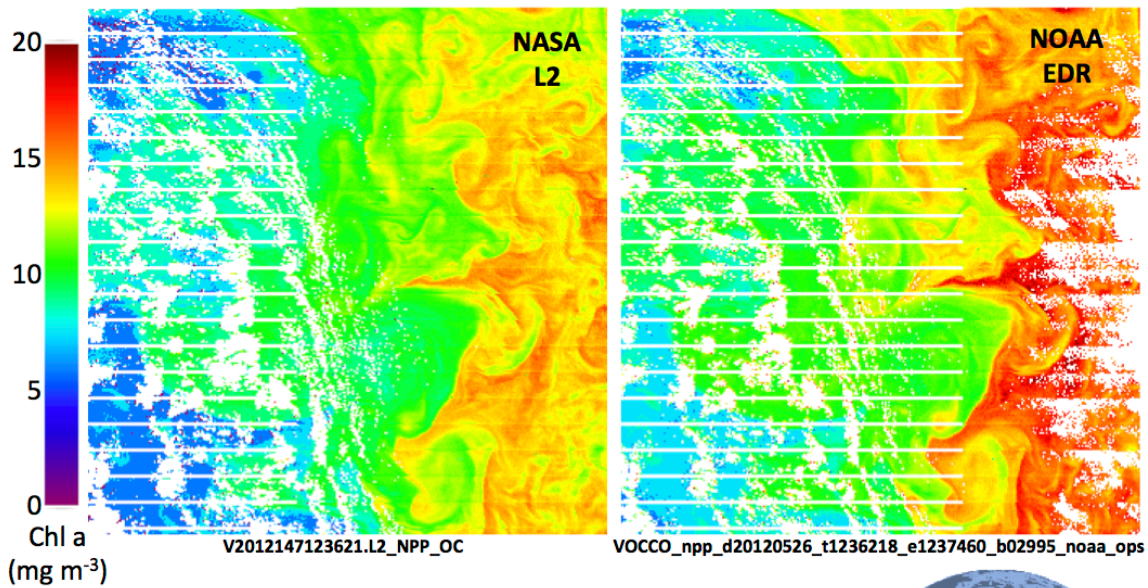


Fig. 46: Level-2 comparison. A subset was extracted from a scene near the coast of Namibia taken on 26 May 2012. The images show chlorophyll *a* concentration in and around a bloom for both the NASA L2 product (left) and the NOAA EDR (right). The strings under each image correspond to the source file name. White = no data.

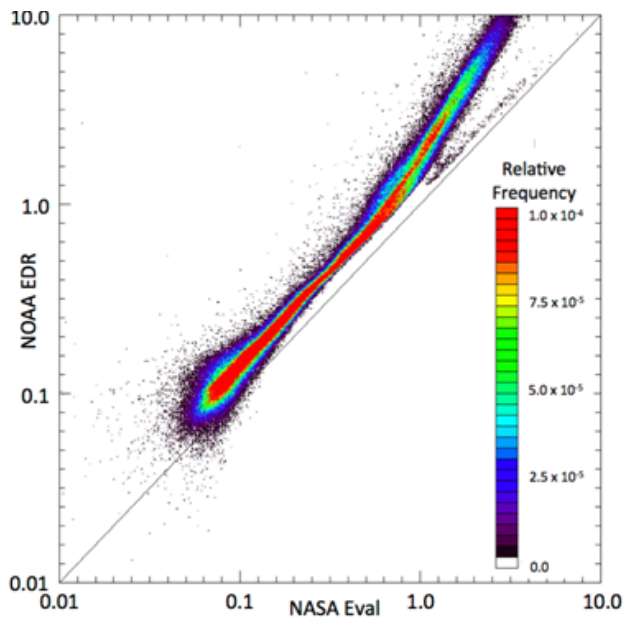


Fig. 47: Density scatter plot of NOAA EDR and NASA evaluation chlorophyll *a* concentration. The data plotted come from the full scene from which the subsets shown in Fig. 46 were taken. Most of the data are open ocean with concentrations  $<1.0 \text{ mg m}^{-3}$ .

---

There are a couple of possible causes for the discrepancy between the evaluation and operational concentration values: calibration differences and differences in the atmospheric correction algorithms. Calibration is expected to account for most of the difference between the operational and evaluation chlorophyll *a* concentrations, which should improve with vicarious calibration of the ocean color EDR. A fraction of the difference can be attributed to a lack of a NIR correction in the EDR atmospheric correction. But, the lack of this correction would primarily affect areas of high concentration, and it does not seem to account for the lower EDR concentrations for values <1.0 mg m<sup>-3</sup>. Other atmospheric correction differences may also have some influence, but further study is needed to verify that hypothesis.

#### 2.5.2.4 COMPARISON OF SATELLITE DATA TO *IN SITU* DATA

SeaBASS was used to search for available matches of *in situ* data and VIIRS measurements. Default criteria were used to select data for the NASA evaluation product matchups as shown in Table 10. Analogous criteria were applied to the EDR when matched to *in situ* observations. Only ten points were found for chlorophyll *a*, which proved to be too small and too variable of a sample to draw any conclusions. Conversely, several hundred matches were found between VIIRS satellite data and AERONET-OC radiometric data (i.e., surface reflectance). This also included several points from the Great Belt II cruise led by Balch. MOBY data was also included for comparisons with the EDR, as it was not vicariously calibrated with the buoy data.

It should be noted that the AERONET-OC sites are in mostly northern hemisphere coastal regions (including the Baltic Sea), which are considered challenging to the atmospheric correction algorithm. As determined in the previous section, these regions can also be problematic for the chlorophyll *a* concentration algorithm. Furthermore, regions with higher chlorophyll *a* concentration, which are often characteristic of coastal waters, tend to have higher spatial and temporal variation. This decreased the chances of getting a match between the satellite and *in situ* measurements and can increase the random variability of the *in situ* data, thus adding noise to the analysis.

A reduced major axis regression (RMA, a type of Model II regression) was performed to account for the fact that considerable random error exists in both the satellite and *in situ* data. This particular method assumes that the bivariate distribution of the data pairs is largely a bivariate normal distribution. This assumption holds somewhat for the surface reflectance, but the distribution becomes increasingly skewed with increasing wavelength.

Fig. 48 shows the scatter plots for the EDR and NASA evaluation surface reflectance, in the form of remote sensing reflectance ( $R_{rs}$ ) in units of sr<sup>-1</sup>. The plots include the one-to-one line and linear regression fit.

Table 10: Criteria for matching *in situ* to satellite data.

Search Criteria and Conditions	Setting
Region	Global
Date	All
Depth 0.0 to 10000	0.0 to 10000m
Investigator/Experiment/Cruise	All
Data Source	All
Minimum Valid satellite pixels (in %)	50
Maximum Solar Zenith Angle (Deg)	70
Maximum Satellite Zenith Angle (Deg)	56
Maximum Time Difference between satellite and <i>in situ</i> (in hours)	3
Maximum Coefficient of Variation of satellite pixels	0.15
Maximum difference between measured and modeled Irradiance (in %)	20
Maximum Windspeed	35
Satellite version	Operational
Most Recent Data Update	2/21/13 21:39

Table 11 and Table 12 show regression statistics for the NOAA EDR  $R_{rs}$  and the NASA evaluation  $R_{rs}$ , respectively. The results indicate that fewer points were available for the EDR, probably because of aggressive masks or flags. The results between the EDR and NASA evaluation data are strikingly similar, except for the NASA evaluation  $R_{rs}$  at 410 nm, which showed a poorer comparison with *in situ* data than EDR. This overall agreement between satellite and *in situ* data is remarkably good for the conditions under which the *in situ* was measured. However, the slope confidence intervals are still a few to several percent. Therefore, it is quite possible that the few to several percent differences noted in L2 surface reflectance likely caused the EDR chlorophyll to be high and erratic (i.e., the surface reflectance biases were within the uncertainty of the regression analysis).

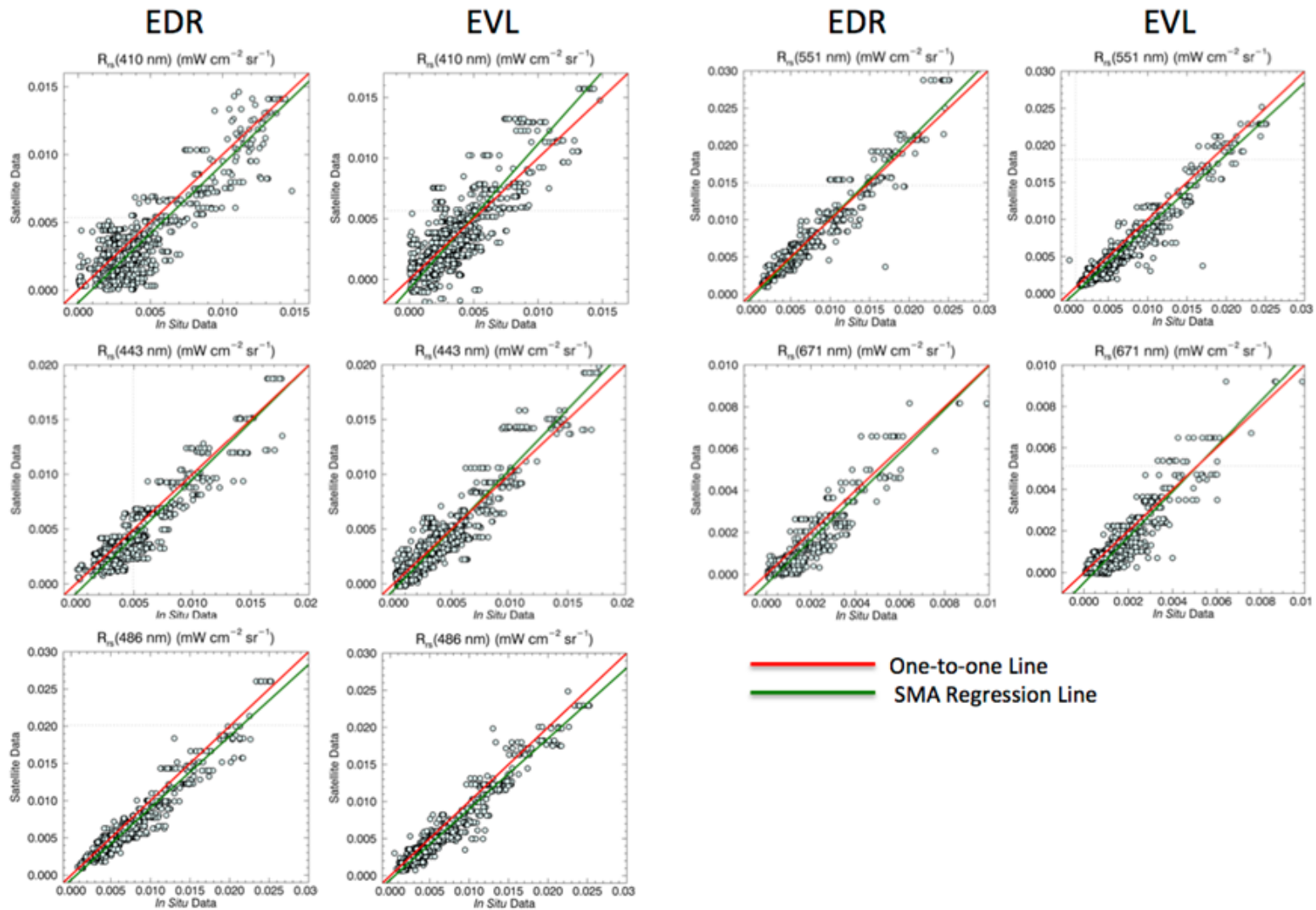


Table 11: RMA regression statistics for the matched NOAA EDR and in situ Rrs data.

### NOAA Environmental Data Records (EDR) Match-Up Analysis

Rrs( $\lambda$ ) nm	Confidence Interval				Confidence Interval				No.	R <sup>2</sup>
	Slope	Std Err	Lower Bnd	Upper Bnd	Intercept	Std Err	Lower Bnd	Upper Bnd		
410	1.02	1.65E-02	9.88E-01	1.05E+00	-9.2E-04	9.00E-05	-1.09E-03	-7.50E-04	1006	0.74
443	1.04	1.42E-02	1.02E+00	1.07E+00	-9.0E-04	8.00E-05	-1.07E-03	-7.40E-04	840	0.85
486	0.96	8.20E-03	9.47E-01	9.80E-01	-6.2E-04	7.00E-05	-7.50E-04	-4.90E-04	963	0.93
551	1.06	8.86E-03	1.04E+00	1.08E+00	-4.8E-04	7.00E-05	-6.20E-04	-3.50E-04	957	0.93
671	1.04	1.44E-02	1.01E+00	1.07E+00	-4.6E-04	3.00E-05	-5.20E-04	-4.10E-04	881	0.83

Table 12: RMA regression statistics for the matched NASA evaluation and *in situ* R<sub>rs</sub> data.

### NASA Evaluation Data Products (L2) Match-Up Analysis (R2013.0)

Rrs( $\lambda$ ) nm	Confidence Interval				Confidence Interval				No.	R <sup>2</sup>
	Slope	Std Err	Lower Bnd	Upper Bnd	Intercept	Std Err	Lower Bnd	Upper Bnd		
410	1.19	1.78E-02	1.16E+00	1.23E+00	-7.6E-04	8.00E-05	-9.10E-04	-6.10E-04	1399	0.69
443	1.10	1.18E-02	1.08E+00	1.12E+00	-5.7E-04	6.00E-05	-6.90E-04	-4.50E-04	1188	0.86
486	0.95	6.43E-03	9.39E-01	9.64E-01	-5.3E-04	5.00E-05	-6.20E-04	-4.40E-04	1399	0.94
551	0.97	6.60E-03	9.59E-01	9.84E-01	-7.1E-04	5.00E-05	-8.00E-04	-6.10E-04	1389	0.94
671	1.09	1.32E-02	1.07E+00	1.12E+00	-4.9E-04	2.00E-05	-5.30E-04	-4.40E-04	1249	0.82

---

### 2.5.2.5 DISCUSSION

Analysis of the EDR product demonstrated that the EDR flags and masks have reduced the number of observations and undermined the product's potential quality. Even though VIIRS can collect more observations than MODIS, the NOAA EDR number of observations is less than that of MODIS. Moreover, it is nearly half of what it could be, as demonstrated by the NASA evaluation data product. Furthermore, masking has eliminated EDR data for all major lakes and preferentially excludes extreme lows for chlorophyll *a* concentration in the open ocean gyres and the extreme highs in the more productive waters. Many of these problems have been recognized by NOAA and are expected to be corrected, eventually. However, without reprocessing, data masked during the first part of the mission are permanently lost. For instance, there is no chlorophyll *a* concentration for all of the Great Lake for all of 2012 and some portion of 2013.

Regional L3 averages and difference maps indicated that NOAA EDR chlorophyll *a* concentration tends to be significantly higher than the long-term record established with SeaWiFS and MODIS. L2 analysis suggests that most of this behavior may arise from differences in surface reflectance. This could arise from differences between the atmospheric correction algorithms, however insufficient calibration of the SDR may be more influential. Vicarious calibration of the SDR may improve the EDR chlorophyll *a* concentration. However, any improvement will only be realized in forward processing. Therefore, without reprocessing, the EDR chlorophyll *a* concentration cannot meet NASA data continuity objects. The NASA evaluation chlorophyll *a* concentration does appear to provide continuity with the SeaWiFS and MODIS Aqua products. This indicates that the VIIRS instrument is potentially capable of maintaining continuity of the NASA chlorophyll *a* concentration record.

Comparison between *in situ* data and NOAA EDR and NASA evaluation surface reflectance showed that both versions of the VIIRS data are in apparent good agreement with the AERONET-OC data. This is remarkable because AERONET-OC stations are mostly situated in coastal waters; some potentially challenging. Too few chlorophyll data were available to perform a meaningful analysis. More chlorophyll *a* concentration data are expected in the coming months. However, whether enough *in situ* data can be collected to provide a useful validation remains to be determined. Uncertainty, even with large samples of matchup data, seems too large to optimally determine product performance (e.g., to fully determine and diagnose deficiencies in data quality). New strategies for data collection (e.g., to improve quality sampling for all data products) and analyses should be considered for future analyses.

## 3. CONCLUSIONS

---

The science team had two primary goals: 1) to evaluate the NOAA ocean color Environmental Data Record (EDR) to determine whether it would support continuity of the establish NASA ocean color data record and 2) to determine whether VIIRS could support the development of new algorithms, including those that could generate data products that were originally part of the NASA data record, but were not supported by the S-NPP operational processing stream. Furthermore, the science team also considered whether calibrated

---

radiometry from the VIIRS sensor could support NASA's data continuity objectives to generate a continuous NASA data record.

More specifically, a goal of the science team was to determine whether the NOAA EDR, or the VIIRS instrument itself, was capable of functioning as a climate data record (CDR) or an Earth System Data Record (ESDR). The determination first requires some definition of terms. In 2004, the National Academy of Science Committee on Climate Data Records from NOAA Operational Satellites defined a CDR to be a data record that can be used to discern variability and change on inter-annual to decadal scales. For the ocean color record, this translates to monitoring the response of the ocean biospheric parameters (e.g., chlorophyll *a* concentration) to climate change or to answer science questions associated with ocean color research, such as those described in Section 1.1. The committee reported that in order to detect small trends or anomalies against a background of intense, short-term variations records must be long-term, highly accurate and stable, consistent, and continuous (NRC, 2004). To that end, CDR production requires repeated analysis and refinement of the data record. Furthermore, a CDR requires "an observing strategy emphasizing a strong commitment to maintaining data quality and minimizing gaps in coverage." Similarly, NASA defined an ESDR as "a unified and coherent set of observations of a given parameter of the Earth system, which is optimized to meet specific requirements in addressing science questions (Maiden and Ramapriyan, 2009)."

In this regard, the prelaunch evaluation identified major issues with the operational system that confuted the premise that the Ocean Color EDR would support NASA science objectives. First, the NOAA operational algorithms for VIIRS are inconsistent with those used to generate the current NASA data record. For instance, they lack a NIR correction in the EDR algorithm, which causes significant differences in chlorophyll *a* concentration in productive or turbid waters. Second, the lack of a mission-level reprocessing capability precludes the generation of a consistent data record. For instance, changes or updates to the calibration, implementation of a vicarious calibration, or making needed updates to algorithms, masks, and flags will only improve the record for the future; the standing record will always hold artifacts, some of which are significant. Therefore, the operational NOAA ocean color EDR cannot meet NASA continuity objectives.

Postlaunch data analysis further supports this conclusion. This is plainly illustrated in Fig. 43 for chlorophyll *a* concentration, which is the only derived product in the EDR suite that corresponds to a standard product in the NASA data record. Fig. 44 puts this comparison of records in context of the MODIS and SeaWiFS records. Deep-water averages of monthly composites shown Fig. 44 are not based on common bins, but any the difference between these monthly curves and the 8-day common bin averages were found to be much smaller than the deviation of the EDR. This is expected given that the monthly composites have fuller global sampling, and so coverage gaps have less influence the signal. Therefore, synoptic averages of the EDR chlorophyll *a* product deviate significantly from the NASA data record spanning 15 years.

However, the overall performance of VIIRS instrument on orbit is good, and so the sensor appears potentially useful for the generation of number of heritage ocean color data products. A consistent calibration of VIIRS can be achieved, but it may take years to reach heritage quality. Likewise, heritage missions (e.g., SeaWiFS and MODIS) took two to three years

---

for calibration teams to fully understand and de-trend solar calibrator data; to collect sufficient data for vicarious calibration; or to accumulate sufficient lunar measurements to fully trend long-term trends in the instrument response. It should be noted that the VIIRS calibration system is degrading at an order of magnitude faster than MODIS, limiting its potential lifespan. The design of the calibration system exposes the solar reference panel to far more ultraviolet light than received by the MODIS Aqua calibration system and its corresponding monitor detectors are degrading in NIR responsivity because of the higher ambient radiation flux at the S-NPP orbital altitude. The same problematic design is planned for future VIIRS instruments, which will also need to be carefully monitored. **However, the quality of the VIIRS evaluation data products at their one-year anniversary appears better than the quality for corresponding products from the SeaWiFS and MODIS at their first anniversary.** This can be attributed to the solid performance of the instrument; the well-seasoned experience of the science team and Ocean PEATE; and the unprecedentedly extensive knowledge gained about the instrument characteristics prior to launch. In addition, the combined engineering resources available across NASA and NOAA to resolve VIIRS instrument anomalies are also much greater than heritage.

As with heritage ocean color missions at this stage, some additional work will be needed to bring VIIRS calibration quality to heritage levels. Calibration will continue to be refined as more lunar and calibration buoy data is collected. The calibration system artifacts will need to be investigated and the effects of changing OOB response will need to be quantified and corrected. Corrections for residual striping and scan effects should be applied to bring VIIRS quality in line with MODIS Aqua, as mentioned in Section 1.3.2. Also, the decreasing signal-to-noise ratio for the NIR bands will need to be monitored to be sure that they do not require further mitigation to boost the signal (e.g., pixel aggregation). However, techniques to address all of these tasks already exist and are straightforward because of the experience afforded by previous missions.

The VIIRS surface radiometry for both the EDR and NASA evaluation products showed good agreement with *in situ* data from fixed stations of the AERosol ROBotic NETwork – Ocean Color (AERONET-OC). Similar results were observed at sea by Balch, but the biases were larger for most of the bands. However, that analysis involved a sample size at least one order of magnitude smaller and the corresponding regression analysis could be more subject to noise associated with ship measurements (related to viewing geometry, pitch and role of the ship, etc.). The good agreement between satellite and *in situ* surface radiometry seems counterintuitive when considering the poor performance of the EDR chlorophyll *a* deep-water time series. However, the slope confidence intervals for the regressions statistics indicate that there is sufficient uncertainty in the comparison between satellite and surface data to allow for large enough biases to adversely affect one or both products (in this case, only the EDR appears to be affected). Observed small, positive biases for chlorophyll *a* concentration of about 10-40% (for the week with maximum difference between the EDR and MODIS) could arise from biases of only a few percent in the surface reflectance over most of the open ocean, provided that the blue band biases go in the opposite direction of the green band bias (i.e., underestimated blue and overestimated green surface reflectance or overestimated blue and underestimated green). Analysis of the EDR surface reflectance (i.e.,  $nL_w$ ) indicates that the EDR blue bands are low and the EDR green band is high, relative to the NASA evaluation product. Improvement in EDR chlorophyll should come with vicarious calibration of the operational product.

---

Comparison between chlorophyll *a* estimates from the satellite with estimate from *in situ* data was limited. SeaBASS protocols eliminated all but ten data pairs (all from the Great Belt II cruise), so no meaningful statistical analysis could be done. Field comparisons by Balch showed reasonable matches between fluorometric chlorophyll *a* concentration and the NASA evaluation product (within the known algorithm uncertainty of a factor of two). Siegel also made comparisons between fluorometric chlorophyll *a* concentration taken as part of Plumes and Blooms, but these showed modest, but significant correlation. Similar results arose when the same analysis was applied to MODIS and SeaWiFS. These smaller correlations likely stemmed from the fact that the region where Plumes and Blooms measurements were taken is particularly challenging for spaceborne remote sensing instruments with limited spatial and spectral resolution.

The amount of *in situ* data available after one year for this analysis was limited. Additional data are expected to be archived into SeaBASS over the next year (PI's have up to one year to deliver data to this archive per NASA policy). Also, per NASA policy, all High-Performance Liquid Chromotography (HPLC) chlorophyll *a* measurements must be performed at a common NASA laboratory to maintain consistency. This necessary approach slows the process for making data available for validation analysis. Furthermore, once all the SeaBASS protocols are applied for matching satellite and *in situ* data, only a small fraction of the collected data remain. However, despite the lack of available chlorophyll *a* data, AERONET-OC stations provided continuous radiometric measurements through most of the year, producing a far greater sample of that parameter than can affordably be collected shipboard during that period. This number of satellite/*in situ* matches has more recently been reduced to about a quarter of the amount because multiple AERONET-OC measurements were being matched to the same satellite measurement, thus increasing the scatter. Therefore, the time constraint in the matching algorithm has been reduced from 3 hours to 1 hour. Even with this reduction, the sheer volume of data is far greater than what we can affordably collect shipboard because of limited time and expense. This is not to say that we should not have cruises, because only cruises can target specific regions, e.g., away from terrestrial sources of pollution and continental dust. However, implementation of new strategies, e.g., advanced buoys or gliders that can take a suite of measurements, could cover much more ground at a lower cost. Also, increasing data sharing with domestic and international sources could expand the available data. For instance, further analysis of the VIIRS EDR and NASA evaluation products could include data from the European data collection activity called the Bouée pour l'acquisition de Séries Optiques à Long Terme (BOUSSOLE), including chlorophyll data. New strategies need to be considered to expand the data available for validation and while minimizing cost.

Another aspect about *in situ* validation was raised by the fact that despite the hundreds of radiometric measurements now available through AERONET-OC, the regression uncertainty was too large to capture significant biases that would have directly explained the poor performance of the chlorophyll *a* algorithm. This is indicative that there are other challenges regarding data collection and analysis that should be addressed. Naturally, there are many sources of uncertainty that can arise when taking measurements at sea and methods to address these are being, and should be, developed. However, there is the so-called "scale issue," in which spurious variation is introduced by matching point measurements with a kilometer-scale

---

satellite pixels. Further work is needed to reduce these sources of uncertainty in the comparison with the *in situ* data.

Finally, evaluation of new algorithms further supported the potential of VIIRS to meet data continuity objectives and possibly the development of novel applications. The heritage algorithms, PIC and PAR, were successfully implemented in the NASA evaluation processing stream and appeared to perform well, relative to MODIS and sea truth. The comparisons between VIIRS-derived PIC and chlorophyll estimates are remarkably close to those achieved with MODIS Aqua. While there are some differences between the two sensors, they show exceedingly similar statistics in terms of the algorithm bias and RMS error. The PAR product showed comparable, but slightly higher values with compared to MODIS Aqua and to *in situ* data. This may improve with further refinement of the VIIRS calibration. The experimental algorithm for estimating chlorophyll *a* using the GSM semi-analytic ocean color model demonstrated similar performance for the Plumes and Blooms data for VIIRS, MODIS, and SeaWiFS. Use of the VIIRS SWIR bands to improve atmospheric correction over coastal waters shows promise. A potential challenge facing this algorithm is proper calibration the SWIR bands. Like the NIR bands, the responsivity of the SWIR bands is also degrading because of prelaunch mirror contamination. Unlike the IR bands, the SWIR bands were not turned on until mid-January, several weeks after the nadir doors of the spacecraft were opened and the degradation began. Therefore, it is difficult to determine much these bands degraded from their prelaunch calibration responses to the point when they were activated. Fortunately, the SWIR algorithm investigated by Wang considers the ratio of two SWIR bands and the same-sign calibration biases in those bands will tend to cancel. Finally, application of data assimilation techniques and the ESRIDS bias correction produces a VIIRS L3 time series of chlorophyll *a* concentration that is more consistent with MODIS Aqua. The technique also provides a method to remove the spurious signal introduced into the climate record by data gaps on regional and global scales.

## 4. RECOMMENDATIONS

---

The following general recommendations were based on the conclusions drawn in the previous section and on experience with heritage missions.

**REPROCESSING** – A mission-level ocean color reprocessing capability should be available for application throughout the mission, as with heritage missions. Moreover, reprocessing should be able to span the multiple sensors of NASA data record to facilitate algorithm updates.

**VIIRS CALIBRATION SUPPORT** – An ocean color-focused calibration should continue for at least the first two to three years, which barring late mission anomalies, is likely a minimum period necessary to bring VIIRS data to NASA data record quality.

**ALGORITHM CONTINUITY AND CONSISTENCY** – Heritage atmosphere correction algorithms should be used to maintain continuity with the NASA ocean color data record. Furthermore, EOS products without an EDR equivalent should be generated (e.g., PIC, PAR, and  $K_d(490)$ ).

**NEW ALGORITHM DEVELOPMENT** – VIIRS is of sufficient quality to be used as an opportunity for the development of new algorithms and remote sensing techniques.

---

**VALIDATION DATA** – New data collection and validation strategies should be developed for more effective validation and data analyses. These include the following example areas:

- Top-level planning for collection of data over a wide diversity of environments;
- Technology or techniques to increase sample size or reduce noise for *in situ* data;
- Strategies to address differences in scale between satellite and *in situ* data;
- Expanded domestic and international collaboration in data collection.

---

## RESULTING PAPERS – 2011-PRESENT

---

Anderson, C.R., R.M. Kudela, C. Benitez-Nelson, E. Sekula-Wood, C. Burrell, Y. Chao, G. Langlois, J. Goodman, and D.A. Siegel, 2011: Detecting toxic diatom blooms from ocean color and a regional ocean model. *Geophysical Research Letters*, doi:10.1029/2010GL045858.

Antoine, D., D.A. Siegel, T. Kostadinov, S. Maritorena, N.B. Nelson, B. Gentili, V. Vellucci and N. Guillocheau, 2011: Variability in optical particle backscattering in contrasting bio-optical oceanic regimes, *Limnology and Oceanography*, 56, 955–973.

Barrón, R.K., D.A. Siegel and N. Guillocheau, 2013: Evaluating the importance of phytoplankton community structure to the optical properties of the Santa Barbara Channel, California. In review, *Limnology and Oceanography*.

Eplee, R.E., Turpie, K.R., Fireman, G.,F., Meister, G., Stone,T.C., Patt, F.S., Franz, B.A., Bailey, S.W., Robinson, W.D., McClain, C.R., (2012). VIIRS On-Orbit Calibration for Ocean Color Data Processing, in *Earth Observing Systems XVII* J.J. Butler, X Xiong, and X. Gu, eds., Proc. SPIE 8510, 85101G.

Gregg, W.W., N.W. Casey, and C.S. Rousseaux, 2012. Assimilating Global Ocean Chlorophyll from Suomi NPP-VIIRS: Prospects for Extending the Ocean Color Time Series. *Transactions of the American Geophysical Society*.

Krause, J.W., M.A. Brzezinski, D.A. Siegel, R.C. Thunell, 2013: Biogenic silica standing stock and export in the Santa Barbara Channel ecosystem. *Journal of Geophysical Research*, DOI: 10.1029/2012JC008070.

Kostadinov, T.S., D.A. Siegel, S. Maritorena, N. Guillocheau, 2012: Optical assessment of oceanic particle size and composition in the Santa Barbara Channel, California. *Applied Optics*, 51, 3171–3189.

Turpie, K.R., B.A. Franz, C.R. McClain, W.D. Robinson, R.E. Eplee, Jr., G. Meister, G.F. Fireman, F.S. Patt, and R.A. Barnes, (2012). Suomi NPP VIIRS ocean color data product early mission assessment, in *Earth Observing Systems XVII* J.J. Butler, X Xiong, and X. Gu, eds., Proc. SPIE 8510, 85101I.

Wang, M., Shi, W., (2012). Sensor noise effects of the SWIR bands on MODIS-derived ocean color products, *IEEE Trans. Geosci. Remote Sensing*, 50, 3280-3292.

---

## REFERENCES

---

- Anderson, C.R., Kudela, R.M., Benitez-Nelson, C., Sekula-Wood, E., Burrell, C.T., Chao, Y., Langlois, G., Goodman, J., Siegel, D.A., 2011. Detecting toxic diatom blooms from ocean color and a regional ocean model. *Geophysical Research Letters* DOI: 10.1029/2010GL045858.
- Anderson, C.R., Siegel, D.A., Brzezinski, M.A., Guillocheau, N., 2008. Controls on temporal patterns in phytoplankton community structure in the Santa Barbara Channel, California. *Journal of Geophysical Research* 113, C04038, doi: 10.1029/2007JC004321.
- Anderson, C.R., Siegel, D.A., Kudela, R.M., Brzezinski, M.A., 2009. Empirical models of toxigenic *Pseudo-nitzschia* blooms: Potential use as a remote detection tool in the Santa Barbara Channel. *Harmful Algae* 8, 478-492.
- Antoine, D., Siegel, D.A., Kostadinov, T., Maritorena, S., Nelson, N.B., Gentili, B., Vellucci, V., Guillocheau, N., 2011. Variability in optical particle backscattering in contrasting bio-optical oceanic regimes. *Limnology and Oceanography* 56, 955-973.
- Balch, W.M., 2004. Re-evaluation of the physiological ecology of coccolithophores, in: Thierstein, H.R., Young, J.R. (Eds.), *Coccolithophores from molecular processes to global impact*. Springer-Verlag, New York, pp. 165-190.
- Balch, W.M., Drapeau, D.T., 2004. Backscattering by Coccolithophorids and Coccoliths: Sample Preparation, Measurement and Analysis Protocols, in: \Mueller, J.L., Fargion, G.S., McClain, C.R. (Eds.), *Ocean Optics Protocols For Satellite Ocean Color Sensor Validation, Revision 5: Biogeochemical and Bio-Optical Measurements and Data Analysis Protocols*. National Aeronautical and Space Administration, Goddard Space Flight Space Center, Greenbelt, Maryland, pp. 27-36.
- Balch, W.M., Drapeau, D.T., Bowler, B.C., Booth, E.S., Goes, J.I., Ashe, A., Frye, J.M., 2004. A multi-year record of hydrographic and bio-optical properties in the Gulf of Maine: I. Spatial and temporal variability. *Progress in Oceanography* 63, 57-98.
- Balch, W.M., Drapeau, D.T., Bowler, B.C., Booth, E.S., Windecker, L.A., Ashe, A., 2008. Space-time variability of carbon standing stocks and fixation rates in the Gulf of Maine, along the GNATS transect between Portland, ME, USA, and Yarmouth, Nova Scotia, Canada. *Journal of plankton research* 30, 119-139.
- Balch, W.M., Drapeau, D.T., Fritz, J.J., Bowler, B.C., Nolan, J., 2001. Optical backscattering in the Arabian Sea-continuous underway measurements of particulate inorganic and organic carbon. *Deep Sea Research Part I* 48, 2423-2452.
- Balch, W.M., Kilpatrick, K., 1996. Calcification rates in the equatorial Pacific along 140 W. *Deep Sea Research Part II* 43, 971-993.
- Balch, W.M., Kilpatrick, K.A., Holligan, P., Harbour, D.S., Fernandez, E., 1996. The 1991 coccolithophore bloom in the central North Atlantic. II. Relating optics to coccolith concentration. *Limnology and Oceanography* 41, 1684-1696.
- Barrón, R.K., Siegel, D.A., Guillocheau, N., 2013. Evaluating the importance of phytoplankton community structure on ocean optical properties in the Santa Barbara Channel, CA. In review, *Limnology and Oceanography*.
- Bishop, J.K.B., 1999. Transmissometer measurement of POC. *Deep-sea research. Part I* 46, 353-369.
- Bishop, J.K.B., Calvert, S.E., Maureen, S.Y.S., 1999. Spatial and temporal variability of POC in the northeast Subarctic Pacific. *Deep Sea Research Part II* 46, 2699-2734.

- 
- Brown, S.W., Eppeldauer, G.P., Lykke, K.R., 2006. Facility for spectral irradiance and radiance responsivity calibrations using uniform sources. *Applied Optics* 45, 8218-8237.
- Carder, K.L., Chen, F.R., Lee, Z.P., Hawes, S.K., 1999. Semianalytic Moderate-Resolution Imaging Spectrometer algorithms for chlorophyll a and absorption with bio-optical domains based on nitrate-depletion temperatures. *Journal of Geophysical Research* 104, 5403-5421.
- Cheng, Z., Zheng, Y., Mortlock, R., Van Geen, A., 2004. Rapid multi-element analysis of groundwater by high-resolution inductively coupled plasma mass spectrometry. *Analytical and Bioanalytical Chemistry* 379, 512-518.
- Clark, D.K., Gordon, H.R., Voss, K.J., Ge, Y., Broenkow, W., Trees, C., 1997. Validation of atmospheric correction over the ocean. *Journal of Geophysical Research* 102, 209-217.
- Eplee, R.E., 2011a. Proposed VIIRS SDR code updates, Internal report. v1.0 24 Jan 2011.
- Eplee, R.E., 2011b. The VIIRS SDR code implementation. Internal report. v1.0 18 Jan 2011, 5 pp.
- Fernandez, E., Boyd, P., Holligan, P.M., Harbour, D.S., 1993. Production of organic and inorganic carbon within a large-scale coccolithophore bloom in the northeast Atlantic Ocean. *Marine Ecology Progress Series* 97, 271-285.
- Frouin, R., Chertock, B., 1992. A technique for global monitoring of net solar irradiance at the ocean surface. I: Model. *Journal of Applied meteorology* 31, 1056-1066.
- Frouin, R., Franz, B.A., Werdell, P.J., 2003. The SeaWiFS PAR product, in: Hooker, S.B., Firestone, E.R. (Eds.), *Algorithm Updates for the Fourth SeaWiFS Data Reprocessing*, pp. NASA/TM-2003-206892, 206822:206846-206850.
- Frouin, R., McPherson, J., Ueyoshi, K., Franz, B.A., 2012. A time series of photosynthetically available radiation at the ocean surface from SeaWiFS and MODIS data, *Proc. SPIE 8525 Remote Sensing of the Marine Environment* DOI: 10.1117/12.981264.
- Gardner, W.D., Walsh, I.D., Richardson, M.J., 1993. Biophysical forcing of particle production and distribution during a spring bloom in the North Atlantic. *Deep Sea Research Part II* 40, 171-195.
- Gordon, H.R., Wang, M., 1994. Retrieval of water-leaving radiance and aerosol optical thickness over the oceans with SeaWiFS: a preliminary algorithm. *Applied optics* 33, 443-452.
- Gregg, W.W., Casey, N.W., 2007. Sampling biases in MODIS and SeaWiFS ocean chlorophyll data. *Remote Sensing of Environment* 111, 25-35.
- Gregg, W.W., Casey, N.W., 2010. Improving the consistency of ocean color data: A step toward climate data records. *Geophysical Research Letters* 37, L04605.
- Gregg, W.W., Casey, N.W., O'Reilly, J.E., Esaias, W.E., 2009. An empirical approach to ocean color data: Reducing bias and the need for post-launch radiometric re-calibration. *Remote Sensing of Environment* 113, 1598-1612.
- Hooker, B., E., F., Acker, J., 1995. Level-3 SeaWiFS Data Products: Spatial and Temporal Binning Algorithms. NASA Technical Memorandum 104566, Vol. 32.
- JGOFS, 1996. Protocols for the Joint Global Ocean Flux Study (JGOFS) core measurements. Report no. 19 of the Joint Global Ocean Flux Study. Scientific Committee on Oceanic Research, International Council of Scientific Unions, Intergovernmental Oceanographic Commission, Bergen, Norway.
- Kostadinov, T.S., Siegel, D.A., Maritorena, S., 2009. Retrieval of the particle size distribution from satellite ocean color observations. *Journal of Geophysical Research* 114, C09015.
- Kostadinov, T.S., Siegel, D.A., Maritorena, S., Guillocheau, N., 2007. Ocean color observations and modeling for an optically complex site: Santa Barbara Channel, California, USA. *Journal of Geophysical Research* 112, C07011. doi: 07010.01029/02006JC003526.

- 
- Kostadinov, T.S., Siegel, D.A., Maritorena, S., Guillocheau, N., 2012. Optical assessment of particle size and composition in the Santa Barbara Channel, California. *Applied Optics* 51, 3171-3189.
- Maiden, Ramapriyan, 2009. NASA's MEaSUREs Program: Making Earth System Data Records for Use in Research Environments. Presentation.
- Maritorena, S., Siegel, D.A., Peterson, A.R., 2002. Optimization of a semianalytical ocean color model for global-scale applications. *Applied Optics* 41, 2705-2714.
- Mobley, C.D., 2013. The Atmospheric Correction Problem," in *Ocean Optics Web Book*, [http://www.oceanopticsbook.info/view/remote\\_sensing/the\\_atmospheric\\_correction\\_problem](http://www.oceanopticsbook.info/view/remote_sensing/the_atmospheric_correction_problem), accessed 18 March 2013.
- Mueller, J.L., Austin, R.W., Morel, A., Fargion, G.S. and McClain, C.R., , 2003. Ocean optics protocols for satellite ocean color sensor validation, Revision 4, Volume I: Introduction, background, and conventions. Goddard Space Flight Center, Greenbelt, MD.
- Mueller, J.L., Morel, A., Frouin, R., Davis, C., Arnone, R., Carder, K., Lee, Z.P., Steward, R.G., Hooker, S., Mobley, C.D., McLean, S., Holben, B., Miller, M., Pietras, C., Knobelspiesse, K.D., Fargion, G.S., Porter, J., Voss, K., 2003a. Ocean optics protocols for satellite ocean color sensor validation, Revision 4, Volume III: Radiometric measurements and data analysis protocols, Goddard Space Flight Center, Greenbelt, MD.
- Mueller, J.L., Pietras, C., Hooker, S.B., Austin, R.W., Miller, M., Knobelspiesse, K.D., Frouin, R., Holben, B., Voss, K., 2003b. Ocean optics protocols for satellite ocean color sensor validation, Revision 4, Volume II: Instrument specifications, characterization, and calibration. Goddard Space Flight Center, Greenbelt, MD.
- Nelson, N.B., Siegel, D.A., 2013. Global distribution and dynamics of chromophoric dissolved organic matter. *Annual Review of Marine Science* 5, 447-476.
- NRC, 2004. *Climate Data Records from Environmental Satellites*, Washington, DC, 150 pp.
- O'Reilly, J.E., Maritorena, S., Mitchell, B.G., Siegel, D.A., Carder, K.L., Garver, S.A., Kahru, M., McClain, C., 1998. Ocean color chlorophyll algorithms for SeaWiFS. *Journal of Geophysical Research* 103, 24937-24953.
- O'Reilly, J.E., Maritorena, S., Siegel, D.A., O'Brien, M.C., Toole, D., Mitchell, B.G., Kahru, M., Chavez, F.P., Strutton, P., Cota, G.F., Hooker, S.B., McClain, C.R., Carder, K.L., Muller-Karger, F., Harding, L., Magnuson, A., Phinney, D., Moore, G.F., Aiken, J., Arrigo, K.R., Letelier, R., Culver, M., 2000. Ocean Color Chlorophyll a Algorithms for SeaWiFS, OC2 and OC4: Version 4. S.B. Hooker and E.R. Firestone, Eds., NASA Goddard Space Flight Center, Greenbelt, Maryland, pp. 8-22.
- Ramachandran, S., Wang, M., 2011. Near-real-time ocean color data processing using ancillary data from the Global Forecast System model. *IEEE Trans. Geosci. Remote Sens.* 49, 1485-1495.
- Raytheon, 2009a. Performance verification report – VIIRS FU1 Crosstalk. Performance Verification Plan. PVP154640-101, Section 4.7.2. 162 pp.
- Raytheon, 2009b. Performance verification report – VIIRS FU1 Relative spectral response. Performance Verification Plan. PVP154640-101, Section 4.6. 204 pp.
- Reynolds, R.W., Smith, T.M., 1994. Improved global sea surface temperature analyses using optimum interpolation. *Journal of Climate* 7, 929-948.
- Robinson, W.D., Patt, F.S., Franz, B.A., Turpie, K.R., McClain, C.R., 2009. A VIIRS ocean data simulator. *Proceedings of the SPIE*, 7452(3-5), 3-5 Aug, San Diego. DOI: 10.1117/12.827058.
- Roesler, C.S., Perry, M.J., 1989. Modeling in situ phytoplankton absorption from total absorption spectra in productive inland marine waters. *Limnology and Oceanography* 34, 1510-1523.

- 
- Siegel, D.A., Behrenfeld, M.J., Maritorena, S., McClain, C.R., Antoine, D., Bailey, S.W., Bontempi, P.S., Boss, E.S., Dierssen, H.M., Doney, S.C., Eplee Jr., R.E., Evans, R.H., Feldman, G.C., Fields, E., Franz, B.A., Kuring, N.A., Mengelt, C., Nelson, N.B., Patt, F.S., Robinson, W.D., Sarmiento, J.L., Swan, C.M., Werdell, P.J., Westberry, T.K., Wilding, J.G., Yoder, J.A., in review. Regional to Global Assessments of Phytoplankton Dynamics from the SeaWiFS Mission. *Remote Sensing of the Environment*.
- Siegel, D.A., Maritorena, S., Nelson, N.B., Behrenfeld, M.J., 2005. Independence and interdependencies among global ocean color properties: Reassessing the bio-optical assumption. *Journal of Geophysical Research* 110, C07011, doi: 07010.01029/02004JC002527.
- Stramski, D., Reynolds, R.A., Kahru, M., Mitchell, B.G., 1999. Estimation of particulate organic carbon in the ocean from satellite remote sensing. *Science* 285, 239-242.
- Swan, C.M., Nelson, N.B., Siegel, D.A., Kostadinov, T.S., 2012. The effect of surface irradiance on the absorption spectrum of chromophoric dissolved organic matter in the global ocean. *Deep Sea Research Part I* 63, 52-64.
- Turpie, K.R., Franz, B.A., McClain, C.R., Robinson, W.D., Eplee, R.E., Jr., Meister, G., Fireman, G.F., Patt, F.S., Barnes, R.A., 2012. Suomi NPP VIIRS ocean color data product early mission assessment, in *Earth Observing Systems XVII* J.J. Butler, X Xiong, and X. Gu, eds., *Proceeding of the SPIE*, 8510, 851011, 12-16 Aug, San Diego.
- Turpie, K.R., Meister, G., Eplee, G., Barnes, R.A., Franz, B., Patt, F.S., Robinson, W.D., McClain, C.R., 2011. Assessment of NPP VIIRS ocean color data products: Hope and risk. *Proc. of SPIE Vol. 8153 81530M0-1*, *Earth Observing Systems XVI*, Butler, J.J., Xiong, X., Gu, X., eds., San Diego, CA. 9 pp.
- Walton, C.C., Pichel, W.G., Sapper, J.F., May, D.A., 1998. The development and operational application of nonlinear algorithms for the measurement of sea surface temperatures with the NOAA polar-orbiting environmental satellites. *Journal of Geophysical Research* 103, 999-928,012.
- Wang, M., 2007. Remote sensing of the ocean contributions from ultraviolet to near-infrared using the shortwave infrared bands: simulations. *Appl. Opt.* 46, 1535-1547.
- Wang, M., Son, S., Harding, J., L. W. , 2009. Retrieval of diffuse attenuation coefficient in the Chesapeake Bay and turbid ocean regions for satellite ocean color applications. *Journal of Geophysical Research* 114, doi:10.1029/2009JC005286.
- Werdell, P.J., Bailey, S.W., 2005. An improved in-situ bio-optical data set for ocean color algorithm development and satellite data product validation. *Remote Sensing of Environment* 98, 122-130.
- Zibordi, G., Mélin, F., Berthon, J.-F., Holben, B., Slutsker, I., Giles, D., D'Alimonte, D., Vandemark, D., Feng, H., Schuster, G., Fabbri, B.E., Kaitala, S., Seppälä, J., 2009. AERONET-OC: A Network for the Validation of Ocean Color Primary Products. *Journal of Atmospheric and Oceanic Technology* 26, 1634-1651.

---

## ACRONYMS

---

ADL	Algorithm Development Library
a	Absorption
AERONET-OC	AERosol RObotic NETwork – Ocean Color
ATMWARN	Atmospheric correction algorithm
bb	Total backscattering
bb'	Acid labile backscattering
BBP	Particulate backscattering coefficient at 443 nm
CDM	Colored dissolved and detrital materials at 443 nm
CDR	Climate Data Records
Chl-a	Chlorophyll <i>a</i>
CHLWARN	Poor chlorophyll <i>a</i> data value
CLASS	NOAA Comprehensive Large Array-data Stewardship System
CLASS	Comprehensive Large Array-data Stewardship System
EDR	Environment Data Records
ESDR	Earth System Data Record
ESRIDS	Empirical Satellite- <i>In situ</i> Data algorithm
GFS	Global Forecast System
GSM	Garver, Siegel, Maritorena semi-analytic model
HPLC	High Performance Liquid Chromatography
HRI	Horizontal Reporting Interval
IDPS	Integrated Data Processing Segment
IOP	Inherent Optical Properties
IOP_A	Absorption quality flags
IOP_S	Scattering flag
Kd(490)	Diffuse Attenuation Coefficient at 490 nm
LUT	Look-up-table
MicroSAS	Satlantic SeaWiFS Aircraft Simulator
MOBY	Marine Optical Buoy
MODIS	MODerate resolution Imaging Spectroradiometer
nLw	Normalized water-leaving radiance
NPP	Suomi National Polar-orbiting Partnership
OCTS	Ocean Color Temperature Scanner
PACE	Pre-Aerosol, Cloud, ocean Ecosystem mission
PAR	Photosynthetically Available Radiation
PAR	Photosynthetically Available Radiation
PIC	Particulate Inorganic Carbon
PnB	Plumes and Blooms program
POC	Particulate Organic Carbon
PVR	Performance Verification Reports
RDR	Raw data records
RDR	VIIRS Raw Data Records
ROLO	RObotic Lunar Observatory model
RRS	Spectral remote sensing reflectance
RSR	Relative spectral response
SDR	VIIRS Sensor Data Records
SDS	Science Data Segment
SDSM	Solar Diffuser Stability Monitor
SeaBASS	SeaWiFS Bio-optical Archive and Storage System
SeaWiFS	Sea-viewing Wide Field-of-view Sensor
SIRCUS	Spectral Irradiance and radiance Responsivity Calibrations using Uniform Sources system
STAR	NOAA Center for Satellite Applications and Research
SWIR	VIIRS shortwave infrared bands
TOA	Top-of-atmosphere radiance/reflectance
VCST	NASA VIIRS Calibration Support Team
VIIRS	Visible Infrared Imaging Radiometer Suite